



Recycling permanent magnets from offshore wind turbines an e-waste approach

Materials Science Engineering

Fay Fang de Waal

Supervised by S. Abrahami

Co-supervised by M. van Regteren, J.P. Jensen, K. Skelton

Materials Science Engineering

Mechanical, Maritime and Materials Engineering

Delft University of Technology

September, 2022

*A thesis submitted in partial fulfilment of the requirements for the degree of
Materials Science Engineering.*



Copyright ©2022 Delft University of Technology | CrossWindHKN | SGRE

www.tudelft.nl | www.crosswindhkn.nl | www.siemensgamesa.com

First edition, August 29, 2022



CROSSWIND

Declaration by Master Students

(a) Authenticity of Thesis

I hereby declare that I am the legitimate author of this Dissertation and that it is my original work. No portion of this work has been submitted in support of an application for another degree or qualification of this or any other university or institution of higher education.

I hold Delft University of Technology harmless against any third party claims with regard to copyright violation, breach of confidentiality, defamation and any other third party right infringement.

Faculty	Mechanical, Maritime and Materials Engineering
Degree	Materials Science Engineering
Title	Recycling permanent magnets from offshore wind turbines an e-waste approach
Candidate (Id.)	Fay Fang de Waal (4345940)

Signature of Student _____

Date August 29, 2022

02.09.2022

Reinventing the wheel.

Het wiel opnieuw uitvinden.

Acknowledgements

I would like to thank Marin van Regteren, Shoshan Abrahami, Jonas Jensen and Kristen Skelton for being my supervisors throughout my second and final master thesis to Yongxiang Yang for providing additional support. A special thanks to Tjalling de Bruin for taking me on at CrossWind and to David Molenaar to getting Siemens on board with this thesis. Moreover, the contents of this thesis would not have been filled without all the people that contributed in interviews and that I spoke with during site visits and at the office. Thank you to all the fun CrossWind colleagues for keeping me company during my long office hours and to all my friends and family who had to deal with me through my many quarter-life crises.

Abstract

OWTs and WEEEs have both been found to contain NdFeB permanent magnets, which are both valuable sources for the recovery of REEs. At the same time, OWTs have been found to contain many electrical components that may not officially fall under the WEEE direct but share many similarities with WEEE. While there is little known about the recycling of OWTs and their electrical components due to their recent introduction, the recycling of WEEE has been studied more extensively and is a more mature industry.

To determine the preferred recycling route for permanent magnets from OWTs, a comparison was made with the characteristics and the recycling routes of permanent magnets from WEEE. The disassembly was found to be the most critical part to enable an efficient recycling process, leading to the objective of how can permanent magnets be disassembled from OWT generators. It was found that the disassembly of magnetised magnets at the scale of OWTs is challenging due to the forces required to move them and the brittleness of the materials. For efficient disassembly, the permanent magnets need to be locally and thermally demagnetised. Through a series of interviews, desk research, a lab visit and a site visit to Cuxhaven a concept for the disassembly of permanent magnets from OWTs was developed.

It was found that induction heating a copper coil wrapped around U shaped core to transfer heat to the permanent magnet via conduction is a potential scalable, automatable and time-efficient solution for demagnetisation. The power required to heat the coil depended predominantly on the time taken to heat the core as well as the contact surface area of the core with the permanent magnet, the mass of the conductor and the material chosen for the conductor. After thermal demagnetisation, the magnet can be removed while the magnetic is still hot or after cooling, dependent on the thermal expansion coefficient, effect of re-magnetisation and remanence of the magnet. Depending on the acceptable remanence to be able to handle the magnet, it may not be necessary to heat the magnet up all the way to the Curie temperature. The solution proposed in this study is just one of many options towards the recycling of permanent magnets, thus alternative solutions such as direct induction of complete thermal demagnetisation should also be considered.

Contents

- 1 Introduction 1**
 - 1.1 Offshore Wind Turbines 2
 - 1.2 Waste Electronic and Electric Equipment 7
 - 1.3 Recycling 13
 - 1.4 Objectives 16
 - 1.4.1 Sub-objectives 16
 - 1.4.2 Case study 17

- 2 Methodology 21**
 - 2.1 Sub-objective 1: Preferred recycling route 23
 - 2.1.1 Permanent magnet properties 23
 - 2.1.2 Recycling routes 24
 - 2.2 Sub-objective 2: Disassembly 25
 - 2.2.1 Assembly 25
 - 2.2.2 Disassembly concept 26

- 3 Preferred recycling route 29**
 - 3.1 Permanent magnets 29
 - 3.1.1 Materials 29
 - 3.1.2 Applications 32
 - 3.1.3 Properties 34
 - 3.2 Recycling routes 37
 - 3.2.1 Process overview 37
 - 3.2.2 Recycling permanent magnets 41
 - 3.2.3 Disassembly 44
 - 3.2.4 Demagnetisation 47
 - 3.3 Summary of results 53

4	Disassembly	55
4.1	Assembly	55
4.1.1	Magnet assembly	56
4.1.2	Generator assembly	59
4.1.3	Disassembly at SGRE	62
4.2	Demagnetisation concept	65
4.2.1	Theory	65
4.2.2	Concept design	69
4.2.3	Theoretical model	74
4.3	Summary of results	83
5	Discussion	85
5.1	Interpretation of results	85
5.1.1	Implications of results	87
5.2	Future research	88
5.2.1	Alternative set-ups	89
5.3	Recommendations and limitations	90
5.4	Conclusion	92
	Appendix A Python	97
A.1	Properties database	97
A.2	Variable Curie temperature	100
	Bibliography	105

List of Figures

1.1	Percentage of global warming contribution from each life cycle stage (gCO ₂ eq/kWh) (Siemens Gamesa, 2014)	1
1.2	Overview of the CrossWind wind turbines' main parts and components (van der Tempel, 2006)	2
1.3	Image of the top of an SG 11.0-200DD which shows the rotor nacelle assembly (RN or RNA) obtained from CrossWind/SGRE	4
1.4	Global warming contribution of main components in the wind power plant (CO ₂ eq) (Siemens Gamesa, 2014)	6
1.5	Global warming contribution per material group in the wind power plant (CO ₂ eq) (Siemens Gamesa, 2014)	6
1.6	Assessment of the environmental impact and uncertainties involved in dismantling, recycling and disposing of wind turbines and their components (Andersen et al., 2014)	7
1.7	Different material compositions in WEEE (Murugappan and Karthikeyan, 2021)	10
1.8	The periodic table with an overview of the elements found in WEEE, precious metals are indicated in green, critical raw materials are shown in teal (Forti et al., 2020)	10
1.9	Overview of the material recycling and recovery process	13
1.10	Flow chart of different recycling options for permanent magnets in WEEE	15
1.11	Overview of the CrossWind wind farm location and size (CrossWind, 2022)	18
1.12	Overview of the CrossWind wind turbines' basic characteristics (CrossWind, 2022)	19
2.1	Overview of the methodology to answer the research question and its sub-research question.	21
3.1	Recycling potential estimate of REEs from (a) hard disk drives and (b) mobile phones in the period of 2010–2019 (München et al., 2021)	35
3.2	Mass and material intensity changes for REEs from 2020 to 2040 (Li et al., 2022)	35

3.3	Nd oxide price in US dollars per metric ton worldwide from 2009 to 2025 (Kapustka et al., 2020)	35
3.4	Extended overview of the entire recycling process including the sub-steps of the pre-processing and end-processing stage.	37
3.5	Overview of the entire recycling process for NdFeB permanent magnets according to (Peelman et al., 2018)	43
3.6	Proposed recycling process for permanent magnets in HDDs (Peelman et al., 2018)	43
3.7	Example of the disassembly processes for two types of WEEE from (Lixandru et al., 2017)	45
3.8	Example of a hysteresis loop (Arora, 2018).	49
3.9	Example of magnetic domains and magnetisation (Arora, 2018).	49
3.10	Induction heating the entire generator structure.	52
4.1	A basic overview from the top of the generator assembly of an OWT.	55
4.2	Zoomed in view of the basic overview from the top of the generator assembly of an OWT.	56
4.3	Permanent magnets in the OWT	57
4.4	Magnet casing containing permanent magnet blocks stacked on top of each other	57
4.5	Breakdown of the magnet casing containing permanent magnet blocks shown from a top view.	58
4.6	Front, top and side view of the magnet casing containing permanent magnets.	58
4.7	Two possible orientations for the permanent magnets, where the pole facing the front plate is used as a reference to describe the polarity of the magnet.	59
4.8	Magnet is inserted into an empty rotor via the slots.	60
4.9	Top view of slots filled with magnets in the outer rotor.	60
4.10	Section view of the outer rotor with north pole magnets being inserted.	61
4.11	Section view of the outer rotor filled with north pole magnets and the last magnet being inserted.	61
4.12	Section view of the outer rotor that is completely filled with magnets.	62
4.13	Illustration of how the magnets are lifted up against a conical shape and collected by a fibre covered magnetic plate	64
4.14	Induction heating through copper wires wrapped around a U shaped core.	65
4.15	Basic diagram of the induction heating principle (RF Heating Consult, 2022)	66
4.16	Local thermal demagnetisation through induction heating	69
4.17	Top view of local thermal demagnetisation through induction heating	70
4.18	Thermal demagnetisation of multiple magnets by utilising multiple cores for induction.	71
4.19	Alternative orientation for the core on the magnets	72
4.20	Diagram of how the heat transfer was calculated.	74
4.21	Illustration of how the heat transfer was calculated in relation to the actual core concept and the corresponding geometry.	75

4.22 Plot of how the power required for heating varies with time taken to heat.	78
4.23 Plot of how the power required for heating varies with the time taken for different conductor materials with different conversion efficiencies.	79
4.24 Plot of the power required for different Curie temperatures.	80
4.25 Illustration of the different height of the conductor.	81
4.26 Plot of the power required for different contact surface areas of the conductor with the magnet with a constant mass.	81
4.27 Plot of the power required for different contact surface areas of the conductor with the magnet with a varying mass.	82
5.1 Induction heating combined with an opposite magnetic field through two sets of copper wires wrapped around a U shaped core.	89
5.2 Direct induction heating by placing coils near the permanent magnet.	90
5.3 Overview of the preferred recycling route for permanent magnets from OWTs.	92
5.4 Induction heating through copper wires wrapped around a U shaped core.	93
5.5 Thermal demagnetisation of multiple magnets by utilising multiple cores for induction.	94
5.6 Core rotated 90° to contact two magnets in the same column.	94

List of Tables

- 1.1 Overview of the different parts and components that can be found in an OWT and their description based on (BVG Associates, 2019) 3
- 1.2 Estimation of materials used in a an 11MW WTG based on data from (Arrobas et al., 2017) 5
- 1.3 Materials and masses per component a for a Vestas 9.5MW, Siemens 11MW and GE 15MW OWT respectively, adapted from (BVG Associates, 2019; Garcia-Teruel et al., 2022) and SGRE 5
- 1.4 Overview of the 6 main categories for e-waste according to (European WEEE registers network, 2018; Forti et al., 2020) along with examples from OWTs based on insights provided by CrossWind/SGRE 9
- 1.5 Hazardous substances found in WEEE compiled from (Ilankoon et al., 2018; Kaya, 2016), where * indicates sources of hazardous materials that may also be found in OWTs. 11
- 1.6 Overview of REEs and their common uses, the non-lanthanide REEs, LREEs and HREEs are indicated in light yellow and dark yellow shading respectively (Izatt, 2016; Jowitt et al., 2018; Omodara et al., 2019; Popov et al., 2021; Ramprasad et al., 2022) 12
- 1.7 Summary of the four different types of recycling according to (Kumar, 2021; Nijkerk et al., 2001) 14
- 1.8 Overview of the different recycling options for magnets (Jin et al., 2018; Yang et al., 2017) 15

- 2.1 Overview of the 14 people consulted/interviewed for data collection. 22

- 3.1 Reported compositions of NdFeB permanent magnets and magnet swarf (Tunsu, 2018) 30
- 3.2 REEs used in different types of generator based on Li et al. (2022) 31
- 3.3 Applications of NdFeB magnets according to (Tunsu, 2018) 32

3.4	Estimated global in-use stocks for the rare-earth elements in NdFeB permanent magnets in 2007 (Du and Graedel, 2011)	33
3.5	Possible quantities of Nd-Fe-B magnet that can be collected from different electronic waste streams at the Halmstad plant owned by Stena (Lixandru et al., 2017)	33
3.6	Overview of the different properties of permanent magnets and approximate ranges for the properties of sintered NdFeB magnets at 20°C based on company websites from various sources (Neorem magnets, Magnet source, Advanced magnet source, Arnold Magnetics, Ee-magnetstuk, Eclipse Magnetics)	36
3.7	Summary of the three types of disassembly (Desai and Mital, 2003; Marconi et al., 2018; Tao et al., 2018)	38
3.8	Overview of the different types of size reduction and the technologies that can be used (Kaya, 2016; Tabelin et al., 2021)	40
3.9	Overview of the different types of materials separation and the technologies that can be used (Ambaye et al., 2020; Cui and Forssberg, 2003; Guo et al., 2016; Kasper et al., 2015; Thompson et al., 2021)	41
3.10	Overview of the different types of metallurgical recycling technologies that can be used (Kasper et al., 2015; Tabelin et al., 2021)	42
3.11	Main principles of magnetism	48
3.12	Overview of the comparison between recycling WEEE and OWT permanent magnets .	53
4.1	Assumed values for the properties of CW OWT permanent magnets and conductor materials based on (Bahl et al., 2020; Dallos, 2019; Kreith et al., 2010; Rudnev et al., 2017)	76
4.2	Approximated geometry of the permanent magnet, casing and conductor	76
4.3	Temperature calculated at different points the the material corresponding to Figure 4.20	77
4.4	Power required for different heating times of the permanent magnet and conductor . .	78
4.5	Power requirements for different Curie temperatures	80
4.6	Overview of the comparison between recycling WEEE and OWT permanent magnets .	84

Introduction

Wind energy is one of the fastest-growing sources of renewable energy and plays a critical role in achieving the energy transition to combat climate change (Bonou et al., 2016; Saraswati, 2020; Tazi et al., 2019; Tota-Maharaj and McMahon, 2021). Since 2010, the offshore wind sector has grown by nearly 30% per year, with an estimated capacity growth of up to 450 GW by 2050 in Europe (Caglayan et al., 2019; Hernandez C et al., 2021). To meet the rising demand, offshore wind turbines (OWTs) have increased in size throughout their development, driven by the need to reduce the Levelised Cost of Energy (LCOE).

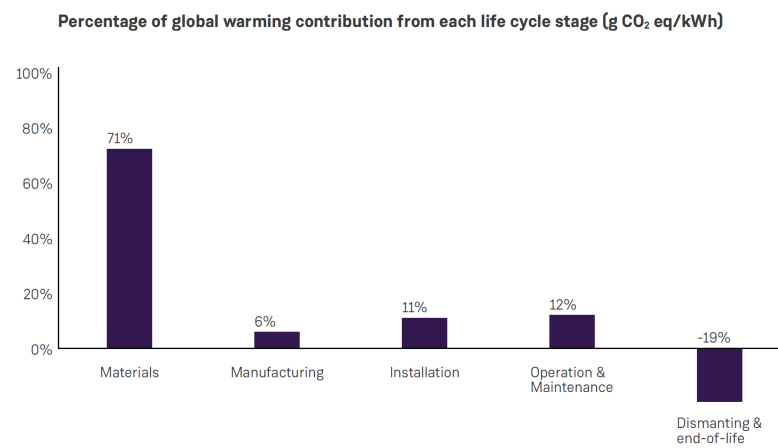


Figure 1.1: Percentage of global warming contribution from each life cycle stage (gCO₂eq/kWh) (Siemens Gamesa, 2014)

The increasing number and size of OWTs will necessitate a substantial quantity of materials. Their extraction is the main contributor to global warming through an OWT's life cycle, as shown in Figure 1.1, which has also been corroborated in various studies (Hernandez C et al., 2021; Jensen et al., 2020; Möller et al., 2012; Yang et al., 2018). Moreover, renewable energy systems, such as wind, also impact the demand and availability of critical raw materials (CRMs) which include various groups of materials such as rare earth elements (REEs), platinum group metals (PGMs) and

precious metals (Farina and Anctil, 2022; Kim et al., 2015).

After 20-40 years of service life, offshore wind turbines typically reach their End-of-Service Life (EoSL) or End-of-Life (EoL) (Ortegon et al., 2013). To ensure there are sufficient resources to meet the rising demand and reduce the environmental impacts of offshore wind turbines, it is important to manage the waste and material flows at their EoL (Jensen and Remmen, 2017; Tazi et al., 2019; Wang et al., 2019). The extraction of raw materials could be significantly reduced if the components and their materials are reused and recycled effectively (Harivardhini et al., 2017; Jensen et al., 2020; Johnson et al., 2007).

Within the OWTs, the nacelle, which is part of the wind turbine generator (WTG), is where the vast majority of the electrical components such as the transformer, converter and generator are located. These components have been found to contain the most valuable materials due to the presence of large quantities of CRMs, including REEs such as Neodymium (Nd), Praseodymium (Pr) and Dysprosium (Dy) among other materials such as Copper (Cu), Nickle (Ni) and Molybdenum (Mo). Therefore this study will focus on the electric components in the nacelle of the WTG.

1.1 | Offshore Wind Turbines

Offshore wind turbines (OWTs) are large industrial products, which can be perceived as either a large piece of machinery or equipment, that converts offshore wind energy into electricity. This electricity is then transferred back to shore via a transformer platform and a grid connection. When multiple OWTs are placed together they create an offshore wind farm (OWF). These OWTs are linked to the grid via cables to a substation which enables energy transfer back to shore.

OWT Components

OWTs are generally split up into two main sections, the wind turbine generator (WTG) and the balance of plant (BoP). The WTG is comprised of components above the water, whereas the BoP consists of infrastructure that supports the WTG, mostly below the water. Figure 1.2 depicts the different components for a monopile type offshore wind turbine, where the components above water in white and remaining components below water correspond to the

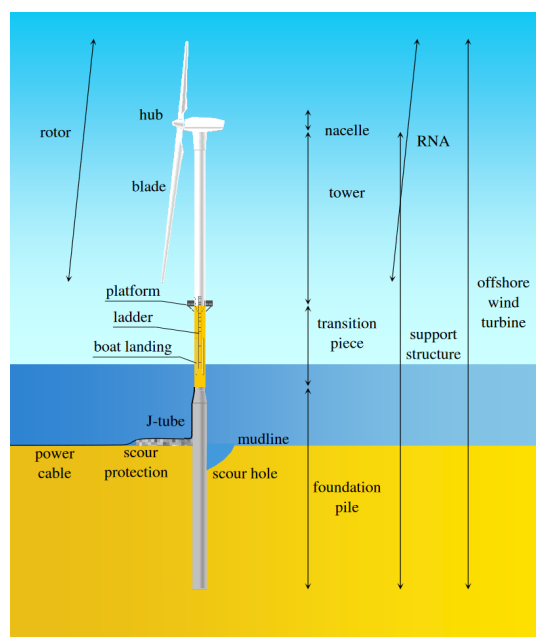


Figure 1.2: Overview of the CrossWind wind turbines' main parts and components (van der Tempel, 2006)

WTG and BoP respectively.

An OWT is constructed of around 25,000 components, of which the three main components of the WTG are the nacelle, tower, and rotor and of the BoP are the platform, foundation, and cabling (Carrara et al., 2020). A more detailed overview of the parts and components of the WTG along with their function and supplementary details is shown in Table 1.1.

Part	Components	Description	Details (approx.)
WTG			
Rotor	Extracts & converts kinetic to rotational energy in the drive chain		Diameter 170-200m, £1.7m
	Blades	Captures & transfers kinetic energy to mechanical torque & speeds in generator	90m long, 6m wide, £1.3m
	Blades bearings	Enable adjustment of pitch angle of blade to control OWT power output	4 point contact ball bearings, 4m diameter rings, £200,000
	Hub	Connects blades to main shaft & transfers loads from blades to generator	£150,000
	Pitch system	Rotate blades to the desired position using a pump station, hydraulic hub assembly, pitch cylinders & auxiliary systems	Utilises oils, cooling system and accumulators
Nacelle	Supports the rotor and transfers loads from generator to tower, carries yaw system and electrical drive chain		20-25m long, 9-12m wide, 7-9m high, £4m
	Cover	Provides waterproof protection, support & access to internal & external components	20t, £100,000
	Main shaft	Extracts & converts kinetic to rotational energy in the drive train, transfers torque from rotor to the generator	£200,000
	Main bearing	Supports rotor, transfers part of the rotor loading to bedplate	£200,000
	Bedplate	Main structural component, supports the drive train & other components	£200,000
	Generator	Converts mechanical torque from rotating hub & blades to electrical energy	Max. 810V, output up to 9400 kW, >£2m
	Yaw system	Orients the nacelle in the wind direction (upwind) while operating to optimise power production	10 yaw motors (1t, 690VAC), gearboxes, 10 yaw brakes, sensors £170,000
	Yaw bearings	Connects the nacelle & tower, yaw system orients nacelle in desired direction	4 point contact ball bearings, 6m diameter rings, 10t, £70,000
	Power electronics	Adjusts voltage & frequency of energy from generator for transfer to OWF electricity distribution system	Cabling, switch gear, transformer and converter, £700,000
	Transformer	Links OWT to the grid, steps up low output voltage from generator to higher distribution voltage level	Transforms 0.69-3.3kV to 33-66kV
	Converter	Keeps the output current and frequency of turbines consistent with the grid	
Tower	Tubular steel structure, supports nacelle & transfers loads to foundation		100-110m height, 5-6m top & 7-8m base diameter, £700,000
BoP			
Monopile	Supports the WTG, transfers loads from tower to seabed		40m depth, 10m diameter, 120m length

Table 1.1: Overview of the different parts and components that can be found in an OWT and their description based on (BVG Associates, 2019)

The different types of offshore wind turbines can be distinguished by their foundation or rotor type, number of blades or power generation system. These types will vary depending on the preferences of the wind park owner as well as the location and conditions of the offshore wind

farm (Hernandez C et al., 2021; Jensen et al., 2020; Smith et al., 2015).

78% of the offshore wind energy sector in Europe are being built with monopile foundations, made of predominantly steel and concrete (Topham et al., 2019). Since monopiles are relatively simple in terms of their materials and construction as can be seen in Table 1.1, these are not interesting to study from a material perspective. Therefore the remainder of this study will focus on the WTG part of an OWT.

The main parts of an WTG are the rotor, nacelle and tower, which are configured as shown in Figure 1.3. The blades are connected to the hub through blade bearings, which allow the pitch system to pitch the blades, collectively making up the rotor. The nacelle consists of the generator which connects the hub and the nacelle via a main bearing that allows the rotor to rotate. An additional yaw system connects the nacelle to the tower, which allows the nacelle to rotate relative to the tower.

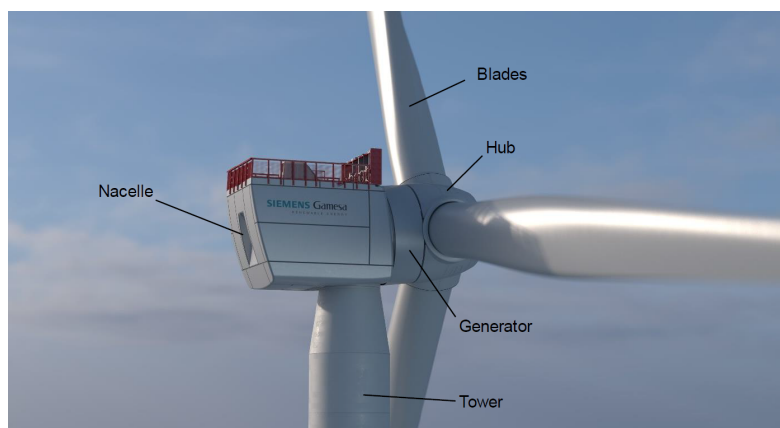


Figure 1.3: Image of the top of an SG 11.0-200DD which shows the rotor nacelle assembly (RN or RNA) obtained from CrossWind/SGRE

An offshore wind turbine will contain several electric and electronic parts and components, such as transformers, converters, cables, generator and motors in order to function. Although it serves as a piece of electrical equipment, it is not formally recognised as WEEE once it reaches its EoL. This will be discussed in more detail in Section 1.2.

OWT Materials

An OWT uses a diverse range of materials, where Table 1.2 provides an overview of the materials used in an OWT based on data from Arrobas et al. (2017), which was extrapolated to determine the quantity of materials for an 11MW turbine. This was compared to data found online on a 9.5MW and 15MW reference turbine in Table 1.3

The global warming contribution, measured in CO₂eq, of the main components of an offshore wind power plant and the contribution per material group in the wind power plant are depicted in

Metal	[kg/MW]	[%]	Mass [t]
Aluminium	-	-	-
Boron	7	0.005	0.077
Chromium	902	0.601	9.922
Copper	3,000	1.998	33.000
Dysprosium	25	0.017	0.275
Iron (magnet)	455	0.303	5.005
Iron (cast)	23,900	15.918	262.900
Lead	-	-	-
Manganese	80.5	0.054	0.886
Molybdenum	136	0.091	1.496
Neodymium	186	0.124	2.046
Nickle	663	0.442	7.293
Praseodymium	35	0.023	0.385
Steel	115,000	76.592	1.265
Terbium	7	0.005	0.077
Zinc	5,750	3.830	63.250

Table 1.2: Estimation of materials used in a an 11MW WTG based on data from (Arrobas et al., 2017)

WTG	Component	Materials	9.5MW [%]	11MW [%]	15MW [%]
Rotor			15.63	19.40	10.42
Blades			9.22	9.59	10.42
	Blades	Glassfibre reinforced plastic, epoxy resin	9.22	9.47	10.42
	Bolts	M30 or M26 grade 10.9 bolts	-	0.12	-
Hub			6.40	9.81	10.12
	Machined hub	Low alloy steel, cast iron	6.40	4.24	10.12
	Blade bearings	Cast iron, rings (42CrMo4), balls (100Cr6)	-	0.65	-
	HPU		-	0.21	-
	Spinner		-	0.26	-
	Others		-	4.45	-
Nacelle			29.13	25.19	33.63
Back-end			15.69	10.26	12.56
	Casted bedframe	Cast iron (ENGJS40018ULT), 355 grade steel	2.37	3.32	3.75
	Yaw system	Low alloy steel, rings, balls	3.37	1.37	5.33
	Cover	Glassfibre reinforced plastic, epoxy resin	0.38	1.01	0.61
	Transformer		1.60	2.22	1.81
	Converters		-	1.04	0.85
	Read end structure		7.75	0.96	0.21
	Others		-	0.33	-
Generator			13.43	14.94	21.07
	Fixed shaft	High grade steel	0.53	1.74	0.84
	Main bearing	Steel	0.27	1.39	0.42
	Segments	Iron, copper, magnets	5.95	4.46	11.41
	Rotor housing	Reinforcing steel	6.68	2.68	8.38
	Brake system		-	1.46	-
	Others		-	3.21	0.02
Tower			55.25	55.41	45.83
Structure		Low alloy steel, concrete	55.25	53.02	45.83
Flanges			-	2.39	-

Table 1.3: Materials and masses per component a for a Vestas 9.5MW, Siemens 11MW and GE 15MW OWT respectively, adapted from (BVG Associates, 2019; Garcia-Teruel et al., 2022) and SGRE

Figure 1.4 and Figure 1.5 respectively. These numbers are based on the absolute quantities of materials and are not relative to the size of component or value of the specific material constituents.

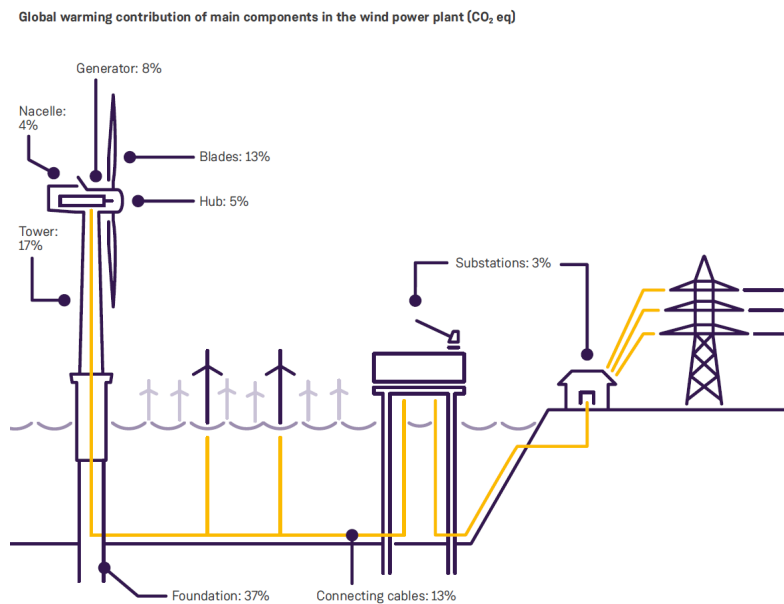


Figure 1.4: Global warming contribution of main components in the wind power plant (CO₂eq) (Siemens Gamesa, 2014)

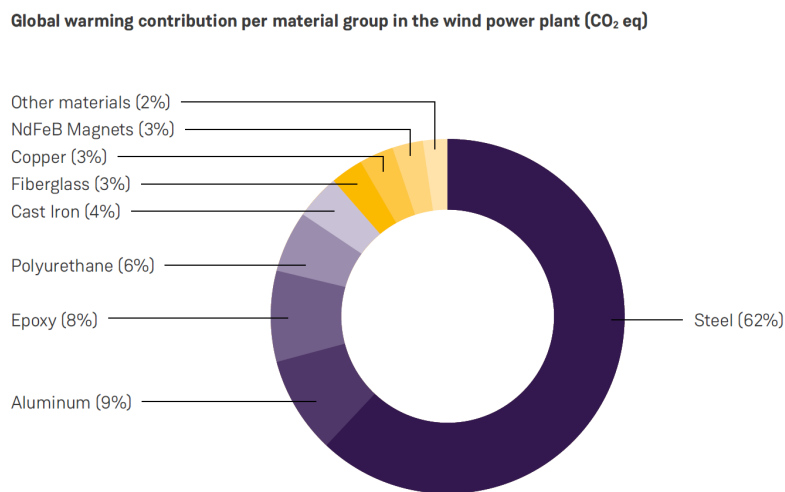


Figure 1.5: Global warming contribution per material group in the wind power plant (CO₂ eq) (Siemens Gamesa, 2014)

Steel has a global warming contribution of 62% and is therefore the main contributor at a material level, as shown in Figure 1.5. On the other hand, the tower and foundation contribute 17% and 37% to global warming at a component level, as seen in Figure 1.4. The impact of steel is related to the fact that the tower and foundation are two of the largest components, by weight, of an offshore wind turbine, which are made up of mostly steel. Furthermore, steel is also a material that is relatively easy to recycle at a high grade due to the maturity of the steel production industry.

When the steel parts in Figure 1.4 and 1.5 are neglected, it can be seen that the blades and

the corresponding epoxy and fibreglass as well as the generator and the NdFeB magnets become prevalent. In the past, studies into the environmental impacts of OWTs have often concluded that the blades made of fibreglass composites, are the major problem as shown in Figure 1.6. As such, recycling studies on OWTs have focused on the blades and composite materials rather than the retrieval of valuable materials and dismantling.

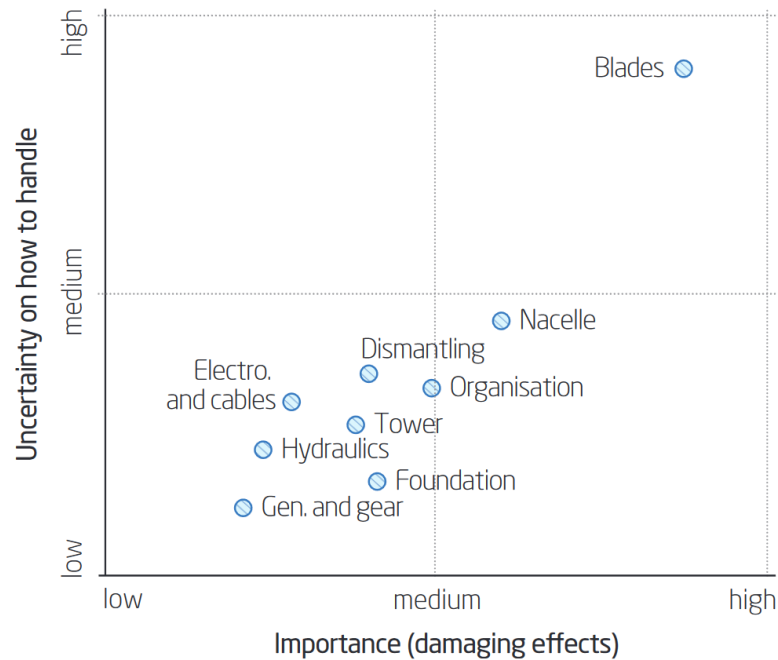


Figure 1.6: Assessment of the environmental impact and uncertainties involved in dismantling, recycling and disposing of wind turbines and their components (Andersen et al., 2014)

While a lot of research has been done into the recyclability of blades, not a lot is known about the recycling of REEs from OWTs. Moreover, based on the recycling rates calculated by Andersen et al. (2014), the electronic components of offshore wind turbines have the lowest recycling rate, where 50% is treated as waste. In addition, studies in the past have not accounted for the increased use of rare earth materials in newer turbines.

Seeing as NdFeB magnets are responsible for 3% of the impact based on Figure 1.5, it is important to know more about how to recycle and recover the magnets and REEs. Therefore, the recovery of NdFeB permanent magnets from direct drive OWTs will be the focus of this study.

1.2 | Waste Electronic and Electric Equipment

WEEE, Waste Electronic and Electric Equipment, otherwise known as electronic waste (e-waste), is defined as “a term used to cover items of all types of electronic and electric equipment (EEE) and its parts that have been discarded by the owner without the intention of reuse” (United Na-

tions Environmental Program, 2018). WEEEs are characterised by their material complexity, which in combination with the presence of hazardous materials can make it difficult to recycle WEEE. To recover the valuable resources from WEEE, a proper waste management strategy is required (Evangelopoulos et al., 2019; Hicks et al., 2005; Pérez-Belis et al., 2015; Vanegas et al., 2018).

OWTs are also known to contain various electronic components such as converters, transformers, generators and motors as mentioned in Section 1.1. While there is little experience in the recycling of OWTs, the recycling of WEEE is well established. As such, this study explores what the offshore wind industry can learn from the recycling of WEEE. This is done by looking at the differences and similarities from a materials perspective, as well as in their processing.

WEEE Classification

The tremendous speed of technological development has led to an exponential growth in the production of WEEE. To contribute to sustainable consumption and production and address the environmental issues related to the rapid growth of discarded electronics, the European Commission introduced the WEEE directive. The directive includes equipment that is used for the generation, transfer or measurement of the currents and field and is limited to equipment designed for use with a voltage rating of up to 1,500 volts or 1,000 volts for alternating and direct currents respectively (European Commission, 2021; Forti et al., 2020).

Not all EEE becomes WEEE at their EoL after it has been discarded. Products that meet specific conditions are excluded from WEEE categories and thus also exempted from the WEEE directive. Examples of exemptions are equipment designed to be sent into space, large scale stationary industrial tools, large, fixed scale installations, equipment designed for research and development and so on. In addition, WEEE also does not include batteries, accumulators, or electrical components of vehicles (Forti et al., 2020).

Since EEE and WEEE are comprised of a wide variety of products, they have been categorised into 54 different product-centric categories, which are sorted into 6 general categories: temperature exchange equipment, screens and monitors, lamps, large equipment, small equipment and small IT and telecommunications equipment. The definitions and examples for the EEE categories that are covered by the WEEE directive are shown in Table 1.4.

Some WEEE components in OWTs are officially classified as WEEE and others are not, dependent on if they meet the criteria of the WEEE Directive. If those components have not been specifically tailored to the large industrial product, such as lighting, switches and sensors, they will fall under the Directive. The larger components such as the generator, converter and transformer, have been designed specifically for OWTs and therefore are not officially WEEE.

It is important to note, that while the European Commission strove to homogenise discrepant definitions and classifications of WEEE, this is not necessarily upheld in practice. There are various organisations and documents that scrutinise the directive for inconsistencies and the European Commission is constantly making amendments the directive to cover any misinterpretations.

Category	Definition	WEEE examples	OWT examples
1 Temperature exchange equipment	EEE with internal circuits where substances other than water are used for cooling, heating or dehumidifying	Cooling and freezing equipment such as refrigerators, freezers, air conditioners and heat pumps	12 50hz coolers in the generator, 3 dehumidifiers, passive and active cooling system (ventilators) on site
2 Screens and monitors	EEE intended to provide images and information on an electronic display regardless of its dimensions	Televisions, monitors, laptops, notebooks, and tablets	Various control panels in the nacelle may contain screens
3 Lamps	Replaceable electronic devices that produce light from electricity and may have other functions	Fluorescent lamps, high discharge lamps and LED lamps	Lighting systems inside the nacelle, lighting on top of wind turbine
4 Large equipment	EEE that doesn't belong to categories 1, 2 or 3, with any external dimensions over 50cm	Washing machines, clothing dryers, dishwashers, electric stoves	Palfinger lifting robot, electric vehicle that drives into blade for inspection, generator, transformer, converter
5 Small equipment	EEE that does not belong to categories 1, 2, 3, 4 or 6, with no external dimensions exceeding 50cm	Vacuum cleaners, microwaves, calculators, video cameras	Many sensors (temperature, humidity, pressure, smoke etc.)
6 Small IT and telecommunications equipment	Information equipment that can be used to the collection, transmission, processing, storage and showing of information. Telecommunication equipment is designed to transmit signals electronically over a certain distance	Mobile phones, routers, printers, Global Positioning System (GPS) devices	3 cabinets that contain many wires and motherboards for data storage and processing

Table 1.4: Overview of the 6 main categories for e-waste according to (European WEEE registers network, 2018; Forti et al., 2020) along with examples from OWTs based on insights provided by CrossWind/SGRE

The WEEE directive states that electronics not tailored the specific application and products containing batteries should fall under WEEE. However, electric vehicles and batteries have their own directives, such that their electric components do not fall under WEEE, which may cause confusion in the scope of WEEE. Another example to elucidate confusion is that while all lighting equipment falls under the directive, a filament bulbs are excluded.

Materials in WEEE

WEEE is a non-homogenous complex mixture of materials that can contain up to 100 different substances, where the composition varies depending on the functionality and design (Shittu et al., 2021). The material constituents of WEEE can be grouped into 5 main categories: ferrous metals, non-ferrous metals, glass, plastics and other (Liu et al., 2019). Figure 1.7 shows the different material compositions in WEEE, where it is clear that metals make up a large majority (approximately 60%), followed by plastics and other constituents (Ibanescu et al., 2018).

An overview of the different elements that can be found in WEEE based on the periodic table is given in Figure 1.8. These include critical and non-critical materials such as platinum group metals (PGMs), Rare Earth Elements (REEs) and precious metals Murugappan and Karthikeyan. The presence and importance of these materials, which are critical for WEEE, make WEEE an interesting source for material recovery.

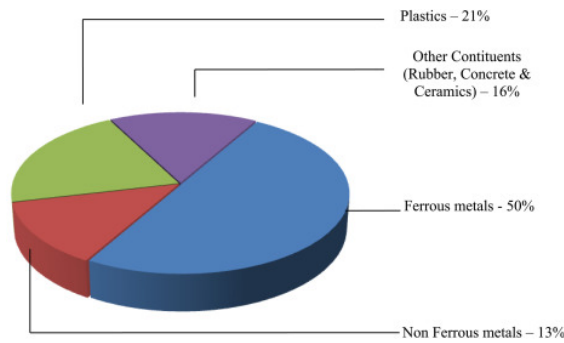


Figure 1.7: Different material compositions in WEEE (Murugappan and Karthikeyan, 2021)

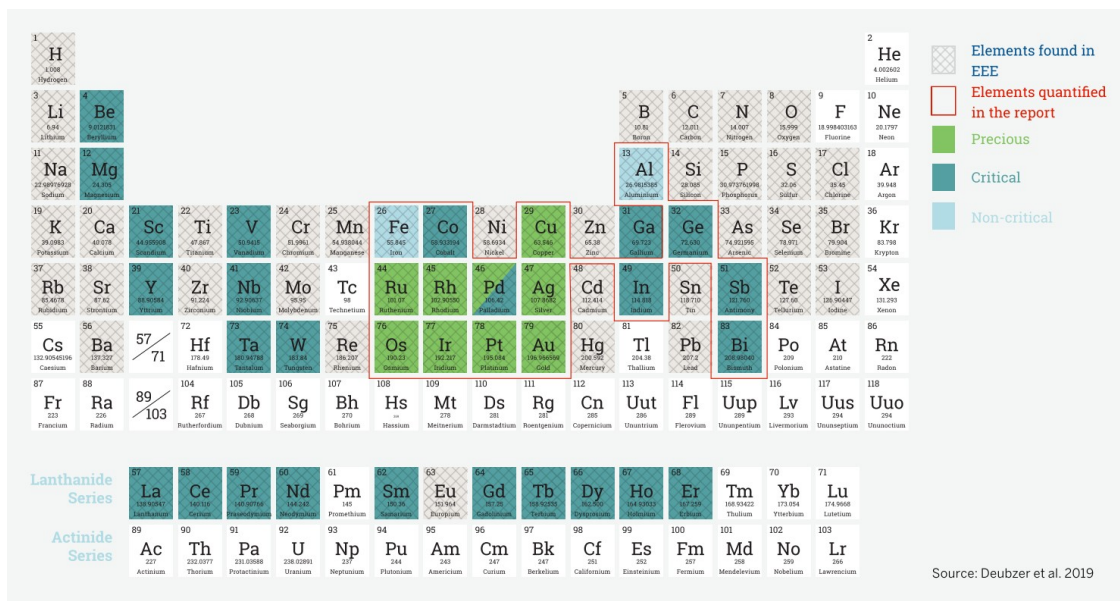


Figure 1.8: The periodic table with an overview of the elements found in WEEE, precious metals are indicated in green, critical raw materials are shown in teal (Forti et al., 2020)

WEEE can contain a mixture of hazardous and non-hazardous materials that require special handling and recycling processes to avoid negative environmental and health related impacts. Examples of hazardous materials include the presence of heavy metals such as lead (Pb), nickel (Ni), cadmium (Cd), mercury (Hg), arsenic (As), selenium (Se), hexavalent chromium (Cr(VI)), and brominated flame retardants (BFRs), polybrominated diphenyl ethers (PBDEs) beyond the threshold quantities (Murugappan and Karthikeyan, 2021). An overview of sources of hazardous materials can be found in Table 1.5, where some elements by themselves, such as Zn and Pb, are not hazardous but their applications are.

Many of the hazardous materials found in WEEE can also be found in OWT components, which are indicated in Table 1.5. This is due to the presence of WEEE-like (sub)components in the OWTs, as shown in Table 1.4, which demonstrates overlaps in WEEE components and similar OWT com-

Substance		Sources
Lead	Pb	CRTs, television sets, monitors, batteries, printed circuit boards*, light bulbs*, lamps*
Cadmium	Cd	Ni-Cd batteries, contacts and switches*, semiconductor chips
Mercury	Hg	Lighting devices for flat screen displays, CRTs, PCBs, thermostats*
Chromium or hexavalent chromium compounds		Metal housing (anti-corrosion coatings)*, data tapes, floppy disks
Nickel	Ni	Ni-Cd batteries, electron gun in CRTs
POPs including BFRs		Circuit boards (fire retardants for electronic equipment)*, plastic casings for computers*, cables*, dielectric fluids in capacitors and transformers*, lubricants and coolants in generators*, fluorescent lighting*, electric motors*, connectors*
Lithium	Li	Li batteries
Barium	Ba	CRTs, fluorescent lamps*
Zinc	Zn	CRTs, metal coatings*, batteries
PVC		Insulation on wires and cables*
Beryllium	Be	Power supply boxes*, computers, ceramic components of electronics
Arsenic	As	Gallium arsenide in LEDs*
Americum	Am	Smoke detectors*
Antimony	Sb	Flame retardants in plastics*
Chlorofluoro carbon		Cooling units*, insulation foams*
Polychlorinated biphenyls		Condensers, transformers*
PBDEs, PBBs		Flame retardants in plastics*

Table 1.5: Hazardous substances found in WEEE compiled from (Ilankoon et al., 2018; Kaya, 2016), where * indicates sources of hazardous materials that may also be found in OWTs.

ponents. Although some of the WEEE components do not officially fall under the WEEE directive, they are still exposed to the same hazardous materials. This is important to take into account during their handling and processing.

WEEEs are also known to contain a high content of REEs, which are high in demand and have been classified by the European Commission as Critical Raw Materials (CRMs) due to their supply risk as can be seen in Figure 1.8 (Amato et al., 2019; Yang et al., 2017). Due to the common usage of REEs in high technology (i.e. electronic equipment), WEEE is seen as a valuable source for the recovery and recycling of REEs. However, only 1% of the REE content from EoL products is recycled (Ambaye et al., 2020). Since Nd was also shown to be a major contributor to global warming for OWTs, where they are predominantly found in permanent magnets, this study will dive further into the use of REEs in WEEEs and the overlaps with OWTs.

REEs in WEEE

Rare Earth Elements (REEs) are a group of 17 chemical elements with similar properties, shown in Table 1.6. They are valued for their special properties that make them increasingly important in the technological advancement of the electronics industry, such as luminescence and magnetism (Ni'am et al., 2019; Williams, 2016).

Although they are abundant in nature, they are rare because they occur together in nature and possess similar trivalent oxidation states (Omodara et al., 2019). The main challenge with regard to

Rare Earth Elements		
Element	Name	Applications
Sc	scandium	Alloys in aerospace engineering, magnets, phosphors, fuel cells, batteries
Y	yttrium	Lasers, superconductors, microwave filters, lighting (low energy lightbulbs, carbon arc), flatscreen TVs, colour television cathode ray tubes, additives in alloys
Lanthanides		
La	lanthanum	Optics, batteries, catalysis, magnets, phosphors, additives in carbon arc lamps, electric welders, projectors
Ce	cerium	Chemical applications, colouring, catalytic converters in cars, phosphors
Pr	praseodymium	Magnets, lighting, optical amplifiers
Nd	neodymium	Magnets, lighting, lasers, optics, fuel cells, batteries, solar panels, electric vehicles
Pm	promethium	Paint, atomic batteries (limited use due to radioactivity and very rare in nature)
Sm	samarium	Magnets, lasers, masers, small motors, headphones, high-end magnetic pickings for guitars and musical instruments, aircraft engine alloys, sports goods
Eu	europium	Lasers, colour TV, lighting, medical application, phosphors, fluorescent glass and lamps, optoelectronic devices
Gd	gadolinium	Magnets, glassware, lasers, X-ray generation, computer and medical applications, television screens
Tb	terbium	Lasers, lighting
Dy	dysprosium	Magnets, lasers, compact fluorescent bulbs, batteries, fuel cells, phosphors
Ho	holmium	Lasers, magnets, microwave equipment
Er	erbium	Lasers, steelmaking, fibre amplifiers in optical communications
Tm	thulium	X-ray generation, high temperature superconductors, lasers
Yb	ytterbium	Doping material in lasers and amplifiers, chemical industry applications
Lu	lutetium	Medical, chemical industry applications, phosphors

Table 1.6: Overview of REEs and their common uses, the non-lanthanide REEs, LREEs and HREEs are indicated in light yellow and dark yellow shading respectively (Izatt, 2016; Jowitt et al., 2018; Omodara et al., 2019; Popov et al., 2021; Ramprasad et al., 2022)

REEs is the extraction and processing due to their widespread geographic distribution and the associated environmental impacts (Williams, 2016). Due to the rising demand for REEs in electronics applications, the recovery and recycling of these materials is becoming increasingly important.

The lanthanide REEs are divided into either lighter rare earth elements (LREEs) or heavier rare earth elements (HREES), based on their electronic configuration (Swain and Mishra, 2019). HREES are elements with an atomic number range from 57 to 63, La and Eu respectively, whereas LREEs are elements with an atomic number range from 64 to 71, Gd and Lu respectively, as well as Sc and Y (Ramprasad et al., 2022). The configuration of the valence electrons of the outermost shell of the lanthanide atoms is the same, while their 4f orbitals are filled progressively with increasing atomic number. As a result of the screening of the 4f orbitals, the elements have extremely similar physical and chemical properties (Jowitt et al., 2018).

The unique electronic structure gives REEs unique electronic, optic, magnetic and conductive properties that are highly desirable for a broad range of technological applications (Ni'am et al., 2019; Ramprasad et al., 2022). Approximately 26.3% of all REEs are used in the production of electronic components such as magnets, batteries, glass and alloys which are needed to manufacture modern computers, lasers and screens, where Table 1.6 gives a few examples (Amato et al., 2019; Jowitt et al., 2018; Omodara et al., 2019).

According to Sprecher et al. (2014) and (Peelman et al., 2018), permanent magnets are the single largest application of REEs, accounting for 21% of the production of REEs by volume and

generating 37% of the total value of the REE market (Ni'am et al., 2019; Nlebedim and King, 2018). Since permanent magnets play a major role in both WEEEs and OWTs, this study will dive further into the use of permanent magnets in WEEE and OWTs and how the REEs can be recovered from them through recycling.

1.3 | Recycling

Recycling is defined as the reprocessing of recovered materials at a product's EoL, returning it into the value chain. The aim of recycling is to conserve raw materials by maximising the value retention of the materials contained in a product in either its component or material form (Chen et al., 1994; Muthu et al., 2012; Nelen et al., 2014; Sabaghi et al., 2015; Tanskanen, 2013; WBCSD, 2019). The recycled material may be referred to as a "secondary" material, as opposed to a "primary" material that is extracted from the environment (Worrell and Reuter, 2014).

To clarify the scope of this study, it is important to distinguish the difference between recycling and recovery, which are often used interchangeably and inconsistently throughout literature. The recycling process encompasses the entire cycle of the material from new to old and old to new (Kumar, 2021; Nijkerk et al., 2001). Recovery is a process within recycling in which the materials are retrieved from waste through sorting and separation. After the recovered materials have been processed and refined, the recovered materials can be recycled to produce new products.

The distinction between the recycling and recovery process is shown in Figure 1.9. In the case of an EoL plastic bottle as an example, the recycling process includes the collection of EoL bottles to the production of a new bottle using the materials recovered from the EoL plastic bottle, the recycled product made of secondary materials. The recovery process is limited to the processing of the collected materials to recover a secondary material, which can be used to produce the recycled product.

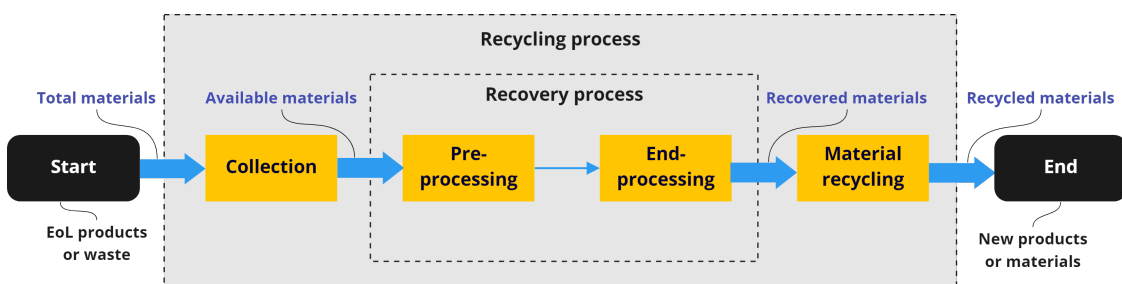


Figure 1.9: Overview of the material recycling and recovery process

The recovery process consists of two main phases, the pre-processing and end-processing phase. The former refers to the initial disassembly and depollution of the product, in which all the hazardous and valuable components are removed, followed by sorting, size reduction and separation. The latter refers to the refining of the materials once they have been sufficiently

separated, such that the recovered material can be used to produce a new product in the recycling process, which is called material recycling (Sethurajan et al., 2019).

Efficient disassembly techniques are needed for material recovery and recycling technologies to benefit from economies of scale and improve the recovery grade (Li et al., 2015; Rademaker et al., 2013). This is because the quality of the recycled and recovered material is highly dependent on the degree of separation of the material. Improved disassembly could enable better separation and thus increase the value of the recovered or recycled material, while reducing refining time and costs (Pan et al., 2022).

The scope of this study will focus on the recovery process, where the aim is to produce the highest possible quality secondary material such that it can be used to produce a recycled product. Depending on the state of the waste product at its EoL, there are four possible options for recycling which have been summarised in Table 1.7. Primary recycling is the most preferred option from a value retention perspective, followed by secondary, tertiary and quaternary as least favourable. However, in practice decisions are often based on economic and technical feasibility.

Primary recycling	Reprocessing to form the original material or a comparable quality level
Secondary recycling	Reprocessing to form a different product at a lower quality level, often mechanically.
Tertiary recycling	Thermal or chemical decomposition of materials, often chemically
Quaternary recycling	Recovery of energy through incineration

Table 1.7: Summary of the four different types of recycling according to (Kumar, 2021; Nijkerk et al., 2001)

In the case of permanent magnet recycling, there are four options: direct reuse, magnet to magnet, waste to alloy and waste to element, these are described in Table 1.8 and shown in Figure 1.10. By recovering the REEs from permanent magnets, the dependence on virgin production (primary materials) can be reduced which will help overcome supply issues related to the extraction of REEs. The preferred recycling method used will depend on technical and economical feasibility, while taking environmental impacts into account.

Due to the rapid development of the offshore wind sector, the continuous changes in technology, size and capacity of the OWTs would suggest that direct reuse is improbable. This is because each OWF has its own design specifications and would require a different properties. Moreover, academia as well as the industry are looking to reduce the quantity of REEs used in permanent magnets and develop new technologies that are not reliant on permanent magnets.

From an environmental and economic perspective, magnet to magnet and waste to alloy would be the preferable and more realistic options for the recycling of permanent magnets from OWTs. Studies have shown that the environmental impact of using recycling magnets is tremendously lower than that of virgin magnets (Li et al., 2019b; Yang et al., 2017). There are variations within the recycling processes, where the shortest and simplest route would be magnet to magnet recycling followed by waste to alloy. In this case it is assumed that the shorter the route and the simpler

permanent magnets from OWTs to enable the effective recovery of REEs.

1.4 | Objectives

To meet the rising demand for offshore wind and address the consequent resource consumption and scarcity, it is important to take the recycling of OWTs into consideration such that valuable materials can be recovered. The NdFeB magnets found in the permanent magnet generator were identified as the most important to recycle due to the impact associated with their extraction. However, due to the recent introduction and relatively long life cycle of OWTs, there is little experience or knowledge on how to recycle permanent magnets from OWTs.

WEEEs have been identified as another important source of NdFeB permanent magnets, which have an established recycling industry and have been studied more extensively. OWTs contain many electrical components that, although they may not fall officially under the WEEE directive, may share many similarities with WEEE. The similarities and differences between permanent magnets found in WEEE and OWTs may provide new insights on how to recovery and recycle the REEs from OWTs.

To contribute to the improved recycling of permanent magnets from OWTs, disassembly was identified as a critical step that enables the recovery of materials and influences the quality of the recycled material. Irrespective of its importance, the disassembly of permanent magnets from OWTs has gained little attention in literature and therefore provides an interesting opportunity for research leading to the following research objective.

Research objective

How can permanent magnets be disassembled from OWT generators to facilitate an efficient recycling process for the effective recovery of REEs based on the established WEEE recycling system?

Due to the broad variety of OWTs available, where permanent magnet generator designs deviate per turbine, this study focused on a single offshore wind turbine, the SG 11.00-200DD direct drive OWT containing a permanent magnet generator. This will henceforth be referred to as the CW OWT. Data on the turbine was provided by the case company where possible. The case study is described in more detail in Section 1.4.2.

1.4.1 | Sub-objectives

To determine how to recover REEs from OWTs, the recovery process of NdFeB magnets from WEEE will be studied and analysed to discern how this might be translated for OWTs. This is therefore referred to as a "WEEE" approach to recovering REEs from OWTs. This objective consists of two sub-objectives. The first aimed to determine what the potential recycling routes are based on the established WEEE recycling system, and how this may be useful for the recycling of

permanent magnets from OWTs. The second followed up on the first sub-objective and identified options for disassembly based on the recycling routes.

Sub-objective 1

What is the preferred recycling route of OWT permanent magnets for effective recovery of REEs based on the established recycling route for permanent magnets from WEEE?

To meet the first sub-objective, different potential recycling routes for the recovery of REEs from permanent magnets were identified by studying existing WEEE recycling practices and adapting them to be applicable for OWT permanent magnets. These routes were then compared to determine which form of recycling, direct reuse, magnet to magnet, waste to alloy or waste to element, was preferable from an environmental and economic perspective.

This sub-objective provided an overview of the key similarities and differences between recycling process for permanent magnets from OWTs and WEEE. These were then used to determine which processes were transferable for OWTs and what aspects require additional considerations. To achieve this objective, information on the permanent magnets in OWTs was needed for comparison on permanent magnets from WEEE.

Sub-objective 2

How can the permanent magnet in the OWT be disassembled to enable the best recycling route?

The second sub-objective will use the outputs from the first sub-objective to determine in what state the permanent magnets should be disassembled and how this can be achieved. The factors identified from the recycling process that affect the disassembly of permanent magnets can be used as constraints for disassembly. This will be done by conducting an empirical observation and developing a theoretical concept as to how permanent magnets can be disassembled.

1.4.2 | Case study

This research is conducted in collaboration with CrossWind in the form of a graduate internship, with the intention to get a better understanding of how the OWTs may be recycled at their EoL. Additionally, this thesis is also supported by Siemens Gamesa Renewable Energies (SGRE), who are responsible for providing the WTG for the wind farm and are also interested in the topic of recycling OWTs. Both parties provide support in the form of knowledge and access to data relevant to the study.

CrossWind is a joint venture between Shell (80%) and Eneco (20%), based in Rotterdam, that will develop and operate a subsidy free offshore wind project in the Hollandse Kust Noord (HKN), located 18.5 km from the Dutch West coast near Egmond aan Zee as shown in Figure 1.11. Their aim is to have an operational wind farm of 759 MW by 2023, generating at least 3.3 TWh per year covering a surface area of 125 km² per year.



Figure 1.11: Overview of the CrossWind wind farm location and size (CrossWind, 2022)

For this wind farm they will install 69 wind turbines that each have a nominal power capacity of 11MW as shown in Figure 1.12. These OWTs with a monopile foundation will be placed at water depths between 15-28 m and have a hub height of 125.5 m. The rotor blades are 97 m long giving a diameter of 200 m, a swept area of 31,400 m² and can take wind speeds up to 9.57 m/s.

Although the wind farm is still in development, CrossWind is ambitious in their mission to innovate, by learning how decisions that are being made during development may affect recyclability in the future. Their incentive is to understand the EoL value of their wind farm when it reaches their EoL and what economic and environmental concerns may arise at the decommissioning stage. Additionally, they want to take these learnings back to their stakeholders for the development of future wind farm.

Due to the increasing importance the rising challenges around resource scarcity, SGRE has a demonstrated interest in studying the recycling of the materials. As the producer of WTGs, they have a business interest in recovering valuable materials, since the prices may fluctuate and rapidly increase as resources are exhausted. Opportunities for recycling may provide an interesting business case for EoL wind turbines.

The advantage of looking into this topic at an early stage is that information regarding the production and assembly process is currently easy to access. Experience in decommissioning oil

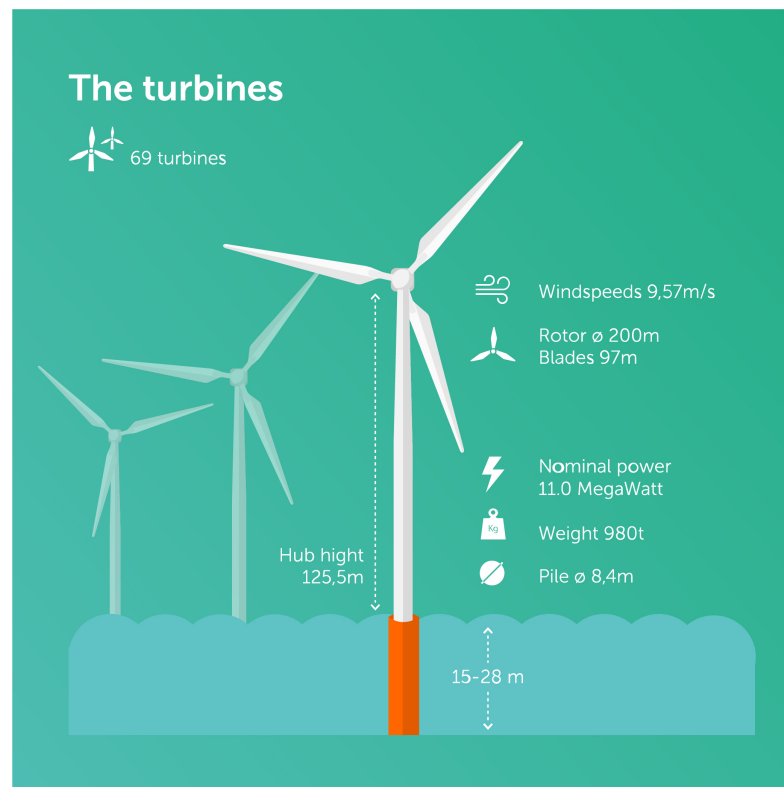


Figure 1.12: Overview of the CrossWind wind turbines' basic characteristics (CrossWind, 2022)

and gas has demonstrated that data quality throughout the life cycle of an offshore project is likely to decrease. Information may become incomplete and difficult to find because the park along with its data may be passed on from owner to owner, not be updated regularly and spread across various stakeholders.

Although information may still be available after the wind farm becomes operational, it may be more difficult to obtain supplementary information about the decision making process, as well as the design and development stage. At the moment, people involved in the project can be directly contacted. Once the project becomes operational, the number of employees will be reduced and people will move on to other projects. Therefore, after 20-40 years it may be harder to locate the relevant persons and they may have forgotten relevant details or moved onto a different industry.

On the other hand, the largest disadvantage is that little information can be collected about the EoL state of the components and materials of an OWT. Therefore, the recyclability in the development phase can only be determined based on data regarding a newly installed offshore wind turbine. As a result, it may be difficult to account for unforeseen circumstances that affect the EoL state of OWTs.

Methodology

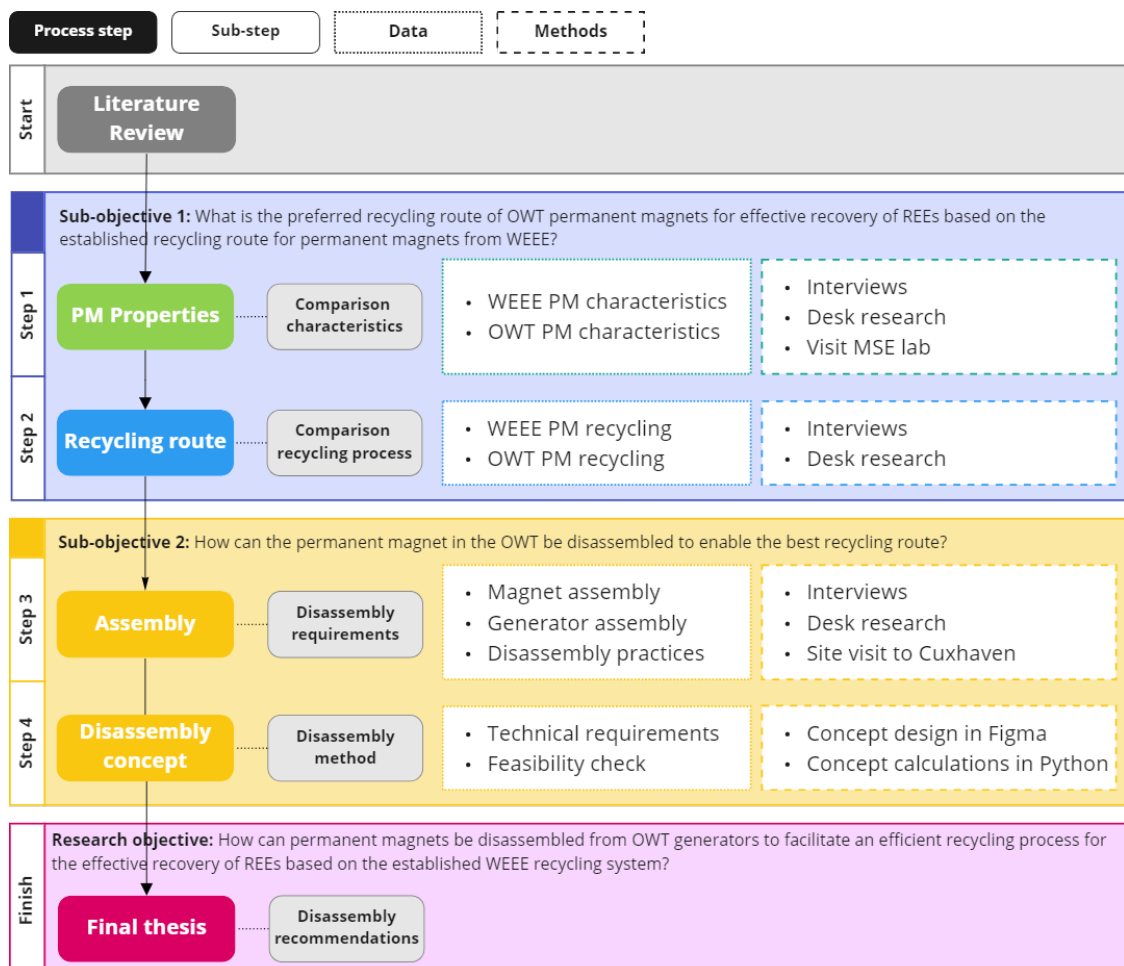


Figure 2.1: Overview of the methodology to answer the research question and its sub-research question.

To achieve the research objective, four main steps were taken which can be seen in Figure 2.1. The main process steps are indicated on the left in solid rounded boxes, with the sub-steps that informed the main step in grey boxes to their right. The data collected and produced is indicated in a white box with dotted lines and the methods are shown in the boxes with dashed lines, with the colours corresponding to the step.

The first two steps address finding the preferred recycling route to meet the first sub-objective, whereas the third and fourth steps address the disassembly required to enable the best recycling route. The results were produced in Figma and processed in Python. Each step and the methods are described in more detail in this Section.

The primary methods of collecting, processing and data was through interviews, desk research and a site visit, where an overview of people interviewed is provided in Table 2.1. The interviews we conducted in a semi-structured manner, where questions were prepared in advance, but the interviewees were allowed to deviate from the topic.

Name	Company	Function	Expertise
Ilse van Andel	Eneco	Sustainability development officer	Circularity and due diligence in renewable energy
Maarten Lo-bregt	ECHT	Quality Process Manager Wind Energy	Technical specialist, inspect of wind turbines, circular decommissioning
Anne Velen-turf	University of Leeds	Senior research fellow in Circular Economy	Sustainable offshore wind development
Rody Kemp	Eneco	Asset management and operations expert offshore wind	Improve offshore wind farms
Lorna Bennet	Offshore Renewable Energy Catapult	Project engineer	Sustainable decommissioning, offshore wind materials handling, mapping and reuse
Martijn Zon-dervan	Eneco	Electrical engineer	Technician and engineer for offshore wind
Brian Wit-tekoek	Coolrec	Outlet manager	Recycling e-waste into secondary materials
Virginie De-cottignies	SUEZ	Head of Advanced Recycling Department	Plastics and precious metals recovery from WEEE, waste and materials characterisation, recycling processes
Marco Kester	Coolrec	Interim business controller	Recycling large e-waste and hazardous materials (cooling and freezing equipment)
Matthew Chapman	Renewable parts	Marketing Manager	Refurbishment in wind industry
Jianning Dong	TU Delft	Assistant Professor	Electrical engineering, permanent magnet machines, electric generators for wind turbines
Elmedin Bratic	SGRE	Team lead generator repair shop	Disassembly and maintenance of OWTs
Paul Breet	General Electric	Retired	Electrical engineer, permanent magnet generators
Henk Polinder	TU Delft	Professor	Electrical engineering, permanent magnets, wind turbine generators

Table 2.1: Overview of the 14 people consulted/interviewed for data collection.

The structure of this thesis follows the methodology by splitting up the results in two chapters. Chapter 3 includes the results comparison of the permanent magnet properties and recycling process in Sections 3.1 and 3.2 respectively. This is followed by Chapter 4, which includes the results

of the assembly process and the disassembly concept in Sections 4.1 and 4.2 respectively.

2.1 | Sub-objective 1: Preferred recycling route

Sub-objective 1

What is the preferred recycling route of OWT permanent magnets for effective recovery of REEs based on the established recycling route for permanent magnets from WEEE?

To determine the preferred recycling route, the first step was to compare the characteristics of WEEE and OWT permanent magnets. This was used as input to evaluate how the differences and similarities in characteristics affect the recycling process for OWT permanent magnets, based on a traditional WEEE permanent magnet recycling route. In the second step, the different options for recycling permanent magnets from WEEE and OWTs were compared based on their characteristics to determine the preferred recycling route.

2.1.1 | Permanent magnet properties

Data on the characteristics of WEEE and OWT permanent magnets was collected through interviews and desk research and complemented with a physical visit to the Materials Science Engineering lab at the TU Delft. Desk research provided quantitative data on the magnet properties based on academic papers, reports and magnet producer websites. The interviews were used to corroborate the quantitative data for relevance and supplement the desk research with additional information. The visit to the lab aimed to view and get experience in handling permanent magnets in real life.

Quantitative data on the material properties of permanent magnets was collected primarily from academic papers and complemented by reports and magnet producer websites where data was lacking. Data on WEEE permanent magnets was more readily available in literature and this was used as the starting point for data collection. Where possible, the corresponding data for OWT permanent magnets was collected, often supported by reports and the producer websites.

First key material properties such as composition, dimensions and density, as well as magnetic properties such as remanence, Curie temperature and coercivity were identified and quantified based on information availability. An iterative process was used to determine the relevance of the different properties and search for additional relevant properties. The characteristics for comparison were then limited to a few most relevant properties for which sufficient data was available.

The interviews were conducted with people that were either working with permanent magnets from OWTs or WEEE, or researching circularity or recycling of permanent magnets. The people interviewed at this stage included Ilse van Andel, Maarten Lobregt, Anne Velenturf, Rody Kemp, Lorna Bennet and Martijn Zondervan. They provided information on their experience working

with magnets and the developments in the industry with regard to magnet design and their recycling. This is necessary as literature and reports may sometimes deviate from what is happening in practice.

A visit to the Materials Science Lab at the TU Delft on the 22nd of June to view and touch the permanent magnets to get a feel for how they feel and behave in real life. This was not used as official data for the study but rather for the researcher to gain experience in how they are handled in real life. The permanent magnets viewed included a sample from hard disk drives that had been disassembled from hard disk drives, where the scraps and hard disk drives themselves were also seen. Additionally, there were permanent magnets from a small wind turbine generator (approximately 7 cm x 5 cm) and a rotor from an electric scooter containing permanent magnets was also viewed.

The combination of desk research, interviews and the lab visit allowed the researcher to collect quantitative data while corroborating this with what is happening in practice and how they look in real life. This helped determine which properties were relevant and what information may be missing in studies or reports.

2.1.2 | Recycling routes

The preferred recycling route was identified by first looking at the existing recycling routes for WEEE permanent magnets. This was collected via desk research consisting of predominantly studies on recycling permanent magnets from hard disk drives and interviews with Brian Wittekoek, Virginie Decottignies, Marco Kester and Matthew Chapman. The interviews aimed to support the desk research by providing additional insights as to what is happening in practice and how it might be different from literature.

Based on the desk research and interviews, an overall overview of the recycling options for WEEE permanent magnets was made. From those options the factors that affect the recycling route for WEEE permanent magnets were determined for the different options and related back to the characteristics found in Section 2.1.1. The recycling route for WEEE permanent magnets was translated to OWT permanent magnets using the comparison of characteristics from Section 2.1.1 to provide input on how the options are affected by differences and similarities.

The translation of the WEEE permanent magnet recycling process to OWT permanent magnets first required the identification of the main characteristics that affect the recycling options. Once these were found, additional quantitative information was searched for to compare the recycling options and determine the feasibility and desirability. If quantitative information was not available for the comparison, qualitative information on the characteristics and recycling process provided in the interviews, lab visit and from desk research was used to form a critical technical analysis.

The aim of this section is to compare the different options for the recycling route of permanent magnets from OWTs based on how permanent magnets from WEEE are recycled. The quantitative and qualitative information were used to compare the options for recycling. The critical technical analysis of the possibilities was used to determine which options might be the most technically and

economically feasible and preferable. The outcomes of the critical and technical analysis formed the preferred recycling route.

2.2 | Sub-objective 2: Disassembly

Sub-objective 2

How can the permanent magnet in the OWT be disassembled to enable the best recycling route?

To determine how the permanent magnets should be disassembled, the first step was a site visit to Cuxhaven to establish how the magnets are assembled and disassembled in practice. Subsequently, desk research, interviews and brainstorming produces a disassembly concept that was visualised in Figma. The concept was analysed by considering the practical and theoretical aspects, where a simplified model was made in Python to make calculations for the latter.

2.2.1 | Assembly

To determine how to disassemble a permanent magnet from a generator it was important to first understand how it is assembled and what the structure looks like. On May 5th 2022, the SGRE nacelle factory in Cuxhaven was visited, henceforth referred to as the site visit. At the site 11 MW OWTs for another OWF were being manufactured but that had predominantly comparable specifications to the CW OWT, with the exception of small customisable details.

Prior to the site visit, a list of desired information on the assembly and disassembly of the generator was made to pose as a basis for things to look out for and ask about during the visit. Based on the preferred recycling route from Section 2.1.2 and desk research, options for disassembly were brainstormed based on provisional information from literature and provided by the case companies. The brainstorm was used to generate ideas for disassembly and prepare questions about potential options during the site visit.

It was not possible to take photos at the site during the visit due to confidentiality of information. Throughout the site visit notes were taken of information that was shared verbally and observed on site to document as many details as accurately as possible. Names of different types of equipment, approximations of sizes of components and descriptions of processes were typed as quickly as possible during the visit.

The first part of the site visit involved climbing into a fully assembled nacelle and visiting all three floors on the inside as well as the deck on top of the nacelle outside. Details such as the presence of specific electric equipment, dimensions of the equipment and details about the installation, operation and maintenance that were shared by the case company were written down.

After visiting the assembled nacelle, the assembly hall was visited, where all the components of the nacelle are put together from scratch. Prior to the walk through the assembly hall a talk was given about the overall process and the layout of the hall. In the assembly hall, the generator

assembly area was the most relevant and exclusive permission was granted to observe the placement of the magnets into the rotor assembly. It was also possible to ask people that worked with the permanent magnets and the rotor assembly questions regarding their assembly and disassembly processes.

Directly after the site visit, the notes were conferred to add any missing details or correct information that was not written down clearly or correctly. As the notes were made while walking around and in discussions with people, there may be some discrepancies in the information provided and the notes taken. Moreover, time was taken to draw some key features about the magnets and the assembly that were observed and add the corresponding details.

To gain additional insights into the disassembly process an attempt was made to schedule a visit to the service and maintenance center in Denmark, however this was not possible due to scheduling issues and time constraints. An interview was scheduled with Elmedin Bractic, the team lead of the generator repair shop at the service and maintenance centre in Denmark was scheduled instead. This provided input as to how OWT generators are disassembled in practice.

The assembly and disassembly practices of the case company were used to inform what is needed for disassembly based on what is happening in practice. There is ample literature on the disassembly of WEEE and the permanent magnets, however information on the disassembly of permanent magnets from OWTs was highly limited. Therefore the site visit and interviews were invaluable to determine disassembly requirements for the CW OWT.

Since the generator and permanent magnets are in a highly magnetic field, it was also necessary to consult literature and experts in the field of electromagnetism and permanent magnets. Firstly, basic textbooks on magnetism, permanent magnets and electromagnetism were consulted to get a better understanding of the workings of the magnetic fields in the generator. Due to the highly specialised nature of OWT generators, additional interviews were conducted with Jianning Dong, Paul Breet and Henk Polinder to further inform what the technical considerations for disassembly should include from an electrical engineering and magnetism perspective.

2.2.2 | Disassembly concept

The disassembly concept was developed using the outcomes of the preferred recycling route in Section 2.1.2 and assembly and disassembly practices in Section 2.2.1. These were in part informed by desk research but also arose from a combination of ideas discussed during the interviews on the assembly and disassembly practices in Section 2.2.1. Hardly any research on the disassembly or demagnetisation of large permanent magnets from OWTs or any comparable application or scale was found.

2.2.2.1 | Concept development

During a discussion with the case company the idea of induction heating for demagnetisation arose and a supporting paper that used induction heating to demagnetise large permanent mag-

nets was provided. The decision was made to use induction heating as a starting point and desk research on heat transfer principles and induction heating was conducted. Textbooks on the principles of induction heating and heat transfer were consulted to gain an understanding of what the possibilities for induction heating were.

Different ideas for induction heating were shared with the case company as well as a few of the interviewees (Jianning Dong, Paul Breet, Elmedin, Henk Polinder) to get their input on the options. From the discussions a few concepts arose and the decision was made to further develop the concept that seemed the most feasible to see how it would work and what the technical aspects would be, this was based on a limited knowledge of magnetism and heating. Since there were hardly any examples in literature or from practice where something comparable has been done had to be fully developed from scratch using a combination of knowledge from materials science, magnetism and heat transfer.

The concept was illustrated using Figma in both 2D and 3D versions from a variety of angles. This was used to visualise the concept and how it would work in practice. The properties and characteristics for the concept were derived from data collected when comparing the characteristics of permanent magnets and the site visit from Section 2.1.1 and 2.2.1. Variations of the concept were also developed in Figma to see how they would work and compare whether one would be better than the other.

After developing the concept in Figma, the first step involved a critical analysis of the application of the concept in the generator and the practical implications for the disassembly of the permanent magnets. This was done by qualitatively looking and how the magnets would be demagnetised and disassembly and what principles of magnetism of heat transfer might affect the concept and how they can be overcome. The assessment was informed by desk research and using input from the case companies and interviews.

2.2.2.2 | Concept modelling

Next, a high level theoretical model was built to conduct a technical analysis of the application of the concept and get an indication of whether the concept is at all feasible. The theoretical model used as much quantitative data as possible to provide orders of magnitude and approximations of the behaviour of the material. The same data on the characteristics of the permanent magnets and the assembly from Section 2.1.1 and Section 2.2.1 were used as inputs for the theoretical model.

The theoretical model focused on the heat transfer between materials to assess whether the Curie temperature can be reached in the permanent magnet. This was done by modelling the system as steady-state heat flow through composite materials. The equations required were obtained from the research done previously on heat transfer and the exact calculations are described in detail in Section 5.2.1. To limit the scope of the study, calculations on the magnetic field and demagnetisation of the magnet were excluded.

2.2.2.3 | Python

The calculations for the theoretical model were programmed in Python, as it is an efficient program to define different variables and plot various outcomes. This was done by first creating a database of relevant properties for different materials, which were selected to be NdFeB, 316 Steel, Al and Cu based on data availability and relevance. The database included geometrical information on the magnets' assembly and can be found in Appendix A.1. These properties and their substantiation can be found in Section 4.2.3.1.

Once the database was created, a function was written to calculate the energy requirements, heat flows and temperatures at different points in the material. In these functions, the time taken to heat the permanent magnet and time taken to heat the conductor were set as the primary input variables throughout the calculations. The power required in the coil to heat up to conductor was the primary output variable of the calculations. A more detailed description of the calculations for the power in the coil can be found in Section 4.2.3.2.

To approximate the effects of other variables, new functions were created in which the time taken to heat the permanent magnet and the conductor were fixed based on the outcomes of the aforementioned calculations. With a fixed heating time, variables such as the material properties of the conductor, the Curie Temperature of the NdFeB magnet and the contact surface area of the conductor could be adjusted. A separate function was written for each of these variables, where an example of the function for changing the height of the conductor can be found in Appendix A.2. The calculations for the variables are described in more detail in Section 4.2.3.3.

Preferred recycling route

3.1 | Permanent magnets

Permanent magnets that contain 27-31 % (w/w) of the REEs are referred to as rare earth (permanent) magnets (Lixandru et al., 2017; Nababan et al., 2021). They can be divided into three types, samarium cobalt (SmCo), samarium iron nitrogen (SmFeN) and neodymium iron boron (NdFeB). Nd-FeB permanent magnets ($\text{Nd}_2\text{Fe}_{14}\text{B}$) have an energy product $BH_{(max)}$ between 200-440 kJm^{-3} , whereas SmCo permanent magnets (SmCo_5 or $\text{Sm}_2\text{Co}_{17}$) and ordinary ferrite magnets have a range of 120-260 kJm^{-3} and 36 kJm^{-3} respectively (Binnemans et al., 2013).

Since the SmCo permanent magnets have a lower energy product, they have been traditionally been more expensive and also have a market share less than 2% (Binnemans et al., 2013). The high energy product of NdFeB permanent magnets has also caused them to be used more extensively in technology products, including offshore wind applications (Ni'am et al., 2019). Therefore, NdFeB permanent magnets will be the focus of this study.

3.1.1 | Materials

NdFeB magnets can be manufactured into either resin bonded alloys that contain 10% epoxy resin or a polymer, or into fully dense sintered magnets with the magnetic matrix $\text{Nd}_2\text{Fe}_{14}\text{B}$ (Binnemans et al., 2013). The manufacturing of complex shaped magnets and processing of magnets is facilitated by embedding an NdFeB powder with a polymer matrix. When the magnetic powder is diluted by a non-magnetic material the overall magnetic strength per volume unit is lower than that of a sintered magnet.

Bonded magnets are a popular option because they lower the costs without an extensive loss in material or magnetic properties (Önal et al., 2020). However, OWTs utilise sintered NdFeB magnets due to their higher performance and low weight and volume (Paredes-Sánchez et al., 2015).

NdFeB magnets consist primarily of Nd, Fe and B while quantities of Dy, Pr, Tb, and Ho are added as alloying agents. The Dy enhances coercivity and improves high temperature performance, increasing the temperature stability against demagnetisation. The Pr and Tb replace the Nd at a lower cost and reduce the quantity of Nd required (Nlebedim and King, 2018; Rademaker et al., 2013). Currently, magnet producers are aiming to reduce REE content, while maximising energy densities at various temperatures (Tunsu, 2018).

Transition metals such as Co, Ga and Cu are added to improve the processing and magnetic properties of the permanent magnets. Additional elements such as Ni, Zr, Mo and Nb are added for other desired properties (Binnemans et al., 2013; Lixandru et al., 2017). For example, Co is used during alloying and Ni is used as a protective surface coating to address corrosion issues (Tunsu, 2018).

The exact composition of these magnets will vary by application, but can also vary within one type of application (Lixandru et al., 2017; München and Veit, 2017; Sprecher et al., 2014). Some computer hard disk drives do not contain Dy, while other hard disk drive applications may include admixtures of Dy up to 1 at% (Binnemans et al., 2013). Table 3.1 demonstrates the varying compositions of NdFeB magnets depending on their application.

Feed	Composition (wt%)									
	Fe	Nd	Pr	Dy	Tb	Gd	B	Ni	Co	Other
Magnets	69	25		4			1			1
	58.16	25.95	0.34	4.21			1	0.02	4.22	1.82 ^a
Magnet swarf	56.2	32.4		1.5			1.04			8.86 ^b
Virgin magnets	66.88	18	4.6	6.15			1.02		2.84	0.51 ^c
Recycled magnets for high temperature applications	64.57	21.63	6.43	3.96			0.93		1.74	0.74 ^c
Ni-coated sintered magnets	68	28		1			1	1		1
Ni-coated magnets	65	22.40	6.79	1.11	0.69		0.86	0.62	1.05	1.31 ^d
High grade magnets for the automotive industry	57.20	23	6.52	6.26		2.25	0.73		0.51	2.89 ^d
Hydrogen decrepitated magnets	61.09	25.38	2.62	1.08			1	2.03	1.42	1.34 ^e
Commercial NdFeB magnets	67	26	5	0.5			1.6			
Notebook spindle motor for HDD		29								
Notebook voice coil accelerator for HDD		29 ^f		2.3						
Notebook loudspeaker		31 ^f								

Table 3.1: Reported compositions of NdFeB permanent magnets and magnet swarf (Tunsu, 2018)

^aAl, C, Cu, Mn, N, Nb, O, Si

^bAl, C, Ca, N, O, Si

^cAl, Cu, Ga, Ti

^dAl, Cu, Eu, Ga, Nb, Si

^eAl, Cu, Mn, Si

^fNd and Pr together

When looking at the material composition, the "other" category in Table 3.1 also gives a good indication of the variations in compositions. The other category is made up of different mixtures of Al, C, Cu, Mn, N, Nb, O, Si, Ca, Ga, Ti and Eu, when looking at the footnotes a to e. The addition

of these materials contribute to a complex material mixture, especially if magnets from a range of applications are treated together.

The different magnet feeds have different wt% of different elements, where the compositions of Fe, Nd and Pr can range from 56.2 - 67 wt%, 18 - 31 wt% and 0.34 - 6.79 wt% respectively. It means that each magnet has slightly different properties, which need to be taken into consideration in their processing, such as different curie temperatures. The properties of NdFeB magnets are discussed in the Section 3.1.3.

Different compositions for the permanent magnets used in different types of offshore wind turbine generators are shown in Table 3.2. This table only accounts for generators that utilise permanent magnets, and excludes gearbox driven generators that currently dominate the market. Based on their study, Li et al. (2022) assume that different types of PM-based generators will take a higher share in the next years.

Generator	Nd	Pr	[t/GW] Dy	Tb	Y	Total	Share [%]
EESG ^a	16 (53.3%)	9 (30.0%)	4 (13.3%)	1 (3.3%)	0	30	3.75
PMSG-GB ^b	39 (76.5%)	4 (7.8%)	4 (7.8%)	4 (7.8%)	0	51	6.35
PMSG-DD ^c	168 (74.7%)	35 (15.6%)	15 (6.7%)	7 (3.1%)	0	225	28.03
PDD ^d	348.9 (74.7%)	72.7 (15.6%)	31.2 (6.7%)	14.5 (3.1%)	0	467.3	58.22
SDD ^e	16 (54.6%)	2 (6.8%)	10 (34.1%)	1 (3.4%)	0.3 (1.0%)	29.3	3.65

Table 3.2: REEs used in different types of generator based on Li et al. (2022)

^aElectrically Excited Synchronous Generator

^bPermanent Magnet Synchronous Generator gearbox based

^cPermanent Magnet Synchronous Generator Direct-drive

^dPseudo Direct-drive

^eSuperconducting Direct-Drive

When looking at the ratios of REE used for different generator types, Table 3.2 does not take into account the variations in material composition of the permanent magnet per generator size, but rather is an overview of the total demand for REEs given in tonnes per GW [t/GW]. Therefore, it does not necessarily give an approximation of the composition of the magnets themselves. Nevertheless, the data can be used as a reference points to compare approximations for the material composition.

In this case, the focus is on the PMSG-DD, however the permanent magnets for other types of wind turbine generators are also interesting to take into consideration. Since the materials overview did not provide explicit information on the magnet, but rather the overall generator, the ratios of the REEs excluding Fe and B can be compared.

For the Ni-coated magnets from Table 3.1, the quantity of Nd, Pr, Dy and Ty used is 72.23 wt%, 21.91 wt%, 3.58 wt% and 2.23 wt% respectively. From Table 3.2, the composition of Nd, Pr,

Dy and Tb for PMSG-DD permanent magnets can be approximated to 74.7 %, 15.6 %, 6.7 % and 3.1 %. This shows that the ratios of REEs used in permanent magnets for WEEE and OWTs are in a similar range, although this only refers to two sources.

The greatest similarities can be seen between PMSG-DD and PDD OWTs, which have approximately the same ratios of REEs at different volumes, containing 74.7%, 15.6%, 6.7% and 3.1% of Nd, Pr, Dy and Tb each. The PMSG-DD accounts for 28.03% of the share of REEs used in generators and the PDD for 58.22%, making it the most REE intensive generator. Although it is not possible to validate the exact ratios, it could be assumed that permanent magnet generators in OWTs use similar ratios.

3.1.2 | Applications

Permanent magnets, are materials that generate a magnetic field, without needing electric power, for conversion between electric and mechanical energy (Campell, 1994). Their unique properties, have caused them to be used in a broad range of high performance technologies such as air conditioners, refrigerators, generators, hard disk drives, electric vehicles and wind turbines (Diehl et al., 2018; Nakamura, 2018; Ramprasad et al., 2022).

The broad applicability of permanent magnets, where both WEEE and OWTs utilise permanent magnets at different scales, has led to an increasing demand for REEs such as Nd, Pr and Dy. The former mass produces products that utilises them at a smaller scale such as hard disk drives, whereas the latter utilises them at tremendous volumes for the permanent magnet generator of a single OWT. Both are seen as a valuable source for materials recovery, which has not yet been done at a commercial scale, but has become increasingly important (Amato et al., 2019; Ni'am et al., 2019; Nlebedim and King, 2018; Rademaker et al., 2013).

Application	Components	Magnet mass/unit	Estimated life-time	Market share
Wind turbines	Generator	250-650 kg/MW	>20 years	15%
Electric transportation (EVs, HEVs, electric bikes)	Electric motor, electric power steering, generator, stop/start technology	1-15 kg in motors, 50-110g for power steering, 0.5 kg for generators, 50-100g for start/stop technology, 300-350g in electric bikes	15 years	15%
Computers	Hard disk drives, speakers, CD unit	1-30 g	10 years	35%
Household appliances and other consumer electronics (air conditioners, headphones, speakers, smartphones)	Compressors, vibration units, speakers in mobile phones	Varies, e.g. 0.5 g in smartphones and less in smaller mobiles	Varies, a few years	5% for household appliances, 25% for audio systems
Magnetic resonance imaging (MRI)			10 years	5%

Table 3.3: Applications of NdFeB magnets according to (Tunsu, 2018)

Between 2005 and 2013 nearly 97% of the REE permanent magnets sold were based on

NdFeB and in 2016 NdFeB permanent magnets accounted for 31% of the metal consumption (München et al., 2021; Ramprasad et al., 2022). As such, NdFeB magnets are also predominantly used in both WEEE and OWTs, making them the most relevant type of magnet to study for the recovery of materials. Applications for NdFeB permanent magnets are found in Table 3.3, which is also in line with the data provided by Yang et al. (2017).

Applications	Nd	Pr	Stock [kt]		Total	Share [%]
			Dy	Tb		
Computers	21.2	5.3	5.3	1.1	32.8	33.8
Audio systems	15.1	3.8	3.8	0.8	23.4	24.1
Wind turbines	10.1	2.5	2.5	0.5	15.7	16.2
Automobiles	9.8	2.5	2.5	0.5	15.2	15.7
Household appliances	3.3	0.8	0.8	0.2	5.1	5.3
MRI	3.0	0.8	0.8	0.2	4.7	4.8
Total	62.6	15.7	15.7	3.1	97.0	100

Table 3.4: Estimated global in-use stocks for the rare-earth elements in NdFeB permanent magnets in 2007 (Du and Graedel, 2011)

Key differences between permanent magnet applications in WEEE and OWTs can be seen in Table 3.3. The primary differences being magnet mass per unit and the estimated life time. Wind turbines contain a large quantity of magnets per unit (around 6,000 kg for an 11MW OWT), whereas the other applications contain significantly smaller quantities per unit ranging from less than 0.5 in mobiles, 30g in computers up to 15kg in motors. While computer and audio systems accounted for the majority of the stock of NdFeB permanent magnets in 2007, the stock of NdFeB magnets is expected to increase rapidly with the introduction of permanent magnet generators for OWTs.

There is a significant difference in life span and quantity of permanent product, such that WEEE permanent magnets provide a more constant flow of waste permanent magnets compared to OWT permanent magnets. Once the CrossWindHKN OWF reaches its end of life, over 400 tonnes of NdFeB permanent magnet will become available instantly. In contrast, WEEE produces a relatively low quantity of NdFeB per product but at a steady rate as shown in Table 3.5. In comparison, the plant will need to wait near 2,500 months, or 200 years to collect the same quantity of NdFeB magnets from WEEE.

Product type	Flow [kg/month]	NdFeB per product [g]			NdFeB flows est. [kg/month]	
		Min	Max	Avg	Low	High
HDDs (3.5")	2,500	6.0	22.0	14.1	27.5	102.5
Laptops	5,000					
HDDs		2.0	5.0	2.5	3.1	5.0
Speakers		0.6	5.3	1.8	1.3	4.0
PC Screens	70,000	1.7	15.0	5.4	7.0	21.0
TVs	45,000	3.0	33.0	12.0	20.0	45.0

Table 3.5: Possible quantities of Nd-Fe-B magnet that can be collected from different electronic waste streams at the Halmstad plant owned by Stena (Lixandru et al., 2017)

Consumer products such as vehicles, computers and household appliances have both a shorter

life time and are produced continuously by various manufacturers. This means that the the flow of NdFeB magnets is continuous, whereas its constituent material composition may fluctuate greatly. The differences in material flows and composition can be seen in Table 3.5 and Table 3.4.

Each application will have a different material composition, coating, size, shape and EoL state. The advantage is that this source of NdFeB magnets is readily available for processing and grows incrementally. On the other hand, the vast range of magnets originating for a myriad of disparate sources create a complex mixture of magnets with divergent characteristics, where information on the exact material composition is difficult to obtain.

It can be assumed that permanent magnets from OWTs within the same OWF are identical in shape, size, composition and coating. Design specifications for OWT permanent magnets are highly confidential, so this was therefore not officially verified. However, based on a visit to the assembly site, this assumption was derived from the fact that a single generator contains nearly 7,000 blocks of permanent magnet, that were not discernibly different. Additionally the production of several different magnets and distinguishing in the production and assembly phase would probably not be efficient from a practical or economical perspective.

The discrepancies in the material flows pose economic and technical challenges for the development of efficient recycling process of materials. The economic viability is dependent on the presentation of a business case for recycling which is contingent on scalability (economies of scale). Developing and installation of a recycling process requires a substantial initial investment (capital expenditure, CAPEX) and thus needs sufficient volumes to be economically attractive.

The technical feasibility notwithstanding, necessitates time, information and a consistent source of materials. It takes time to design a process and develop technology for the processing of magnets. Information is needed on the incoming material flow to determine the best way to process the materials for optimal outcome. Once a process is developed for the specific material flow, the actual flow of incoming materials needs to be consistent with that which it was designed to process.

In a broader context, as the global share of OWTs is growing along with the size and capacity has resulted in a rapid increase in demand for REEs in OWTs as shown in Figure 3.2. Additionally, the increasing price of Nd and unstable market of magnetic materials seen in Figure 3.3 and Figure 3.1 is a reason for the importance of minimising REE consumption, magnet protection and development of magnet recovery processes (Kapustka et al., 2020). Combined these create an economic incentive to recycle and may pose a viable business case in the future.

3.1.3 | Properties

To determine how to disassemble the permanent magnets from the generator information on the properties of the magnets is needed. However, data on the permanent magnets of OWTs is not readily available due to confidentiality. Additionally, OWTs have an expected life span of 25-35 years, meaning that no OWTs of this magnitude have been decommissioned yet such that it is not possible to know what the exact EoL state of the magnets will be.

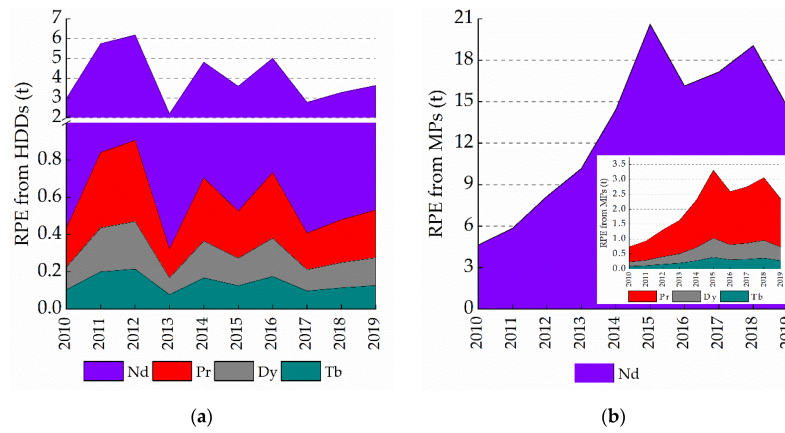


Figure 3.1: Recycling potential estimate of REEs from (a) hard disk drives and (b) mobile phones in the period of 2010–2019 (München et al., 2021)

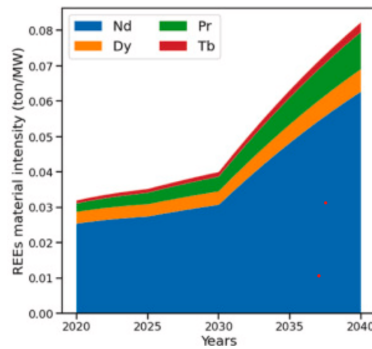


Figure 3.2: Mass and material intensity changes for REEs from 2020 to 2040 (Li et al., 2022)

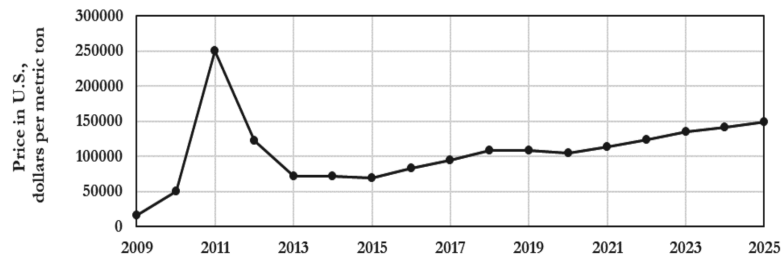


Figure 3.3: Nd oxide price in US dollars per metric ton worldwide from 2009 to 2025 (Kapustka et al., 2020)

In contrast, permanent magnets in WEEE have been around for a much longer time and provide a constant stream of EoL waste permanent magnets due to their shorter life span. As such, data on permanent magnets extracted from WEEE can be used to approximate the properties of permanent magnets in OWTs. This was complemented by data from literature and practice on permanent magnets from OWTs where possible.

For commercial purposes, permanent magnets are often classified by their maximum energy product, BH_{Max} , which is simply the product of the magnetic flux density, B , and coercivity, H .

Other properties relevant properties such as remanance, flux density and Curie are defined in Table 3.6.

Property	Units	Definition	Range (approx.)	
Magnetic flux density	B	Tesla, T	Force acting per unit current per unit length	1.0 - 1.4
Magnetic field strength	H	kAm^{-1}	Intensity of the magnetic field that arises from an external current	750-2000
Maximum energy product	BH_{Max}	kJm^{-3}	Maximum magnetic energy stored in a magnet, BH	180-414
Remanence	B_r	Tesla, T	Remnant flux density, measure of the ability of a material to retain magnetisation	1 - 1.5
Coercivity	H_C	kAm^{-1}	Measure of the field required to magnetise and demagnetise a specimen	875 - 2790
Permeability	μ_0	-	Ease of magnetisation, measure of a materials' resistance to the magnetic field	1.05
Temperature coefficient of B_r	α	$\%K^{-1}$	Measure of change in remanence per unit temperature	-0.12 to -0.09
Temperature coefficient of H_C	β	$\%K^{-1}$	Measure of change in magnetic field strength per unit temperature	-0.75 to -0.313
Curie temperature	T_C	$^{\circ}\text{C}$	Critical temperature at which the material loses its magnetic properties	310-400
Density	ρ	gcm^{-3}		7.3 - 7.7
Thermal conductivity	λ	$\text{Wm}^{-1}\text{K}^{-1}$	Number of watts conducted per meter thickness of a material, rate at which heat flows through a given material	8-9
Thermal expansivity	α	K^{-1}	Increase in size of a material due to changes in temperature	$1-4 \times 10^{-6}$

Table 3.6: Overview of the different properties of permanent magnets and approximate ranges for the properties of sintered NdFeB magnets at 20°C based on company websites from various sources (*Neorem magnets, Magnet source, Advanced magnet source, Arnold Magnetics, Ee-magnetstuk, Eclipse Magnetics*)

Although there are many differences between permanent magnets from WEEE and OWTs, data from permanent magnets on WEEE is readily available and provides a starting point for approximating the properties. The scope of this study however is not to derive the exact composition but to determine the most effective recycling route for the effective recovery of REEs. As such, fluctuations in the properties of permanent magnets, such as the density, need to be taken into account in calculations.

When looking at permanent magnets in WEEE, there is an abundance of literature on the material composition. Approximations are also needed because material properties can change with time as demonstrated by Diehl et al. (2018), who compared the properties and composition of scrap magnets from WEEE with primary materials. Therefore, even if precise data on permanent magnets from OWTs in the design phase, their properties at the EoL may have changed.

It is known that the permanent magnets are NdFeB based and are coated, the exact composition of these specific permanent magnets and their coating is however unknown due to confidentiality and lack of EoL OWTs that have already been decommissioned. These details determine the magnet's exact properties such as the density, conductivity, and Curie temperature. Information on these properties are necessary to determine an efficient recycling process for the effective recovery of REE.

3.2 | Recycling routes

The recycling process covers the entire chain of the materials from the product's EoL, the starting point, to the development of a recycled material that is ready to use in a new application, the end point. A more detailed overview of the recycling process based on Figure 1.9 is shown in Figure 3.4. The sub-steps of the pre-processing stage are shown in the green blocks, while those of the end-processing stage are shown in the red block.

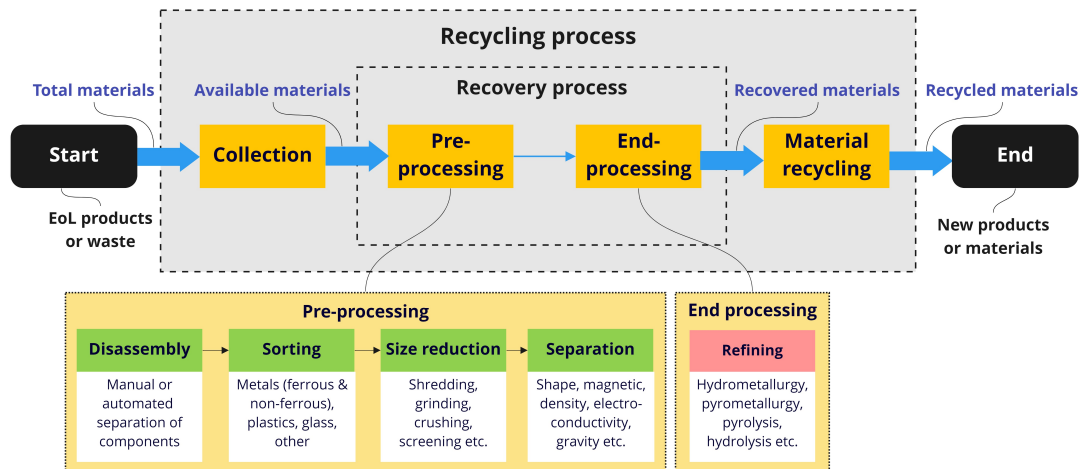


Figure 3.4: Extended overview of the entire recycling process including the sub-steps of the pre-processing and end-processing stage.

3.2.1 | Process overview

The pre-processing phase is often referred to as physical or mechanical separation, whereas the end-processing is often referred to as chemical, or metallurgical for metals, refining of the material to obtain pure materials, metals or alloys. The following sections will provide a brief overview of the sub-steps of the pre-processing and end-processing stage to understand how these might be applied to permanent magnets from WEEE and OWTs. This will provide insights into how the characteristics might affect the quality of the recycled material and which factors influence it.

The pre-processing phase is a central step in the recycling chain of WEEE and complex products that channels secondary raw materials into a designated recovery process through liberation and separation (Marra et al., 2018). These outputs are then subjected to the end-processing phase in which a targeted set of materials are recovered. However, there is always a probability that the presence of certain types of impurities may lead to a lower quality end product after processing (Ueberschaar et al., 2017).

3.2.1.1 | Disassembly

Disassembly refers to the physical dismantling of the product, whereas depollution refers to the removal of hazardous materials to ensure the safety of the remaining process. Disassembly is a crucial step in the pre-processing phase of the recycling process that aims to separate parts, components, and materials for material recovery (Kopacek, 2017; Song et al., 2014). There are three underlying goals of disassembly according to Sodhi et al. (2010); Vanegas et al. (2018):

- Service or repair a product while it is in use
- Remove hazardous or toxic parts or materials
- Recover valuable parts or materials through separation at the EoL

Disassembly is often a requisite step for the removal of hazardous substances and extraction of components or parts containing valuable materials, such as REEs and precious metals. The hazardous materials that have to be removed can be found in Table 1.5 and is often obligated by law depending on the location of the facility. Targeted components will be separated from the product for specific treatments or for the recovery of target materials.

Depending on the goal of disassembly, three different types of disassembly can be used, which can be done either non-destructively, keeping the parts and components intact or destructively, where the parts and components are destroyed in the process (Sethurajan et al., 2019). The three possible types of disassembly are defined in Table 3.7. In the depollution phase for example, selective disassembly would most likely take place, which may be followed by complete disassembly to extract the remaining valuable components.

Complete	The product is separated into all its parts
Partial	A systemic approach for the removal of a single component, part or group of components and parts from a product, DSP is used to determine the disassembly depth and optimal sequence.
Selective	Targeting specific components for which the end point is determined, often the case for either hazardous or high-value components, similar to partial disassembly

Table 3.7: Summary of the three types of disassembly (Desai and Mital, 2003; Marconi et al., 2018; Tao et al., 2018)

Disassembly sequence planning (DSP) is a process in which the order in which the components of a product need to be disassembled is established. In conventional disassembly processes only the joints between components are removed, whereas in destructive disassembly, the whole target product is destroyed into pieces. Partial destructive disassembly, on the other hand, only destroys the connectors and low valued components. DSP is therefore only conducted for conventional and partial destructive disassembly processes (Song et al., 2014).

3.2.1.2 | Sorting

Sorting takes place on several occasions after the disassembly, it can be seen as an iterative process by which each sorting step aims to sort parts at components at a different level. Disassembly and size reduction are requisite steps for sorting to enable the separation of parts, components and materials based on their characteristics (Maisel et al., 2020).

The initial sorting process, also referred to as pre-sorting, takes place at a high level, where the components are sorted based on their classification and subsequent processes, which also serves as a basic form of decontamination (Maisel et al., 2020). At this stage, hazardous materials are removed and grouped according to their classification and contaminants, such as batteries, smoke detectors, fluorescent lighting. Depending on the disassembly level, components containing valuable materials such as cables, printed circuit boards or hard disk drives are also sorted and collected separately.

The remaining components will be sorted by size and basic materials to undergo the first stage of size reduction. At the high level, it is preferable to sort materials based on their general categories (ferrous metals, non-ferrous metals, glass, plastics and other) where possible. For example, a component that is predominantly metal and another that is mostly plastic should be sorted separately if economically and technically feasible. The more the materials are sorted at this level, the lower the level of contamination in later stages.

3.2.1.3 | Size reduction

Size reduction is a process based on comminution which aims to liberate the materials and enable physical separation of the materials in the product by decreasing the particle size. The liberation degree is the percentage of a phase or material that occurs as free particles in relation to the total sample (Kasper et al., 2015). Multiple stages of size reduction may be necessary to achieve the desired liberation degree and particle size, which can strongly impact the success of the subsequent mechanical processing and the subsequent recovery grade (Ruan and Xu, 2016).

Different technologies may be applied to reduce the size of components or particles. The main ones are shredding and cutting, crushing and milling and grinding and pulverisation, which are described in Table 3.8. Each of the processes has different types of equipment built to handle different types of feeds, which may vary in sizes and materials (Cui and Forsberg, 2003).

The method and technology used depends on the characteristics of the incoming feed and desired output. The desired output particle size is dependent on the separation method used in the next stage, which can range from 0.075mm to 10mm as each separation technology has a different optimal feed characteristics (Ambaye et al., 2020; Ruan and Xu, 2016). According to Kasper et al. (2011) metals present in WEEE are easily separated when the technology used is able to reach particles under 2 mm, which would virtually achieve total liberation (Kasper et al., 2015).

Size reduction	Description
Shredding and cutting	Shear force by cutting, tearing or extruding is used to reduce the size of feed materials through shear (industrial shredders, granulators)
Crushing and milling	Using impact force to reduce the size of particles (impact crusher, hammer mill)
Grinding and pulverising	Selective comminution process to reduce and change the size or shape of particles

Table 3.8: Overview of the different types of size reduction and the technologies that can be used (Kaya, 2016; Tabelin et al., 2021)

After the pre-sorting stage, the first stage of size reduction can take place where shredding and cutting is predominantly used for large WEE equipment such as ashing machines, refrigerators and air conditioners. Industrial shredders can take on components with dimensions between 1-2m in width, breadth and length and produce particles with sizes below 100mm (Batinic et al., 2018). Once particles have been reduced to this size, they are processed again in other size reduction technologies to be further reduced down to the desired particle size.

Size reduction utilises a significant amount of energy, such that the time and energy consumption for different materials should be taken into consideration. The comminution energy efficiency, which determines the degree of liberation, and the energy required is inversely proportional to the size of the particle produced (Kasper et al., 2015). On the other hand, excessive crushing can deteriorate the liberation grade making it difficult to separate metals and decrease the recovery rate of materials (Ruan and Xu, 2016).

3.2.1.4 | Separation

After undergoing size reduction, the liberated materials of varying particle sizes are separated based on material properties such as their size, shape, magnetism, density or electro-conductivity. Physical separation technologies employed include magnetic separation, eddy current separation, air current separation, corona electrostatic separation and vacuum metallurgy separation (Am-baye et al., 2020; Cui and Forssberg, 2003; Kasper et al., 2015). Other examples of technologies include flotation, sieves, shaking tables and air classification. Examples of the different separation characteristics and technologies are shown in Table 3.9.

After the initial screening, the ferrous and non-ferrous materials are segregated through magnetic separation, most commonly with a low intensity magnetic drum. Subsequently, an electro-conductive separation technique, commonly the eddy current or corona electrostatic separation, will separate the non-ferrous metals from the other materials, such as plastics, glass and so on. Next, a density or gravity based technology will be used to further separate particles by their specific gravity (Batinic et al., 2018).

Separation	Description	Examples
Size	Particles classified and distinguished by size to prepare a uniformly sized feed and upgrade metal content, also known as screening	Sieves (vibrating, rotating, vibration)
Shape	Particles separated by velocity differences when tilted on a solid wall, time taken to pass through a mesh aperture, cohesive force to a solid wall and settling velocity in a liquid	Inclined conveyor and vibrating plate used as a particle shape separator
Gravity or density separation	Use density of materials to differentiate acceleration and speed in laminar flow, sedimentation rates and interstitial consolidation to separate heavy and light materials	Air current separation, dense medium separation, jigs, suspensions, flowing film concentrators, froth flotation
Magnetic	Particles exposed to the magnetic field and forces acting on them, result in the attraction or repulsion of the same field to recover ferromagnetic materials from non-ferrous metals and non-magnetic waste	Dry separators, wet separators, magnetic drum
Electro-conductivity	An electric field with sufficient intensity to separate an electrically charged particle and particles with a superficial electrical charge or with induced polarisation are influenced by an electric field	Eddy current separation, corona electrostatic separation, triboelectric separation

Table 3.9: Overview of the different types of materials separation and the technologies that can be used (Ambaye et al., 2020; Cui and Forssberg, 2003; Guo et al., 2016; Kasper et al., 2015; Thompson et al., 2021)

3.2.1.5 | Refining

The end-processing phase refers to the refining of the material from the pre-processing phase such that the targeted metals can be extracted. There are a broad range of refining methods and technologies available dependent on the type of material that is to be processed. For metals the most commonly used processes are either hydrometallurgical, pyrometallurgical or electrochemical, although some biotechnology options are also available. A short summary and the advantages and disadvantages of the processes can be found in Table 3.10.

3.2.2 | Recycling permanent magnets

From the different recycling options for magnets given in Table 1.8, magnet to magnet and waste to alloy are the most realistic and preferred options. If magnets can be separated completely from EoL with minimal levels of contamination, this would enable the preferred recycling options. These routes are not suitable for shredded materials due to the high levels of contamination Yang et al. (2017).

The quantities of permanent magnets that can be collected from different electronic waste streams is very low compared to its constituent product. For every incoming kg of HDD between 11 - 41 g of permanent magnet can be recovered. In contrast, for every kg of laptop, PC screen and TVs only 0.9 - 1.8 g, 0.1 - 0.3 g and 0.4 - 1 g of permanent can be collected, based on Table 3.3. The amount of permanent magnet retrievable from a HDD that has been disassembled prior to processing is at least 12 up to 150 times more than that of the other WEEE products. Therefore,

Process	Description	Advantages	Disadvantages
Pryometallurgy	Incineration, smelting, drossing, sintering and smelting to recover non-ferrous and precious metals, metals concentrated in metallic phase and remainder is rejected in a gas and/or slag phase	Applicable to many types of WEEE, no pre-treatment required, shorter process	Air pollution, metals lost, presence of ceramics/glass increases loss of precious and base metals, low recovery for some metals
Hydrometallurgy	Uses acids or caustic watery solutions to selectively dissolve and precipitate metals, solutions separated through solvent extraction, precipitation, cementation, ion exchange, filtration and distillation to isolate and concentrate target metal	High selectivity, lower processing costs, risk of air pollution and power consumption, reusable chemical reagents	Difficult to process complex WEEE scraps, size reduction required, corrosive waste water
Electrochemical	Electrowinning performed in aqueous electrolytes or molten salts, metal concentrates from hydrometallurgical processes are electrodeposited from aqueous solutions on the cathode	High selectivity, electrolyte can be reused, few steps, possible to extract pure metals	Mechanical or hydrometallurgical pre-treatment needed

Table 3.10: Overview of the different types of metallurgical recycling technologies that can be used (Kasper et al., 2015; Tabelin et al., 2021)

it is clearly preferable to disassemble the products as much as possible to increase the quantity and quality of permanents for recycling.

OWTs on the other hand, contain permanent magnets that weigh approximately 10g each and are enclosed in a casing containing approximately 10g of permanent magnets. As such, every kg of magnet contains 10g of permanent magnet that can be recovered. This is three times more than the quantity of permanent magnet that can be extracted from the HDDs. Also, a single permanent magnet in the magnet casing is at least 10 times larger than than the average quantity of permanent magnet in an entire WEEE product.

Taking the size and concentration of permanent magnets into consideration, the technical and economic feasibility of recovering the magnets in a state that is suitable for magnet-to-magnet or waste to alloy-recycling is a lot higher for OWTs. Ideally, the permanent magnet would be extracted from the magnet casing and decoated to provide the purest possible materials stream for end-processing.

The recycling of EoL permanent magnets can be split into two categories, the first is small magnets from WEEE and large magnets from OWTs as shown in Figure 3.5. There are two different strategies for the recycling of permanent magnets from WEEE, the first entails disassembly and pre-sorting prior to size reduction and refining, while in the second the WEEE undergoes size reduction without prior separation and relies on mechanical separation for physical upgrading followed by refining.

If the first route is followed, then the shredded materials are thermally demagnetised in a furnace and undergo further size reduction via grinding and screening to obtain a NdFeB magnet concentrate. Subsequently the concentrate undergoes metallurgical separation and recovery which can be either a hydrometallurgical or pyrometallurgical process.

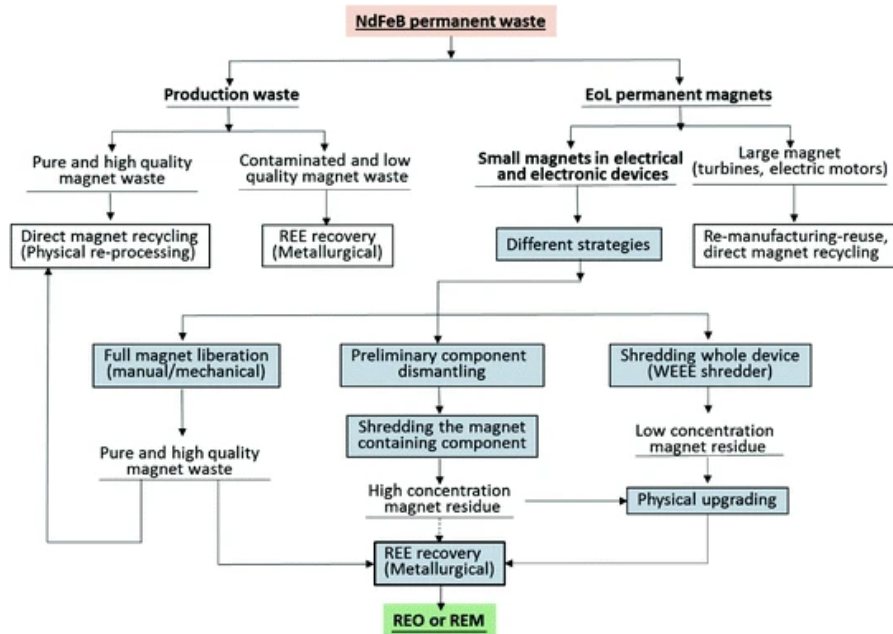


Figure 3.5: Overview of the entire recycling process for NdFeB permanent magnets according to (Peelman et al., 2018)

A more detailed example of the first route is shown in Figure 3.6, which is the proposed recycling process for permanent magnets from HDDs. The HDDs are first dismantled from their component and then shredded to liberate the magnetic materials from the non-magnetic materials, such that approximately 70% of the magnetic particles could be recovered. The separately collected magnet residues then undergo a thermal demagnetisation process followed by grinding and screening, which represented approximately 63% of the total collected shredder residue.

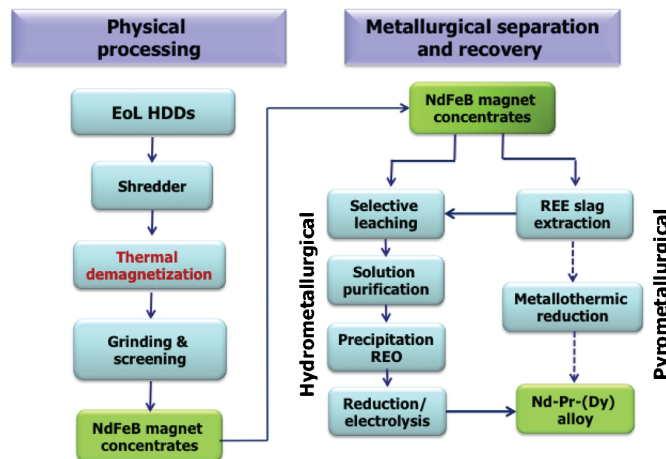


Figure 3.6: Proposed recycling process for permanent magnets in HDDs (Peelman et al., 2018)

For recycling permanent magnets from OWTs, shredding the whole device, in this case the

generator, is not technically feasible as the largest industrial shredders process waste up to 2 m x 2 m while the generator has a diameter of 8 m and height of approximately 1.5 m. Therefore, if the generator is to be shredded as a whole it would have to undergo a crushing stage first in order to fit.

If it was technically feasible to shred a generator containing the magnets after crushing, this would be undesirable due to the low concentration of magnet in a high volume of waste. The concentration of recovered REEs from dismantled HDDs was between, 5-20% after physical processing. In contrast, an approximated ratio of the volume of permanent magnet to the outer rotor and casings alone is 1.5%, meaning that the quantity of desired materials for recovery is relatively low in comparison to the total available material.

Industrial shredders are commonly used to shred equipment such as washing machines and refrigerators and are also known to be magnetic, where magnetic materials can get stuck in the shredder causing it to break. Considering that the permanent magnets in generators are highly magnetic, it may not be possible to shred in a magnetised state and the remanence in a demagnetised state may still pose a safety risk.

It may be difficult to separate the permanent magnets from the casing and rotor, as they are likely made of steel or other ferrous materials that have magnetic properties. In WEEE, the permanent magnets can be magnetically separated from non-ferrous metals and non-magnetic waste such as plastics used in the casings. If the structure is made of predominantly ferrous metals, separation may also be more challenging.

A recycling route in which the magnets are first removed from their main component, the generator, is in this case preferred. The permanent magnets in OWTs are significantly larger and present in higher quantities in comparison to WEEE, the disassembly of the magnets has to take into consideration additional effects of the magnetic field. Since this is not the case for permanent magnets in WEEE, it is important to determine how to disassemble the magnets from the generator in a safe and effective manner.

3.2.3 | Disassembly

Disassembly describes the separation of parts, components and materials of a product either manually, automatically or robotically (Kopacek, 2017; Sethurajan et al., 2019). A product may be joined mechanically, chemically or at an elemental level. Disassembly can involve either an unfastening action or a destructive action, where the former involves the removal of a fastening element and the latter refers to breaking a fastener joint (Sodhi et al., 2010).

Disassembly can be done either manually, automatically, or robotically often with a combination of destructive and non-destructive methods to target specific components and materials (Kopacek, 2017; Sethurajan et al., 2019). The method chosen depends on the goal of disassembly, which could be to recover valuable materials or separate hazardous substances. In the case of hazardous substances, more caution may be necessary and destructive may not be suitable as there may be risks of contamination or leakage.

3.2.3.1 | Disassembly of WEEE

If the goal is to recover the REEs from a WEEE product containing permanent magnets, the components containing hazardous substances will be removed first. Based on the interviews with Brian, Virginie and Marco from Coolrec and Suez, this is done through a selective disassembly process executed by dedicated specialists who are experts at the quick removal of targeted components. These experts have experience in the selective disassembly of a broad range of devices and can quickly locate, recognise and remove target components.

At the same time, companies will often also aim to separate components containing valuable materials such as hard disk drives containing permanent magnets. The degree of liberation of the permanent magnets from their hard drives is dependent on the economic and technical feasibility. For this reason, it is economically viable to separate the hard disk drive from a desktop computer but further manual liberation is too time consuming.

Examples of a manually and non-destructively disassembled laptop and television are shown in Figures 3.7a and 3.7b. These depict the complexity of the product and quantity of steps that need to be taken to extract the valuable components such as the permanent magnet.



Figure 3.7: Example of the disassembly processes for two types of WEEE from (Lixandru et al., 2017)

The size of permanent magnets in comparison to the WEEE product is relatively small. A laptop is around 20-30cm and a TV can range from 50cm to over 2m, the magnet containing components

are around 2-5cm and the permanent magnets are 1cm or less, which can be seen in Figure 3.7. This means that manual separation would require many precise actions, which is labour intensive for the retrieval of 1-3g of magnet (Lixandru et al., 2017).

The wide range of products in which permanent magnets can be found in WEEE means the actions vary per product. As such, a scalable, affordable and efficient automated disassembly process for WEEE has not yet been introduced and is often done manually or skipped altogether and directly undergoes size reduction (Li et al., 2015). This was also corroborated during the interviews, where Virginie and Brian confirmed that specialists manually selectively disassemble products such as laptops.

During the visit to the MSE lab at the TU Delft it was found that liberation of the permanent magnets from a hard disk drive can be done through an automated cutting process. The permanent magnet within the component is located and that section of the component is then cut off and separated from the remainder of the hard disk drive, which is then sent for further processing. This is also a form of size reduction which aims to increase the quantity of permanent magnets per volume processed.

The advantage of the large size and uniformity of OWTs means that it may be possible to standardise and automate the disassembly process. WEEE is a consumer product that can be casually disposed of, whereas OWTs are large industrial products with a clear owner and strict regulations that need to be met. Therefore, if an OWF is decommissioned, multiple identical OWTs will need to be disassembled at once.

The manual disassembly of permanent magnets from WEEEs is labour intensive due to the effort required to separate the magnet relative to the quantity of magnet retrieved. During this disassembly process they are still magnetised and only demagnetised after they have been collected and sorted separately. This is different for the disassembly of OWTs.

3.2.3.2 | Disassembly of PMGs

There are limited examples in literature and reports that describe the disassembly of permanent magnets from OWTs. Nevertheless, some comparable examples were found for the disassembly from permanent magnet electrical machines from electric vehicles and scooters. A permanent magnet generator of an electrical scooter was available during the MSE lab visit, however it had not yet been demagnetised or disassembled and could only be viewed as an assembly.

In a study by Li et al. (2019b), a study explored several measurements of magnet disassembly from traction motors of hybrid and electric vehicles that contained surface mounted and interior permanent magnet synchronous machines. The machines were disassembled from the vehicles prior to attempting to remove the permanent magnet, which is comparable to the removal of the HDD from a computer to isolate the part.

The magnets of the machines in the study were fixed to the rotor using an adhesive, which was also seen at the lab for the permanent magnets in the scooter. In the study, the main challenge was

the separation of the magnets due to the adhesive and the behaviour of the magnetised magnet once it was liberated from the assembly.

Mechanical treatments caused damage to the permanent magnets due to their brittleness and absence of appropriate tools. Thermal treatments dissolved the glue before reaching the Curie temperature required to demagnetise the magnet, causing them to fly uncontrollable out of the rotor. Furthermore, the heating of adhesives also produced a heavy amount of smoke.

3.2.4 | Demagnetisation

To determine how to demagnetise and disassemble permanent magnets it is important to understand a few basic principles of magnetism. These principles can then be used to determine which properties are relevant for disassembly and recycling and how they might affect the process. Theories of magnetism do not directly fall under materials science but rather under electrical engineering, however magnetic properties are related to material structures and properties and therefore important to understand.

3.2.4.1 | Magnetism

The basic principle of magnetism starts with the movement of electric charges that produce an electric current. The direction is determined by the direction of motion of a positive charge. The charged particles experience magnetic forces perpendicular to their direction of motion, producing a magnetic field around the current. The strength of the magnetic field produced is referred to as the Magnetic Field Strength, \mathbf{H} , which can be measured at different points in a field and varies depending on the distance from the center of the current.

Charged particles moving between two magnetic fields experience a force that is perpendicular to the field direction and velocity of the particles. The magnitude of that force is proportional to the speeds of the particle, its charge and the sine of the angle between the velocity and field direction. This leads to the Lorentz force law, which can be used to calculate the magnetic field and the force between those fields.

Lorentz Force Law

$$\mathbf{F} = q\mathbf{v} + \times\mathbf{B} \quad (3.1)$$

$$\mathbf{F} = q\mathbf{E} + q\mathbf{v} \times \mathbf{B} \quad (3.2)$$

The permeability of free space, $\mu_0 = 4\pi \times 10^{-7}$ is a constant measured in $[\text{TmA}^{-1}]$. For linear, homogeneous and isotropic media the magnetic field, \mathbf{B} , and magnetisation, \mathbf{M} , are proportional to the magnetic field strength, \mathbf{H} as shown in Equation 3.3 and 3.4. Where μ and χ_m are the permeability and susceptibility of the material.

Magnetic field strength, H	The strength of the magnetic field is determined by the strength of the current, measured in Amperes per unit length [Am ⁻¹]. It measures the influence of a magnet on an electric current.
Magnetic field, B	The magnitude of the force on a moving charge, also referred as the magnetic flux density.
Magnetisation, M	The volume density of magnetic moments given in Tesla [T]. It measures the net magnetic dipole moment per unit volume.
Flux, Φ	The measure of the total magnetic field that passes through a given area measured in Tesla [T]

Table 3.11: Main principles of magnetism

B & H	$\mathbf{B} = \mu\mathbf{H}$	(3.3)
	$\mathbf{M} = \chi_m\mathbf{H}$	(3.4)

The coefficients μ and χ_m are related to each other by Equations 3.5 and 3.6.

Coefficients	$\mu = \mu_0(\chi_m + 1)$	(3.5)
	$\chi_m = \frac{\mu}{\mu_0} - 1$	(3.6)

The magnetisation of ferromagnets exhibit hysteric behaviour and is shown in the hysteresis loop in Figure 3.8. An increase in strength of the magnetic field leads to a non-linear increase in magnetisation until the saturation point M_S . When the field is reduced from the positive value, there is some remnant magnetisation, M_r . The field at which the magnetisation changes direction is the coercive field of the magnet, H_C . The magnetisation decreases with increasing temperature due to the thermal energy that affects the magnetic order.

The hysteric behaviour of magnetisation is caused by the presence of magnetic domains in a material. Magnetic materials contain domains, separated by domain walls, where the magnetisation is saturated locally in the individual domains as shown in Figure 3.9. When the magnetic material is exposed to a magnetic field above H_S , the moments in each domain orient along the field resulting in the saturation magnetisation M_S .

Magnetisation is linked to the easy magnetic direction (EMD), which is the energetically favourable direction of spontaneous magnetisation referred to as the minimum anisotropy energy E_A . The hard magnetic direction (HMD), is described as the maximum E_A . In most magnetic materials, the magnetisation is not completely free to rotate, where the directional dependence of the magnetisation is known as magnetic anisotropy (Li et al., 2019a; Sechovský, 2001).

Magnetic anisotropy is one of the most important characteristics of materials considered for permanent magnet applications because the magnetisation must be pinned in a provided direction.

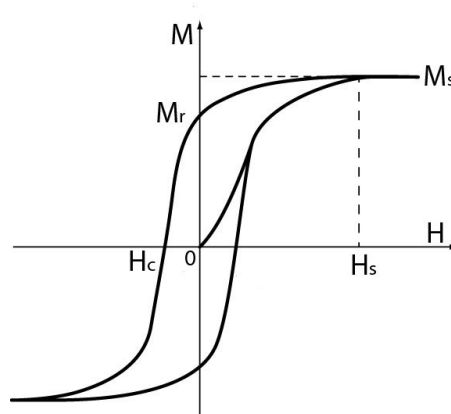


Figure 3.8: Example of a hysteresis loop (Arora, 2018).

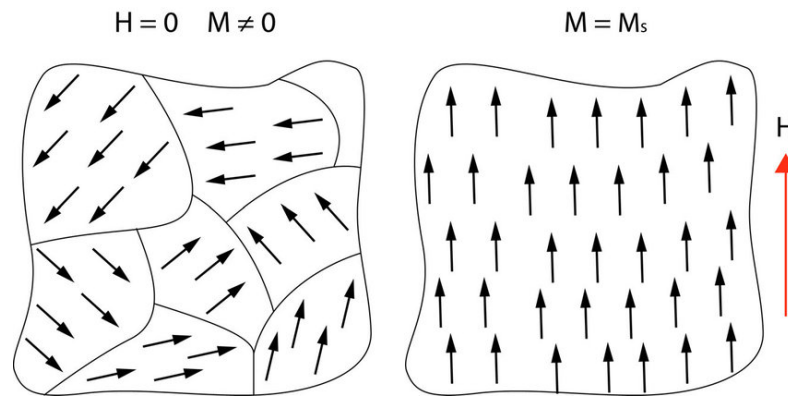


Figure 3.9: Example of magnetic domains and magnetisation (Arora, 2018).

The most common type of magnetic anisotropy is magneto crystalline anisotropy, which is the tendency of magnetisation to align itself along a preferred crystallographic direction, caused by the spin-orbit coupling. (Li et al., 2019a; Sechovský, 2001). This is due to the phenomena in which the internal energy, the magnetic anisotropy energy (E_{MCA}), varies by the direction of the material (Azuma, 2018).

The spin-orbit coupling is a relativistic effect that occurs when a particle with non-zero spin moves around a region with finite electric field. It is the interaction between an electron's spin and its orbital motion around the nucleus, linking the electron orbits to the crystallographic structure (Ito and Tanaka, 2014; Majumdar et al., 2016). They make the spins prefer to align along the well defined crystallographic directions by their interaction with the spins.

The high energy product of a permanent magnet originates from the high uni-axial magneto-crystalline anisotropy of a magnet which produces a high coercivity (Li et al., 2019a). Where the intrinsic coercivity is a measure of the field required to magnetise and demagnetise a specimen, which can be derived from the constitutive relation in Equation 3.7.

B-H

$$\mathbf{B} = \mu_0(\mathbf{H} + \mathbf{M}) \quad (3.7)$$

Spontaneous magnetisation in a material occurs at low temperatures until the material becomes saturated, such that the atomic moments tend towards perfect alignment. As the temperature increases, the magnetisation gradually decreases until T approaches the Curie temperature, T_C , which is where the magnetisation drops dramatically to zero. The Curie temperature of a material is dependent on α , the mean field constant, μ_0 , the permeability of free space, N , the number of non-interacting atomic magnetic moments per unit volume, m , the magnitude of the magnetic moment and k_B , the Boltzmann's constant shown in Equation 3.8.

Curie temperature

$$T_C = \frac{\mu_0 N \alpha m^2}{3k_B} \quad (3.8)$$

Permanent magnets are hard magnetic materials that have a low permeability and high coercivity which makes them difficult to magnetise and demagnetise. Once they become magnetised they tend to remain magnetised. Properties of permanent magnets that are primarily looked when selecting a magnet are the coercivity H_C , saturation magnetisation M_s and remanence, B_r .

The coercivity of a magnet is the value of H required to reduce B to zero, H_C , while the remanence is the value of B when H is reduced to zero, B_r based on Equation 3.7. The coercivity can also be described as a measure of the ability of a ferromagnet to resist changes in magnetisation. The saturation magnetisation M_s is when all the moments within a magnetic domain align parallel to one another and all the domains are also uniformly aligned.

Structural changes through oxidation may take place throughout the life cycle of the permanent magnets in OWTs, which create a layer with lower intrinsic coercivity than the body of the magnet and thus is more easily demagnetised. This causes a reduced working volume and blocks the field from the magnet's interior resulting in a poorer performance of the magnet. For this reason, the composition of the magnet is varied through the addition of alloying elements and coatings such as Ni, Zn and Al with thicknesses of 10-20 μm or epoxy with thickness 20 -30 μm are applied (Constantinides, 2022; Hogberg et al., 2017).

3.2.4.2 | Thermal or non-thermal demagnetisation

In practice, permanent magnets from WEEE and OWTs are disassembled, separated, shredded and demagnetised, although the order depends on the product, before end-processing. The disassembly of magnetised magnets from OWTs is a lot more challenging than WEEE due to the size of the magnet and its resultant force (Li et al., 2019b). Therefore it is worthwhile to explore how the magnets may be demagnetised before disassembly.

The magnetic properties of a material is dependent on temperature, pressure and applied magnetic field and changes to those properties can be either reversible, irreversible or structural. For

OWTs, if the goal is magnet to magnet recycling, it is desirable to invoke an irreversible change in magnetisation to avoid the magnet becoming re-magnetised after demagnetisation.

The first consideration for demagnetisation is if this should be done thermally or with an opposite magnetic field, non-thermally. Thermal demagnetisation, by heating the permanent magnet to its Curie temperature is a form of irreversible demagnetisation. Non-thermal demagnetisation involves the application of an external demagnetising field that exceeds the intrinsic coercivity of the material such that the magnetisation is flipped in the opposite direction.

Thermal demagnetisation is most commonly used in practice for both WEEE and the permanent magnets that have been disassembled before demagnetisation. Thermal demagnetisation requires heating the permanent magnet to a temperature above the Curie temperature, irrespective of the magnet's polarity, shape or size. As such, it can be applied to a wide range of shapes and sizes and is likely the reason that it is the most commonly used form of demagnetisation in practice. However, it is important to note that in thermal demagnetisation excessive heating has been shown to degrade the properties of recycled permanent magnets (Hogberg et al., 2016).

The application of an opposite magnetic field requires knowledge about the direction of the magnetic field and the coercivity of the magnet. These properties vary per magnet and are not always known, which may make it difficult to apply. There is limited literature on non-thermal demagnetisation for permanent magnets from WEEE and interviews also have also been primarily focused on thermal demagnetisation, therefore the remainder of this study will look into thermal demagnetisation.

3.2.4.3 | Complete or local demagnetisation

Complete thermal demagnetisation refers to the heating of the entire structure that contains permanent magnets, whereas local demagnetisation refers to the process of heating the permanent magnets locally within their structure. This option is not necessarily applicable to WEEE permanent magnets, as they are disassembled, separated and reduced in size before they are heated up together. For the larger structures, the aim is to demagnetise them before disassembly to enable their physical removal.

For OWTs, the former would require fitting the entire generator into a very large furnace or heating the structure through other means such as large scale industrial induction. Large scale furnaces that fit an 8 m diameter generator do exist and are used in industrial processes that use large autoclaves such as the steel making or aerospace industry. Large scale induction, as shown in Figure 3.10, have not been seen in literature and are likely to be very complex and unrealistic and will thus not be discussed in more detail.

Complete heating of the generator in a large furnace would have several logistical implications. The first of which is the transportation to the facility at the EoL of the OWT. The generator would either have to be disassembled offshore and be transported separately from the other decommissioned OWT components or they would have to be transported from a site where the disassembly of the generator is possible.

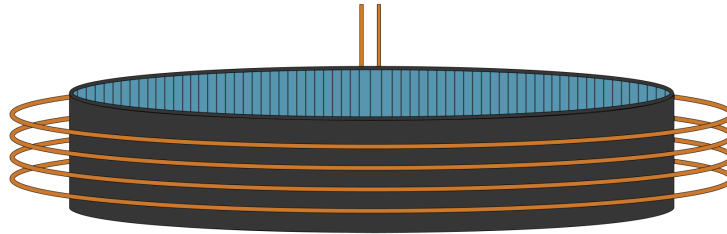


Figure 3.10: Induction heating the entire generator structure.

At the assembly site in Cuxhaven for example, they have all the tools and structures in place to disassemble the generator to a desired state, where for example the inner stator and rotor brake can be removed prior to thermal demagnetisation. From there it can be transported to a site containing a large autoclave who will provide the oven and conduct the heating. Nevertheless, this facility needs to be able to move the structure on site or remove the internal parts since they may not have the space or lifting tools to do so.

The removal of the stator and rotor brake would be preferable from an efficiency perspective as additional masses of material are not unnecessarily heated. However, these components also provide structural stability and it may be difficult to lift and move the outer rotor without its internal support structure due to the relatively thin walls in comparison to the diameter. If the internal parts were to be removed and it is not possible to lift the structure horizontally, it may have to be rotated and lifted vertically.

The presence of the stator and rotor brake also influences the furnace requirements, such as the power needed to heat the generator to the Curie temperature. The larger the mass, the more energy and time is needed to heat the structure. On the other hand, if the internal structure is removed and the outer rotor has to be transported vertically, the logistical challenge would be how to fit this into the oven.

Another consideration of complete demagnetisation at a large furnace at another site that may contain magnetic materials. The generator contains many permanent magnets, such that even small magnetic materials at the maintenance site are not allowed near the disassembly area. This may mean that it is not safe to move an entire generator across a facility.

The reason that the generator would have to be transported to a heating facility by ship is because it is not physically possible to move an 8 m generator on land. There are no vehicles that could carry this nor is it safe because the magnets are still hot during transport.

Due to all the logistical challenges that come with complete demagnetisation, this study will look into the possibilities of local thermal demagnetisation. Although this is not done for WEEE, the size of the permanent magnets and the assembly of the rotor provide an interesting opportunity that could be technically and economically viable for the optimal recovery of the permanent magnets from the generator.

3.3 | Summary of results

A summary of the key differences and similarities between the permanent magnets in WEEE and OWTs for the characteristics as well as the recycling processes involved can be seen in Table 3.12. The table collected the main findings from each of the previous steps to provide an overview for comparison.

	WEEE	OWTs
Characteristics	<ul style="list-style-type: none"> • Life span <10 years • Quantity per product range 0.5-300g • 0.144% recoverable from total inflow • Constant flow 178kg/month • Broad variety of compositions and applications 	<ul style="list-style-type: none"> • Life span, 20-35 years • Magnet size about 100-1kg • Quantity per product >1000 kg per turbine • Instant flow >400t • Uniform magnets & assembly for one wind farm
Recycling grade	<ul style="list-style-type: none"> • Magnet to element more realistic due to impurities • Increased liberation improves recovery grade • Complex material mixture 	<ul style="list-style-type: none"> • Magnet to magnet feasible due to purity • Size reduction challenging due to magnetism and scale • Sorting and separation of ferrous metals difficult
Disassembly	<ul style="list-style-type: none"> • HDDs manually disassembled from main component • Labour intensive due to small scale • PM still magnetised during disassembly 	<ul style="list-style-type: none"> • Mechanical methods damage magnets due to brittleness and force required • Thermal treatment dissolves adhesive before magnet is demagnetised • Difficult to disassemble when magnetised
Demagnetisation	<ul style="list-style-type: none"> • Smaller magnets have smaller magnetic forces • Done after disassembly, shredding and separation • Mostly thermal in a furnace • Mix of permanent magnets, varying Curie temperatures 	<ul style="list-style-type: none"> • Larger magnets have stronger magnetic forces • Needs to be done before disassembly • Thermal and local demagnetisation preferable • Identical permanent magnets, same Curie temperatures

Table 3.12: Overview of the comparison between recycling WEEE and OWT permanent magnets

Disassembly

4.1 | Assembly

The permanent magnet generator consists of a moving outer rotor, fixed inner stator, a rotor brake and permanent magnets, indicated in blue in Figure 4.2 and 4.1. The outer rotor has a diameter of ■■■ mm and has ■■■ magnet casings distributed over ■■■ columns in ■ rows fixed to the inner wall using slots. Each casing contains 6 permanent magnet blocks which are placed in the center of the casing.

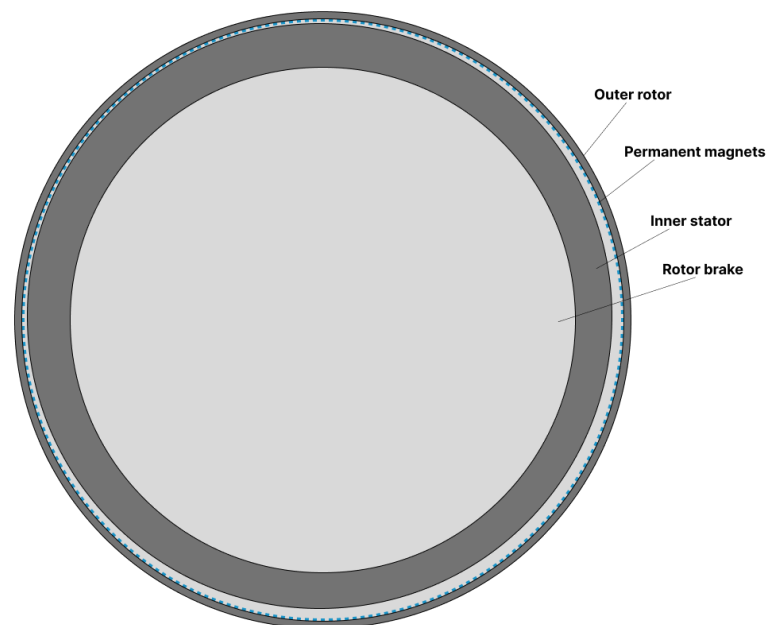


Figure 4.1: A basic overview from the top of the generator assembly of an OWT.

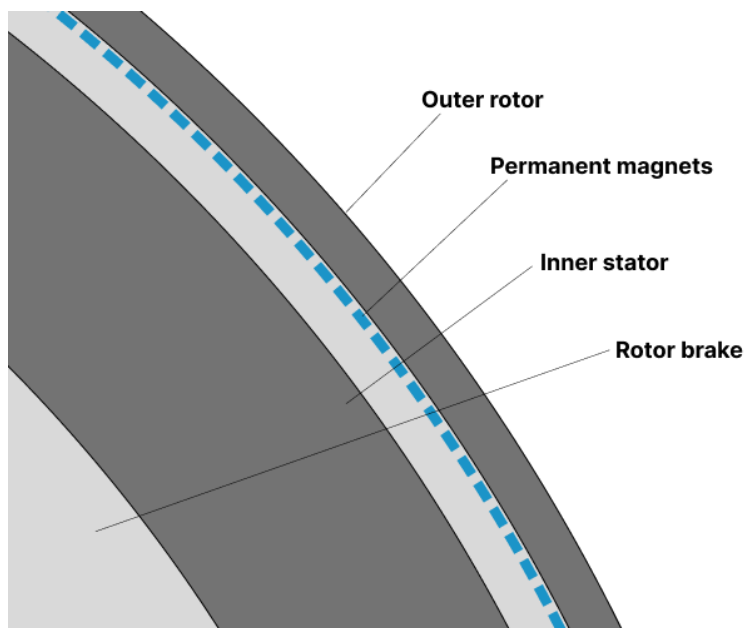


Figure 4.2: Zoomed in view of the basic overview from the top of the generator assembly of an OWT.

Since disassembly is often the reverse of the assembly process it is important to understand how an OWT is assembled. Information on the assembly of the OWT generator was obtained through a visit to the SGRE nacelle assembly site in Cuxhaven, Germany, with Crosswind on the 5th of May 2022. At this site, nacelles for the SG 11.00-200DD direct drive OWTs, referred to as the CrossWind OWT (CW OWT), are assembled.

4.1.1 | Magnet assembly

The shape of the permanent magnets in the CW OWT is shown in Figure 4.3a. The exact dimensions of the permanent magnets are unknown, but were derived from information provided by the case companies. Based on the rotor diameter and the number of magnets the magnets' dimensions were estimated to be \blacksquare mm (l), \blacksquare mm (w) and \blacksquare mm (h).

In the CW OWT, \blacksquare permanent magnets are stacked on top of each other as shown in Figure 4.3b, which gives a stack of permanent magnets with dimensions \blacksquare mm (l), \blacksquare mm (w) and \blacksquare mm (h). This stack of permanent magnets is then encased in a steel casing as shown in Figure 4.4. The exact material composition and type of steel for the casing are not known.

The magnet casing is composed of a back plate and front plate which are attached to each other through an unspecified adhesive. The permanent magnets are enclosed by the casing when the two plates are glued to each other. However, it is uncertain whether there is an adhesive between the magnets and the casing. The exact type of adhesive is also not known. The back plate and front plate of the magnet casing, permanent magnet and adhesive can be seen in Figure 4.5.

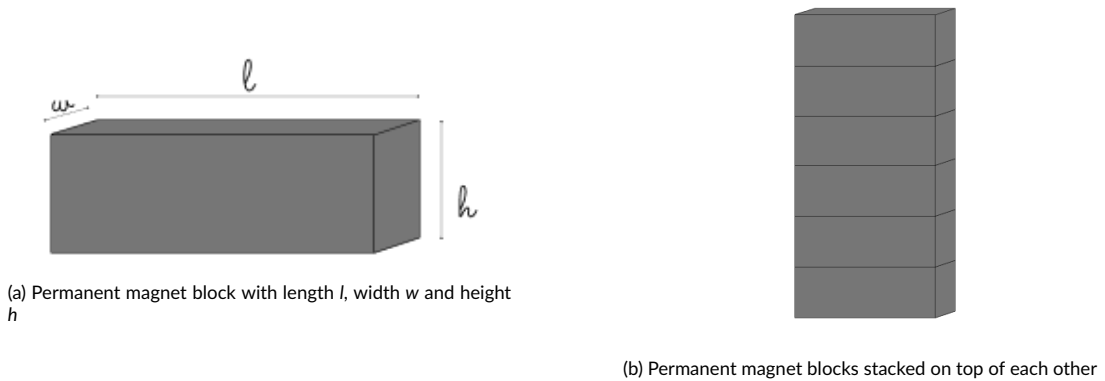


Figure 4.3: Permanent magnets in the OWT

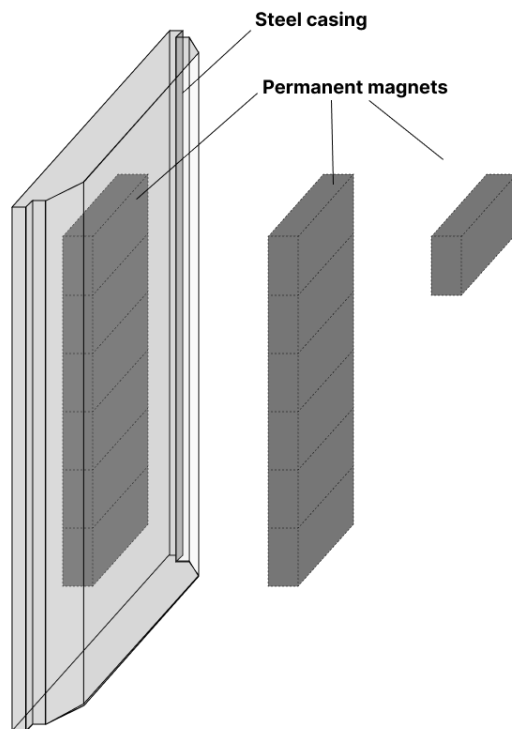


Figure 4.4: Magnet casing containing permanent magnet blocks stacked on top of each other

Since the magnet casings and permanent magnets find themselves in a moving outer rotor, it is important for them to stay in place to avoid damaging the magnet during operation. Therefore, it is possible that an adhesive is used to fix the magnets into place and prevent damage to the magnets. If this is not the case, they may be geometrically bound and physically held by the casing, where it is known that they are hermetically sealed to avoid exposure to external conditions.

There may be an air gap between the magnets and the casing due to small margins of error

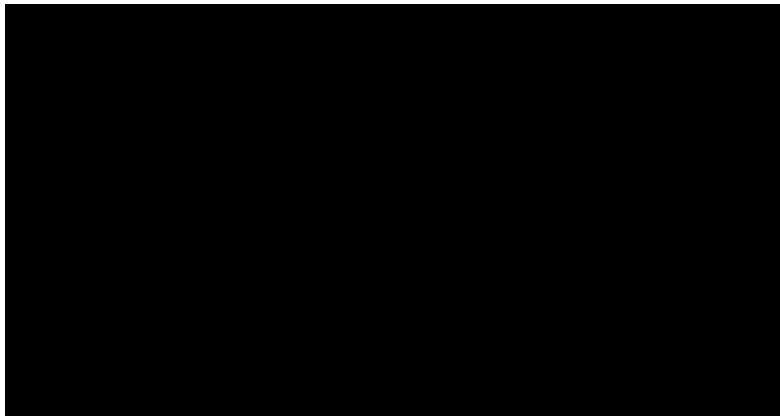


Figure 4.5: Breakdown of the magnet casing containing permanent magnet blocks shown from a top view.

in the manufacturing process of the casing and magnets. However, the physical constriction and the magnetic forces after magnetisation may further prevent movement of the magnets inside the case.

The back plate for each casing is slightly wider than the front plate such that it protrudes slightly from the front plate. This is done to create a small segment of the back plate that sticks out, referred to as strips, which will be used to fix the casing to the rotor assembly using slots. The strips can be seen sticking out from the front plate in Figure 4.6.

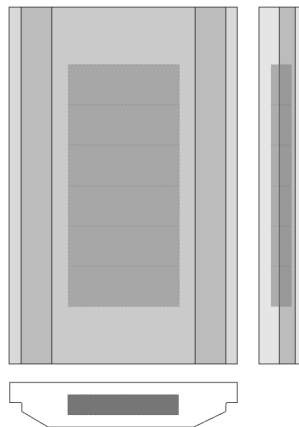


Figure 4.6: Front, top and side view of the magnet casing containing permanent magnets.

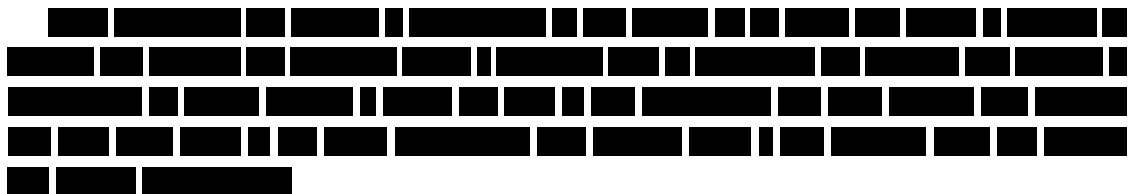
At the assembly site it was visible that each slot could stack 2 casings giving 4 rows. To determine the number of columns, the number of magnet casings which was given to be 1140 was divided by 4. This produced 285 rows, which was not possible and therefore rounded off to the nearest even whole number, 284, which has been used throughout the rest of the study. As the magnets must always be inserted in pairs, an uneven number of rows is not possible. This produced 284 rows containing 2 casings each giving a total 1140 casings.

The length of the casings were then estimated by dividing the circumference by the number of columns, which produced [REDACTED] mm. To account for the distance between the slots and keep the width easy to work with, the length of the casing was approximated to be [REDACTED] mm. The height of the casing had to be guessed based on memory of the ratio of the magnet casing and was estimated to be [REDACTED] mm. The width of the casing was determined through iterations based on the mass per casing given by the case company and density of the materials producing an estimation of around [REDACTED] mm. The approximated dimensions were used to derive the weight of the permanent magnets and may be necessary for the disassembly concept.

4.1.2 | Generator assembly

The permanent magnets are delivered to the assembly site in Cuxhaven inside their casings as a completed product in a demagnetised state, henceforth referred to as magnets, as shown in Figure 4.6. Demagnetised magnets are referred to as cold magnets, whereas magnetised magnets are referred to as hot magnets. Due to the strength of the magnets and the consequent safety issues, the magnets are primarily handled by robots.

The magnets are brought to the generator assembly area, which consists of two floors that are separated from the rest of the assembly hall in a Faraday cage. On the first floor, the magnets are stored, removed from their packaging, and transported upstairs where they are inspected, magnetised and inserted into the rotor. This process is entirely automated through the use of various robots.



The magnets are magnetised such that the opposite poles are facing the back and front plate of the casing as shown in Figure 4.7. [REDACTED], for example a North facing magnet in Figure 4.7a.

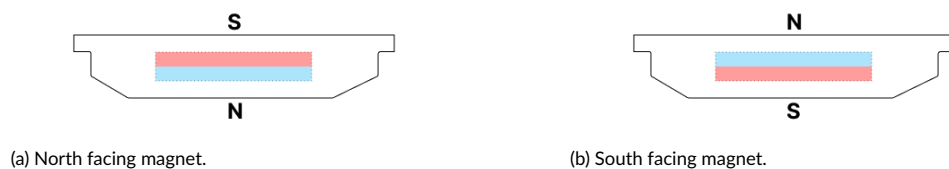


Figure 4.7: Two possible orientations for the permanent magnets, where the pole facing the front plate is used as a reference to describe the polarity of the magnet.





After the magnetisation, the magnets are transferred to the area where the rotor is positioned in the orientation shown in Figure 4.8.

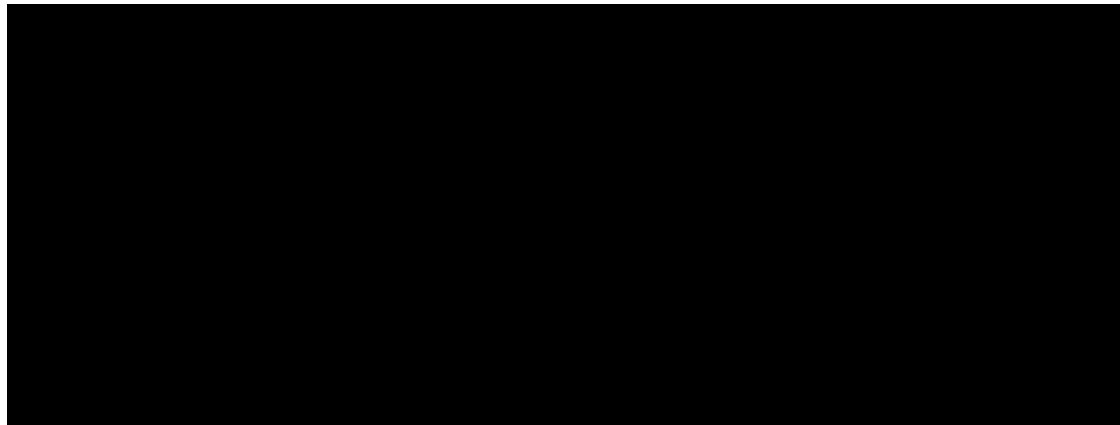


Figure 4.8: Magnet is inserted into an empty rotor via the slots.

The rotor is held in place using an exterior support system which also aims to help it maintain its shape. The inner stator and rotor brake are inserted into the outer rotor prior to inserting the magnets because they have to be placed very precisely. Once the magnets are inserted, the magnetic fields will make it difficult to move the inner stator into the desired position.

To ensure there is enough space for the magnets, spacers are spread out along the perimeter of the outer rotor between the stator and the rotor. These are also critical for the removal of magnets in case of an error. Once the permanent magnets are installed the spacers are removed.



A top view of the slots is shown in Figure 4.9. Nevertheless,

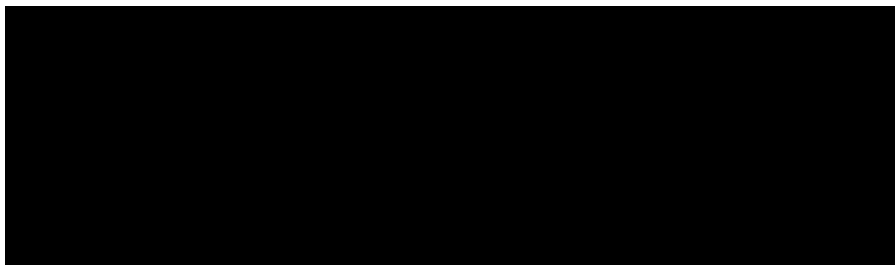


Figure 4.9: Top view of slots filled with magnets in the outer rotor.

[REDACTED]

4.1.3.2 | Service and maintenance site

SGRE has a facility in Denmark specialised in the service and maintenance of OWT generators, where they remove, clean and inspect all the magnets from the generator. It was not possible to visit the facility in person, so an interview was conducted with Elmedin on the 8th of August 2022, team lead of the repair shop of the generator, to collect information on their disassembly process.

This facility is experienced in working with and disassembling 6 to 8 MW generators and demagnetising the magnets for prototypes of the 3 to 12 MW offshore wind turbines. Although not all the generators they work with are specifically direct-drive permanent magnet generators, they have significant experience working with magnets and receive specialised training in handling magnets. Therefore, their experience provides valuable input to how the magnets might be disassembled from the rotor.

When a generator needs to undergo service and maintenance it is brought to a the facility in Denmark where the inner stator and rotor brake are removed to gain access to the interior of the rotor. In this case, all the magnets are still activated, magnetised, such that they can only take out one magnet at a time. This is due to the strong force of the permanent magnets that can potentially cause dangerous situations.

[REDACTED]

[REDACTED] This magnet was not shown but is assumed to be similar or identical to the magnet used at the assembly site. [REDACTED] as shown in Figure 4.13.

[REDACTED]

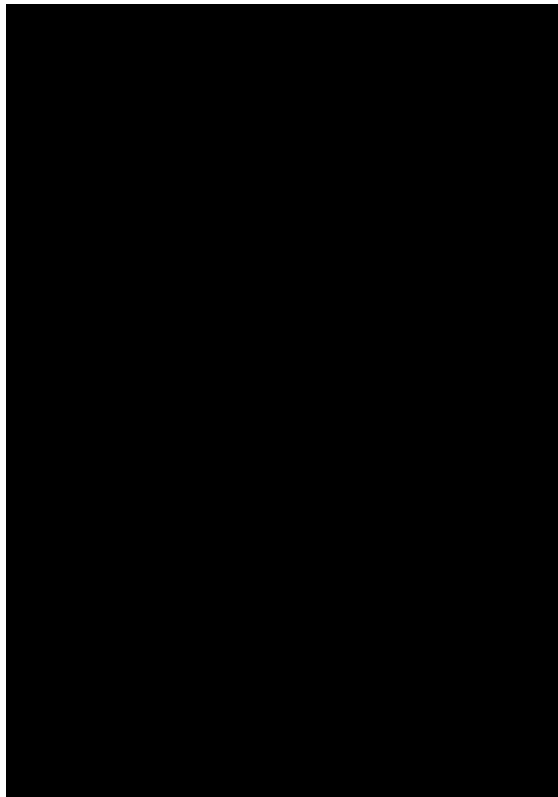


Figure 4.13: Illustration of how the magnets are lifted up against a conical shape and collected by a fibre covered magnetic plate



This holder is handled manually by an employee who then moves the magnet to another area for inspection, after which they are moved into a flamingo box. The flamingo box was also seen at the assembly site and appeared to be made of a styrofoam like material that diminishes the effects of the hot magnets. Once they are in the box, the magnets are taken to a furnace where they are demagnetised.

After this process, they have to clean the magnets and the entire rotor house, which were described to contain a variety of contamination. Examples included the presence of various fluids, which could be a mixture of lubricants or cooling liquids, and small metal parts or rust, which can destroy an entire rotor.

Throughout this entire process, no two magnetised magnets are allowed to be handled near each other and only one magnet is moved at a time. It takes approximately two days to disassemble the magnets from a single generator, meaning that the manual disassembly of the entire HKN OWF containing 69 OWTs would take at least 138 days, since the turbines are larger and contain more magnets.

4.2 | Demagnetisation concept

To demagnetise the magnets locally the permanent magnets need to be heated to the Curie temperature, which can range from 310-400 °C as found in Table 3.6. This can be done by heating a U shaped core via induction, henceforth referred to as a the core or conductor, as shown in Figure 4.14, placing it against the magnet and transferring the heat via conduction. The concept for demagnetisation and the associated principles of heat transfer are described in this chapter.

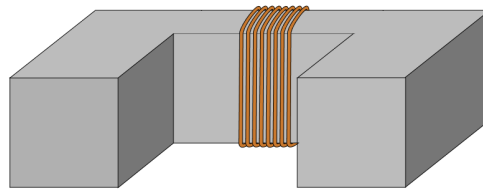


Figure 4.14: Induction heating through copper wires wrapped around a U shaped core.

4.2.1 | Theory

To understand how the magnets are thermally demagnetised, it is important to have a basic understanding of the heating principles applied. In this case a combination of induction heating is used to transfer heat via conduction. Before going into more details on the designed concept, the main principles of induction heating and heat transfer applied to the concept and its calculations are explained.

4.2.1.1 | Induction heating

Induction is the heating of a heating of an electrically conductive material through electromagnetic induction. When an alternating voltage passes through an induction coil, this produces an alternating current (AC) flow. This produces a rapidly alternating magnetic field in its surroundings that matches frequency of the current in the coil, which is characterised by magnetic flux, Φ . A basic figure of induction heating is shown in Figure 4.15.

When an electrically conducting work piece is placed inside the rapidly alternating magnetic field, electric currents are produced inside the conductor. The current inside the conductor is in the opposite direction of the applied magnetic field and are known as eddy currents. Heat is induced in the work piece due to the alternating magnetic field by joule heating and magnetic hysteresis.

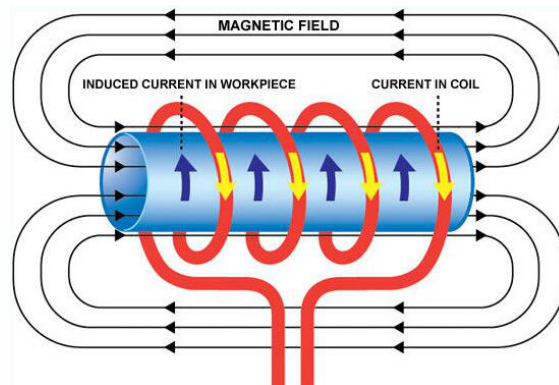


Figure 4.15: Basic diagram of the induction heating principle (RF Heating Consult, 2022)

Magnetic hysteresis only applies to magnetic metals that are below the Curie temperature, and are heated by the friction caused by the changing direction of the imposed magnetic field. Joule heating is related to the Joule Effect, which is the conversion of energy to heat in any electrically conducting material when a current passes through it. When a current I [A] flows through a conductor with resistance R [Ω], the power is dissipated into the conductor. This is given by Equation 4.1.

Joule effect

$$P = R \times I^2 \quad (4.1)$$

Due to the high frequency needed to induce the alternating magnetic field, the current density in the work piece decreases deeper within the surface of the work piece because the eddy currents are lower. This is also known as the skin effect, where the penetration depth, δ , is the depth at which the current density has dropped to $1/e$. At higher frequencies, there is a lower penetration depth whereas at lower frequencies there is a higher penetration depth. This is given by Equation 4.2, where ρ is the resistivity of the material in [Ωm], f is the applied frequency [Hz] and μ is the magnetic permeability [Hm^{-1}].

Penetration depth

$$\delta = \sqrt{\frac{\rho}{f\mu}} \quad (4.2)$$

The permeability is related to the constant $\mu_0 = 4\pi \times 10^{-7}$, which is the magnetic permeability of a vacuum, and the relative permeability, μ_r , of a material.

Magnetic permeability

$$\mu = \mu_0 \mu_r \quad (4.3)$$

The magnetic intensity inside a work piece can be roughly calculated by

Magnetic field strength

$$H = \frac{N_t I}{L} \quad (4.4)$$

Induction heating is known for being highly controllable and reproducible, with short heating times. As such, it is also possible to automate the process and avoid working with high temperatures at the work place, since it heating a material from the inside. Nevertheless, is also important to take into account heat losses from radiation and convection by the heated work pieces. Therefore, induction systems often use insulation methods to decrease the power requisites.

The material of the work piece, size, desired temperature increase and time to reach that temperature determine the power required. Materials with a higher resistivity heat more easily and require less power, than those with a low resistivity. When it comes tot he size of the work piece, it is important to consider the operating frequency of the induction heating system because of the skin effect. Finally, there are also different types of coil geometry that can be used in the design of an induction heating system.

4.2.1.2 | Heat transfer

To determine the power required to heat up the permanent magnet to the Curie temperature, the energy required to heat the system needs to be calculated. The heat required to heat a body of mass, m [kg], is given by the total energy, Q [J]. This can be calculated by following Equation 4.5.

Energy to heat a system

$$Q = mc\Delta T = mc(T_1 - T_2) \quad (4.5)$$

Where m is the mass [kg] of the material to be heated, c is the specific heat capacity [$\text{Jkg}^{-1}\text{K}^{-1}$] of the material, ΔT [$^{\circ}\text{C}$] is the change in temperature of the material such that $T_1 > T_2$, where T_1 and T_2 are either the initial and final temperature of the material. To calculate the heat flow through the material, \dot{Q} [Js^{-1}] or [W], over a given time t [s], Equation 4.6 was used.

Heat flow

$$\dot{Q} = \frac{Q}{t} = \frac{mc(T_1 - T_2)}{t} \quad (4.6)$$

Assuming a constant heat flow through a material, the temperature at two points of a wall can be calculated using the thermal resistance to conduction of a material, R_k [$^{\circ}\text{CW}^{-1}$], which is given by Equation 4.7. Where L is the distance the of the heat transfer in [m], A is the contact surface area in [m^2] and k is the conductivity of the material in [$\text{Wm}^{-1}\text{K}^{-1}$].

Thermal resistance

$$R_k = \frac{L}{kA} \quad (4.7)$$

The conduction of heat by a material is described by Fourier's Law of heat transfer shown in Equation 4.8. Thermal conductivity, k [$\text{Wm}^{-1}\text{K}^{-1}$], is a material property given by the rate of energy flow per unit time across a unit area in the presence of a temperature gradient. The thermal conductivity of a material changes with temperature, however for the purpose of simplification is assumed to be constant in the subsequent calculations.

Fourier's Law

$$q_k = -kA \frac{dT}{dx} \quad (4.8)$$

The temperature distribution through a plane wall by conduction with a constant thermal conductivity, k , can be calculated using the thermal resistance R , change in temperature ΔT and heat flow \dot{Q} . It is important to note that the conductivity is different for each material, therefore the heat flow for each material section is calculated separately to give the temperatures at different points.

Rate of heat flow through a wall

$$\dot{Q} = \frac{1}{R}(T_1 - T_2) = \frac{kA}{L}(T_1 - T_2) \quad (4.9)$$

It should be noted that power P measured in $[\text{W}]$ is equivalent to $[\text{Js}^{-1}]$ and can therefore be calculated from \dot{Q} , such that $\dot{Q} = P$ for a given material. In theory on induction heating the power of the coil P_{coil} $[\text{W}]$ is related to the power of the work piece $P_{\text{workpiece}}$, in this case the conductor, by Equation 4.10.

Power in coil

$$P_{\text{coil}} = \frac{P_{\text{workpiece}}}{\eta_{\text{el}}\eta_{\text{th}}} \quad (4.10)$$

4.2.2 | Concept design

The induction system for heating involves a set of copper wires, the coils, wrapped around a U shaped work piece made of a conductive material, referred to as the core or conductor. When an alternating current passes through the coils internal heat is generated in the core, which will then spread through the core via conduction. Depending on the material of the conductor, heating will be a combination of magnetic hysteresis and the joule effect or solely the latter.

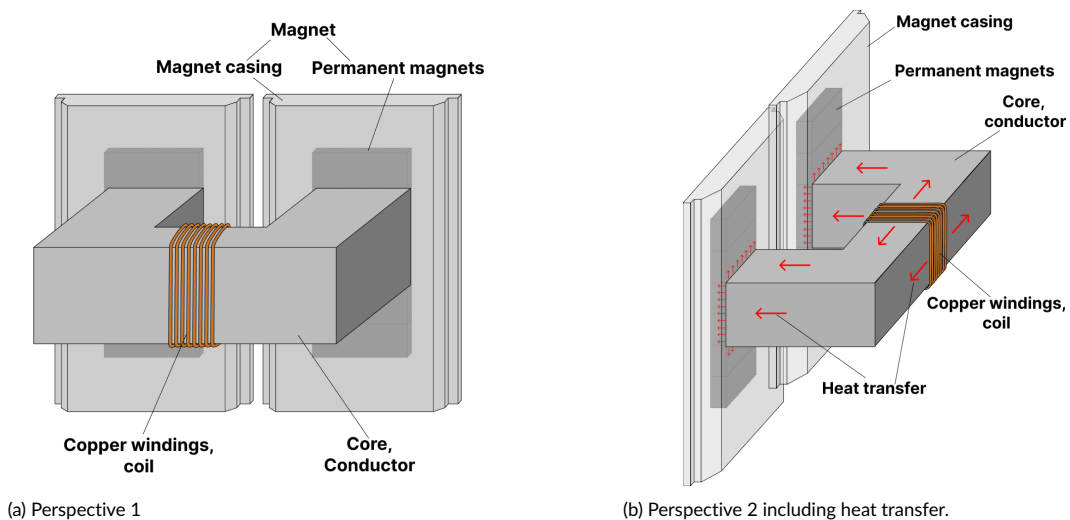


Figure 4.16: Local thermal demagnetisation through induction heating

The core can then be placed against two casings that contain permanent magnets inside the rotor as shown in Figures 4.16a and 4.16b. Due to the contact between the core and the casing and the temperature gradient between the core and the casing, heat transfer via conduction will take place between the core and the casing.

4.2.2.1 | Concept application

This system can be applied to the magnets by inserting the core from the top of the rotor and lowering it down into the rotor against the desired magnet. As the inner stator and rotor brake are removed prior to disassembly there is sufficient space to fit the core. A top view of how the core would be positioned inside the rotor is shown in Figure 4.17.

The trolley system used to insert the magnets into the assembly can be used to conduct the induction in an automated process. The trolley would have to be adapted to be able to hold the induction system and position the core correctly against the magnet for a designated amount of time. It can then move the induction block across the magnets in a controlled and automated way.

In terms of heat conduction there are many variables to take into account, such as the properties of the permanent magnet, its casing, the magnet assembly as well as the conductor and its materials, shape and size. Factors such as the Curie temperature varies for different compositions

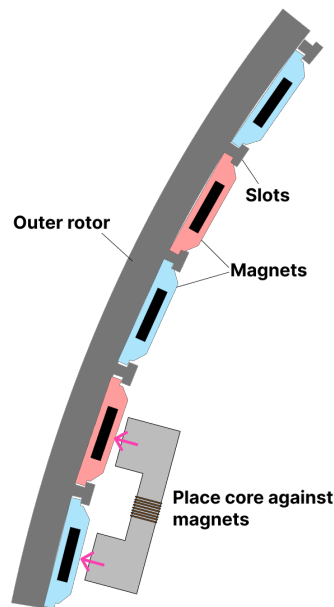


Figure 4.17: Top view of local thermal demagnetisation through induction heating

of the permanent magnet, the presence of coatings, adhesives or an air gap in the magnet assembly, the conductivity of the casing and conductor as well as the contact surface area will affect how heat is transferred. These variables are discussed in Section 4.2.3.

As there are n magnets spread over m columns and k rows, the ideal situation would be to replicate the core not only for both sides but also to heat multiple rows. Depending on the power capacity and current required for induction, n cores can be used concurrently to heat multiple magnets. An example of how the cores can be duplicated and stacked on top of each other to heat multiple rows is shown in Figure 4.18.

A maximum of k cores can be used to heat up n magnets on one side of the rotor, such that a total of n magnets can be heated up synchronously. If each trolley were to heat n magnets at once, that means each trolley would have to repeat the induction process k times to demagnetise all the magnets. However, if the cores are not stacked and each trolley only demagnetises two magnets at once, then they have to demagnetise $2k$ magnets at most.

4.2.2.2 | Practical aspects

In practice, when placing the system inside the generator assembly and demagnetising all the magnets, there are multiple aspects that need to be accounted for such as polarity of the magnets, order of demagnetisation and scalability. Since the magnets are placed against the inner walls of the outer rotor, in large cylindrical shape, there will be a magnetic field inside the generator assembly. The presence of the magnetic field will influence the behaviour of the demagnetised magnets and the remaining magnets.

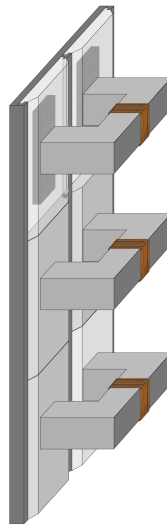


Figure 4.18: Thermal demagnetisation of multiple magnets by utilising multiple cores for induction.

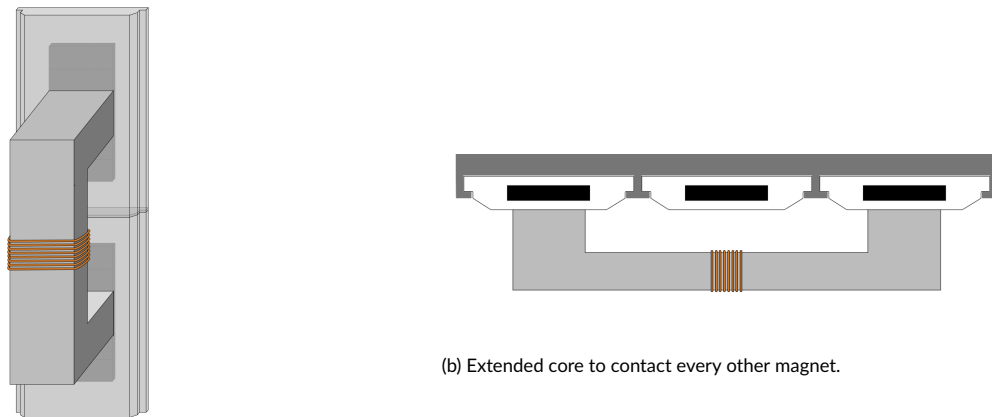
During assembly the magnets are installed one pole at a time, as a safety precaution and to balance the magnetic field which prevents buckling and deformation of the outer rotor. At the service and maintenance site, all the poles of one polarity are removed before the other polarity is removed, while also alternating between opposing sides during removal. When one or more magnets within the magnetic field are demagnetised this may affect the behaviour of the magnetic field.

Removing magnets on one side or both poles at once can cause the magnetic field to become unbalanced and result in safety hazards. For example, the study on the disassembly of permanent magnets from electrical machines mentioned in Section 3.2.3 described magnets flying around. From the interviews with experts in electromagnetism and permanent magnet machines Elmedin, Paul, Jianning and Henk from SGRE, General Electric and TU Delft, it was clear that the exact impacts are not precisely known at themoment.

As a first precaution, the induction system would have to be applied simultaneously on opposing sides of the rotors on the corresponding poles to account for the balance of the internal magnetic field. The controllable nature of the induction heating system means the heating concept of one core and coil can be duplicated and utilised to demagnetise the opposite side. The two trolleys that also install the magnets on opposing sides can be used to execute the heating process for demagnetisation on opposing sides.

The core in Figure 4.16 is the smallest possible size to contact two adjacent magnets that have different polarities, as the magnet columns alternate in North and South facing magnets. In practice, this is may not be preferable due to safety and buckling of the outer rotor, thus it is also possible to either rotate the core or extend the core as shown in Figures 4.19a and 4.19b.

To transfer heat efficiently via conduction the contact area of the U shaped core needs to be



(a) Core rotated 90° to contact two magnets in the same column.

(b) Extended core to contact every other magnet.

Figure 4.19: Alternative orientation for the core on the magnets

fully in contact with the permanent magnet. Since the outer rotor is circular, the rounding may create a small angle between the core and the magnets. The advantage of the vertical core is that it may be easier to ensure that the magnet is fully in contact with the magnet. The elongated U shaped core would be more susceptible to the curvature of the rotor.

The cores in Figure 4.19a and 4.19b would have different geometries from the original core concept, where the mass of Figure 4.19a would be 24.5% smaller and that of Figure 4.19b is 69.4% larger. The core in Figure 4.19a has 10mm less distance between the permanent magnets in the vertical direction than in the horizontal direction, due to the presence of the slots, which are assumed to be around 1mm. The core in Figure 4.19b requires an elongation of at least 10mm.

The vertical orientation of the core will require the cores to be stacked differently, such that only 1 core would fit in one column. To heat more magnets, another stack of three on the alternate column would need to be added. The elongated core can still stack 1 core to heat 1 magnet, but its larger size means that more mass that needs to be heated and more heat will be lost due to the greater surface area by radiation and convection. This may also inadvertently heat the middle column if heat is transported via radiation and convection.

In a broader context, the other advantage of the vertical orientation would be that it is less sensitive to the curvature, such that it may also be applicable to permanent magnet generators with different diameters. However, the size of the permanent magnets, casings and distance between rows may vary for different generator types. Thus the core would need to be optimised or altered to accommodate different geometries.

Another critical consideration is the material of the core, which needs to be conductive. Based on basic induction theory, a magnetic and conductive material is preferable due to combined heating via hysteresis losses and Joule heating. However, the additional heat from hysteresis losses

only applies to materials that are magnetic, once a material loses its magnetic properties this is no longer the case.

The aim is to heat the permanent magnet to the Curie temperature, which means that the conductor will have to be heated above the desired temperature to transfer the heat. Therefore, it can be assumed that the conductor will exceed the Curie temperature and also lose its magnetic properties. Thus it is not necessarily preferable to use a magnetic material, the heat transfer would rely predominantly on the material's conductivity.

Another aspect is the effect of using a magnetic material as a conductor in a highly magnetic field. If the conductor were to be made of a magnetic material, it may be difficult to control the movements and thus the positioning the core within the generator assembly. Additionally, this may be unsafe as other magnetic materials are also not allowed near the generator assembly on site, as mentioned during interviews with the SGRE representative. Therefore, it would be undesirable to use a magnetic material inside the generator assembly as a conductor, unless it is already heated beyond the Curie temperature and demagnetised itself.

4.2.2.3 | Disassembly aspects

The current concept aims to locally demagnetise the magnets inside the generator assembly with an active magnetic field. Once a pair or group of magnets is demagnetised, it is possible that the magnets may become re-magnetised due to the effects of its neighbouring magnets and the presence of the magnetic field. Based on interviews with Jianning, Henk, Paul and Elmedin, this is possible but it is unlikely that they will reach a magnetisation close to their original magnetisation.

From a high level theoretical perspective, magnetism arises from the alignment of the magnetic domains within the material. If the material is exposed to a magnetic field above H_S , this may cause the material to become re-magnetised. However, if a material is exposed to a temperature beyond the Curie temperature, the thermal energy should disorient the domains sufficiently that they will not re-align. The most magnetisation they might theoretically be able to regain would be its remanence.

During the period of this study, there were no other sources found that could validate or provide any example of what would happen to the magnetisation after demagnetisation. The main underlying consideration is whether the magnets should be disassembled when they are still hot, directly after demagnetisation, or after all the magnets have been demagnetised and cooled down.

The disassembly of the magnets while they are hot, would minimise the potential effects of re-magnetisation and ensure that they are fully demagnetised during their mechanical removal. However, the removal of magnets while they are hot means that they need to be handled at temperatures up to the Curie temperature, which ranges from 310-400°C, and stored somewhere safe for cooling.

The study by [Bahl et al. \(2020\)](#), addresses the fact that magnets may not have to be fully demagnetised in order to handle and remove them. It may still be possible to remove the magnets with some remnant magnetisation, depending on the strength of the magnetisation. This means

that there is an allowable remanence for the magnets to be handled, and realignment of magnetic domains within a limit is acceptable. This also means the magnets would not have to be heated all the way up to the Curie temperature exactly.

Another consideration that needs to be taken into account after thermal demagnetisation is the thermal expansion of the materials based on the thermal expansion coefficients of the different materials. If the magnets expand too much during heating it may not be possible to remove the magnets while they are hot, and cooling is required for them to compress sufficiently for handling.

4.2.3 | Theoretical model

The concept design is highly theoretical and has not been tested. Moreover, exact data on the material properties, such as geometry, conductivity, density, Curie temperature and so on, were not available due to intellectual properties. Therefore, the technical feasibility was assessed with rough calculations based on assumptions derived from the data collected throughout the study.

The rough calculations were done to provide estimates as to the heat flow, power required and effects of different parameters. These calculations were made at a very high level to provide approximate insights as to what the energy requirements are and order of magnitudes for temperatures that need to be reached. This would give an idea of whether or not the power and temperature requirements are realistic and factors need to be considered.

To determine the power required to heat the permanent magnet to the Curie temperature the heat flow was approached as a steady state conduction between composite walls. The approach is highly simplified and mainly aimed to give an idea of what type of power might be needed and the impacts of distinct variables on the power requirements. The simplified model used is shown in Figure 4.20.

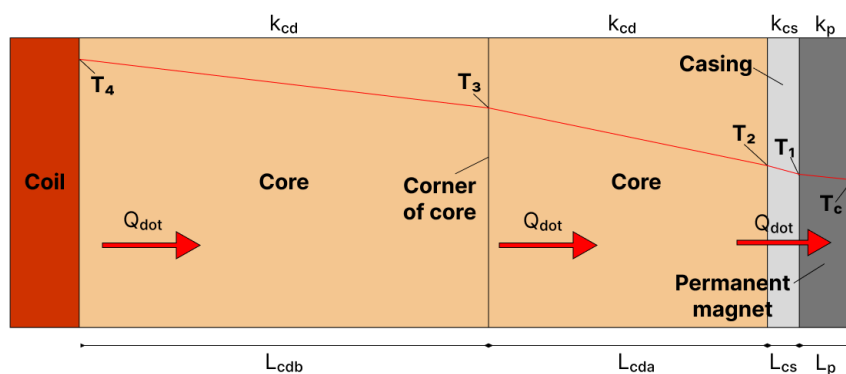


Figure 4.20: Diagram of how the heat transfer was calculated.

In the subsequent calculations, the basic core concept from Figure 4.16 is used as a starting point. The conductor was split up into two sections, where the back section refers to the long

section of the U around which the coil is wound. The front section is one of the two identical parts that stick out from both ends of the back section as shown in Figure 4.21.

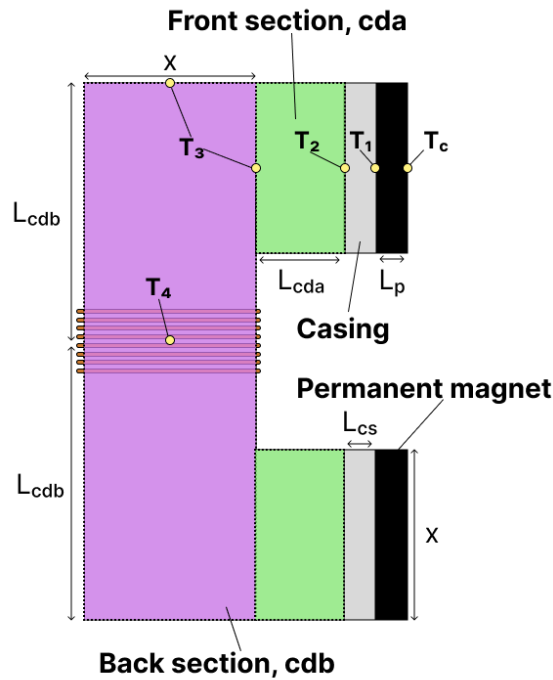


Figure 4.21: Illustration of how the heat transfer was calculated in relation to the actual core concept and the corresponding geometry.

4.2.3.1 | Assumptions

The assumed values for properties of the NdFeB permanent magnet were taken from [Bahl et al. \(2020\)](#), as the study is one of the only ones that focused on demagnetising permanent magnets from OWTs and on larger permanent magnets. The values used for different material properties are found in Table 4.1, where Nd refers to NdFeB permanent magnets, 316 refers to 316-grade steel alloy, Cu refers to a copper alloy and Al refers to an aluminum alloy from [Kreith et al. \(2010\)](#). The calculations below assume that copper is the material used for the conductor.

The Curie temperature in literature ranges from 310-400°C, as seen in Table 3.6, while [Bahl et al. \(2020\)](#) assumed it to be 300°C. Based on an insights shared by SGRE, the industry is aiming to reduce the use of REEs in their permanent magnets, which in turn reduces the Curie temperature, as these cause the resistance to temperature. A Curie temperature of 310 °C was considered on the high side for permanent magnets in OWTs based on information provided by the case company. To stay on the safe side for the calculations the estimate of 310°C was kept.

The mass the of the permanent magnets, casing and conductor were calculated by using their geometry to determine the volume and their respective densities found in Table 4.1. The geometry

Property		Units	Nd	316	Cu	Al
Specific heat	c_p	$\text{Jkg}^{-1}\text{K}^{-1}$	460	500	410	833
Thermal conductivity	k_p	$\text{Wm}^{-1}\text{K}^{-1}$	7.6	16.3	83	164
Density	ρ_p	kgm^{-3}	7500	8060	8600	2787
Relative permeability	μ_p	-	1.05	-	-	-
Curie temperature	T_{Cp}	$^{\circ}\text{C}$	310	-	-	-
Induction efficiency	η_{tot}	-	-	0.45- 0.5	0.05- 0.15	0.35- 0.40

Table 4.1: Assumed values for the properties of CW OWT permanent magnets and conductor materials based on (Bahl et al., 2020; Dallos, 2019; Kreith et al., 2010; Rudnev et al., 2017)

for the different parts are given in Table 4.2. The estimated density and geometry of the permanent magnet and casing give an approximate mass of 6.5kg which is in line with the approximate information provided by the case companies.

Part	x [m]	y [m]	z [m]	mass [kg]
Permanent magnet	■	■	■	■
Casing				■
Backplate	■	■	■	
Frontplate mid	■	■	■	
Frontplate front	■	■	■	
Conductor (Copper)				■
Back section	■	■	■	
Front section	■	■	■	

Table 4.2: Approximated geometry of the permanent magnet, casing and conductor

The permanent magnet refers to the dimensions of a single magnet block. For ease of calculation the casing was split up into three sections, the back plate, the midsection of the front plate, where the magnets are located, and the front of the front plate which is on top of the magnet. The volume of the 6 magnets was deducted from the volume of the midsection during calculations.

In the simplified model, the corner of the core is approached by splitting the core into two parts. L_{cda} is the distance until the corner and L_{cdb} is the distance of the edge of the back section to the center of the core where the coil is as shown in Figure 4.21. This is done because there is usually a shape factor, however this complicates the model and is therefore taken as a long straight piece with two separate core sections, as shown in Figure 4.20.

This system does not take heat losses of the conductor or permanent due to the surrounding through conduction to other magnets or convection and radiation in the air into account. The rest of casing around the permanent magnet was also not included in the calculations. In addition, the adhesives, coating or potential air gap between the permanent magnet and the casing are considered negligible.

It was assumed that heat flow \dot{Q} and surface area A is constant throughout the system, such that T_1 was determined using Equation 4.9, for conductivity k_p and length $L_p/2$. Using T_1 , T_2 was calculated for conductivity k_{cs} and length L_{cs} , followed by the calculation of T_3 and T_4 in the same

way. Next T_4 was used to determine the energy required to heat the core to T_4 using Equation 4.5.

In this model, the temperature of the permanent magnet is T_C at the back of the magnet, such that $L_{pp} = \blacksquare$ m is the thickness of the magnet. The thickness of the front plate of the casing against the magnet is $L_{cs} = \blacksquare$ m, which is equal to the y measure of front plate front in Table 4.2. The length of the front section of the core is given by $L_{cda} = \blacksquare$ 5m and the length of half of the back section of the core is given by $L_{cdb} = \blacksquare$ m.

4.2.3.2 | Calculations

For this calculation $m = \blacksquare$ kg, the mass of \blacksquare permanent magnets inside a magnet casing, T_1 is the Curie temperature, $T_1 = T_C = 310^\circ\text{C}$ and T_2 is the ambient air temperature set at $T_2 = T_a = 20^\circ\text{C}$. The energy required to heat the magnet to the Curie temperature was calculated to be $Q_p = \blacksquare$ kJ based on Equation 4.5.

The energy required to heat the permanent magnet to the Curie temperature, $Q_p = \blacksquare$ kJ, was used to calculate the heat flow, \dot{Q}_p , using Equation 4.6. Time taken to heat the permanent magnets from ambient air temperature T_a to the Curie temperature T_C , t_p , is an unknown variable in the heat flow equation and therefore needs to be set based on the desired heating time. The heat flow, \dot{Q}_p , was calculated for different heating times starting with 60s and up to 300s at 60s intervals and assumed to be constant throughout the material. The temperatures at different points in the material, based on different heating times t_p are shown in Table 4.3.

t_p [s]	T_1 [$^\circ\text{C}$]	T_2 [$^\circ\text{C}$]	T_3 [$^\circ\text{C}$]	T_4 [$^\circ\text{C}$]	Q_{cdb} [kJ]
60	\blacksquare	\blacksquare	\blacksquare	\blacksquare	\blacksquare
120	\blacksquare	\blacksquare	\blacksquare	\blacksquare	\blacksquare
180	\blacksquare	\blacksquare	\blacksquare	\blacksquare	\blacksquare
240	\blacksquare	\blacksquare	\blacksquare	\blacksquare	\blacksquare
300	\blacksquare	\blacksquare	\blacksquare	\blacksquare	\blacksquare

Table 4.3: Temperature calculated at different points the the material corresponding to Figure 4.20

Table 4.3 gives an idea of how the temperature at different points in the material varies throughout the materials based on different heating times for t_p . The shortest heating time $t_p = 60$ s gives the highest temperature at the coil $T_4 = 527^\circ\text{C}$ and the longest heating time $t_p = 300$ s gives the lowest temperature at the coil $T_4 = 353^\circ\text{C}$. The higher the temperature at the coil T_4 , the higher the energy needed to heat the back-section of the conductor Q_{cdb} .

The different heating times for t_p lead to different energy requirements Q_{cdb} to heat the back-section of the conductor to T_4 . The energy required to heat the back-section of the conductor Q_{cdb} with mass m_{cbd} to T_4 from the ambient temperature T_a was calculated using Equation 4.5. Where the mass is taken over the entire length of the back-section rather than just half, as indicated in purple in Figure 4.21. This is done because the entire mass will need to be heated to the desired temperature, even if only one side is being considered in this model.

Using the total energy to heat the back-section Q_{cdb} , the power required to the conductor P_{cdb} and the power required to heat the coil P_c [W] can be calculated. The power required to heat the conductor P_c depends on the time taken to heat the conductor t_{cd} [s]. Due to the larger mass of the conductor, the range of t_{cd} set between 120s to 600s with 120s intervals.

From P_{cd} the power required to heat the coil P_c was calculated based on a fixed assumed thermal and electrical efficiency using Equation 4.10. The electrical and thermal efficiency of the coil, η_{el} and η_{th} respectively, depend on various parameters for the coil and were therefore simplified and approximated to a fixed total efficiency $\eta_{tot} = \eta_{el}\eta_{th} = 80\% \times 80\% = 64\%$. The power requirements for varying t_p and t_{cdb} is given in Table 4.4.

t_p [s]	$P_c(t_{cdb})$ [W]				
	$P_c(120s)$	$P_c(240s)$	$P_c(360s)$	$P_c(480s)$	$P_c(600s)$
60	██████	██████	██████	██████	██████
120	██████	██████	██████	██████	██████
180	██████	██████	██████	██████	██████
240	██████	██████	██████	██████	██████
300	██████	██████	██████	██████	██████

Table 4.4: Power required for different heating times of the permanent magnet and conductor

Analogous to the heating of the permanent magnet, the shortest heating times $t_p = 60s$ and $t_{cdb} = 120s$ gives the highest power requirement $P_c = \text{██████}$ W, while the longest heating times $t_p = 300s$ and $t_{cdb} = 600s$ gives the lowest power requirement $P_c = \text{██████}$ W. The relationship between the power requirements for the permanent magnet and conductor and time taken to heat them are shown in Figure 4.22.

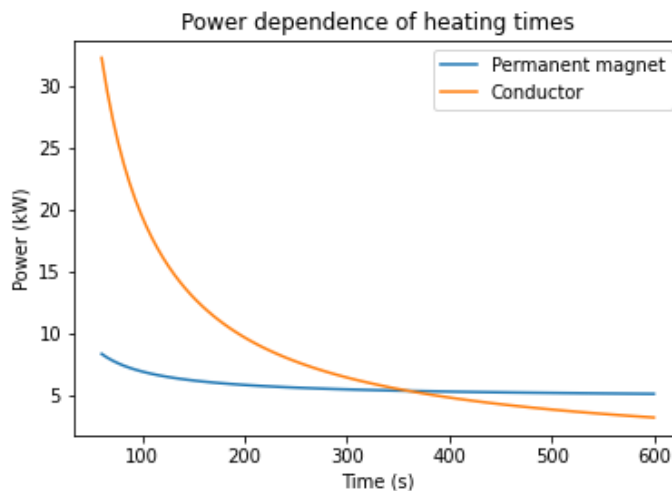


Figure 4.22: Plot of how the power required for heating varies with time taken to heat.

The blue line indicates the power required to heat the permanent magnet P_p for a varying heating times t_p , whereas the orange line indicates the power in the coil P_c required to heat the

back section of the conductor with varying heating times t_{cdb} . There is an exponential relationship between the power and time, where the gradient of the orange line is significantly steeper than that of the permanent magnet. The range of P_c is [REDACTED] W compared to P_p ranging from [REDACTED] W.

It is also clear that there is a trade-off between the time taken to heat the material and the power required. For the permanent magnet, the gradient in the exponential graph becomes lower after about $t_p = 120s$, whereas this is around $t_{cdb} = 360s$ for the conductor. As time increases, the power saved beyond these points become smaller with time due to the decreasing gradients.

4.2.3.3 | Variables

In the basic calculations the conductor was selected to be made of copper at a set efficiency of 64%. Nonetheless, it is also possible to select other materials for the conductor and take into account their respective conversion efficiencies. The power required in the coil for conductors made of different materials and their respective conversion efficiencies is plotted in Figure 4.23.

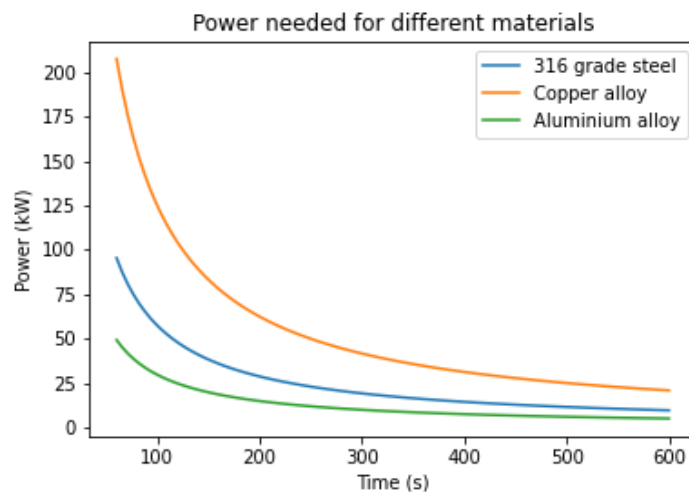


Figure 4.23: Plot of how the power required for heating varies with the time taken for different conductor materials with different conversion efficiencies.

The properties of the materials are found in Table 4.1, however since the efficiencies are not known exactly the upper limit was chosen as the material would be selected based on the the highest possible efficiency. When comparing the copper alloy with a lower efficiency of 15% in contrast to the efficiency of 64% seen in Figure 4.22, it is evident that the induction efficiency has a tremendous impact on the power requirements, raising the range for a copper conductor from [REDACTED] W to to [REDACTED] W. Steel with an efficiency of 50% has a range of [REDACTED] W, while aluminium has the lowest power range of [REDACTED] W at an efficiency of 40%.

When $t_p = 120$ and $t_{cdb} = 360$ s are fixed, and the conductor material is chosen to be aluminium with a power efficiency of 40%, other variables such as the impact of the Curie temperature can also be considered. The power required to heat the permanent magnet to $T_C = 310^\circ\text{C}$ is $P_c = \blacksquare$ W for the above conditions.

Since, precise data on the composition of the permanent magnet is not available, the power required for different Curie temperatures can be found for a range from 200°C up to 400°C . The power required was found to vary linearly with an increasing Curie temperature, with a few values shown in Table 4.5.

T_C [$^\circ\text{C}$]	P_c [W]
200	\blacksquare
250	\blacksquare
300	\blacksquare
350	\blacksquare
400	\blacksquare

Table 4.5: Power requirements for different Curie temperatures

The linear relationship gives a gradient of \blacksquare [$\text{W}^\circ\text{C}^{-1}$], meaning that the power required increases with \blacksquare W for each degree increase of the Curie temperature. When plotting the relationship for different heating times t_{cdb} , the gradient is steeper with shorter heating times and flatter for longer heating times, as shown in Figure 4.24.

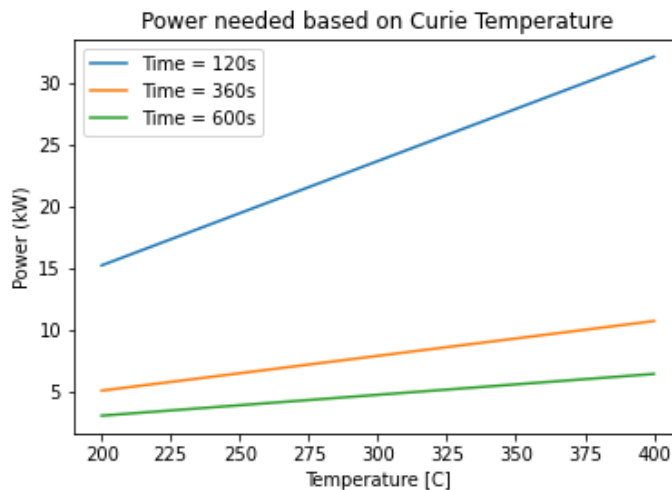


Figure 4.24: Plot of the power required for different Curie temperatures.

The size of the conductor can also be varied to adjust the surface area that is in contact with the magnet. This was done by changing the height of the conductor as shown in Figure 4.25, which was set to be at least equivalent to the height of one permanent magnet block at \blacksquare m and

at most the height of the entire magnet at 0.075 m . The power was plotted against the changing heights in Figure 4.26, where the x-axis was plotted in cm to make it easier to read.

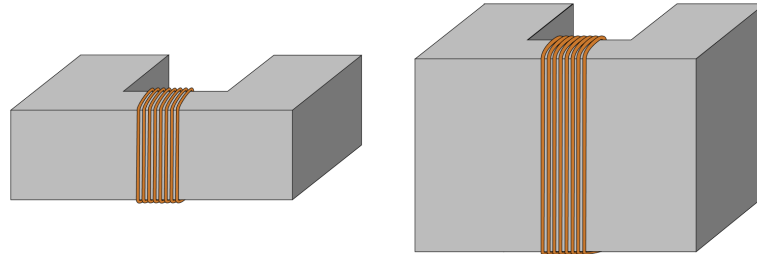


Figure 4.25: Illustration of the different height of the conductor.

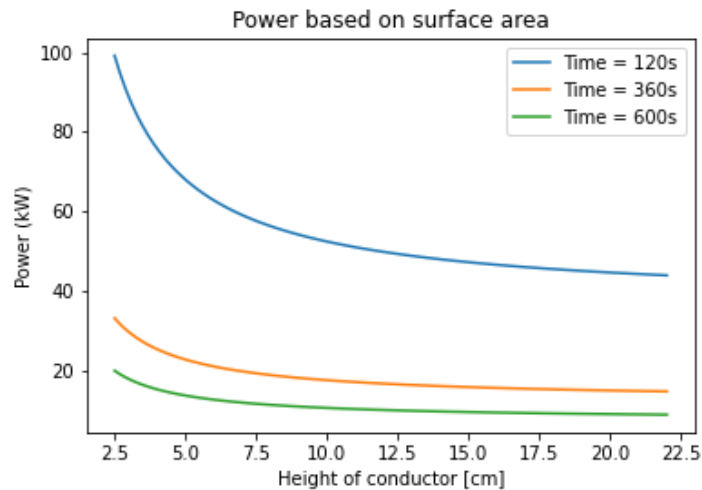


Figure 4.26: Plot of the power required for different contact surface areas of the conductor with the magnet with a constant mass.

Figure 4.26 shows that the power and area are exponentially related but with a milder curve in contrast to the material selection in Figure 4.23. From a height of at least 0.075 m upwards the gradient of the curve gradually becomes flatter such that the surface area does not have a large impact on the power usage anymore. The longer the heating time of the conductor t_{cdb} , the more dependent the power is on the surface area, where t_{cdb} is a dominating factor. This is in line with the pattern in Figure 4.22 and 4.24.

When the mass of the conductor also varies with the surface area the power and height of the conductor are related as shown in Figure 4.27. This shows a linear relationship between the power and area, where the power increases with an increasing surface area and thus also an increasing conductor mass.

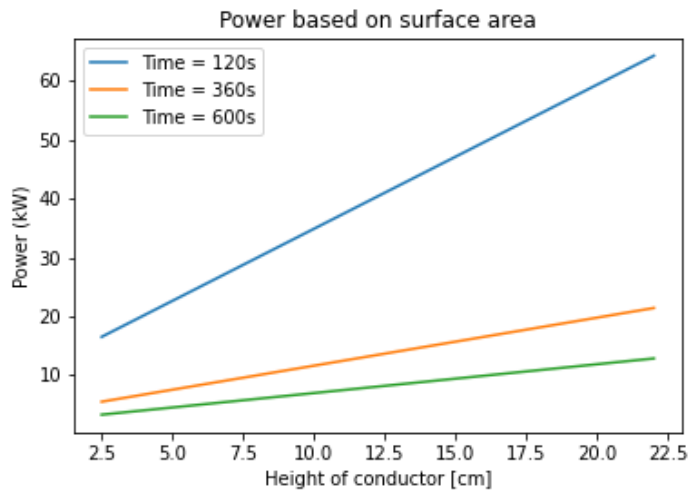


Figure 4.27: Plot of the power required for different contact surface areas of the conductor with the magnet with a varying mass.

4.2.3.4 | Disassembly time

Based on the calculations in this section, an approximation of the optimal time taken to heat the magnet would be $t_p = 120s$ and that of the core would be $t_{cdb} = 360s$. Using an aluminium core at an efficiency of 40% to heat the magnet to $T_c = 310^\circ C$ would require the power in the coil to be $P_c = \blacksquare$ W.

If it takes 2 days to disassemble a single OWT without demagnetisation, the disassembly of the CW OWF would take 138 days in total. It would take \blacksquare hours to demagnetise all the magnets if only \blacksquare magnets were heated at once \blacksquare , where an additional \blacksquare s was approximated for the time taken to move the core between positions such that the time taken per magnet $t_{tot} = t_p + 20 = 140s$.

If \blacksquare cores are stacked on top of each other on both sides of the rotor, \blacksquare magnets could be heated simultaneously which would require \blacksquare movements of both of the trolleys. Using the same $t_{tot} = \blacksquare$ s, the time taken to demagnetise the entire generator would be \blacksquare minutes. When only \blacksquare cores are stacked for the vertical orientation in Figure 4.19a, the time taken would be \blacksquare minutes.

If the disassembly time per magnet is assumed to take \blacksquare s per magnet it would take an additional 6 hours in each case to disassemble the entire generator after demagnetisation. The shortest possible disassembly time for an OWT generator including the demagnetisation would be 8 hours. This means that an entire OWF with 69 OWTs could be demagnetised and disassembled in 23 days and could take up to 49 days if only 4 magnets are demagnetised at a time.

4.3 | Summary of results

An overview of the results for the disassembly of the permanent magnets from OWTs can be found in Table 4.6. The table provides an overview of the key findings from the site visit, disassembly concept, the technical aspects and its variables.

Discussion

5.1 | Interpretation of results

5.1.0.1 | Analysis of calculations

Looking at the results in Figure 4.22, it is clear that the power required in the coil is a lot more sensitive to heating time than the permanent magnet. This is because the exponential curve is a lot steeper, which also caused the range to be a lot greater. Therefore, when it comes to controlling the power of the demagnetisation concept, setting the appropriate heating time for the conductor is more important than the permanent magnet.

The reason the power is sensitive to the heating time is because the shorter the time given to heat a material the more power is required to heat it in that time. As the conductor as a greater mass a shorter time will affect it more than the permanent magnet of a smaller mass. From this perspective it would be preferable to heat a smaller conductor to reduce the power required, however this influences the contact surface area.

A larger contact surface area is preferred for heat transfer between two materials, as shown in Figure 4.26, where the mass is constant. As the height of the conductor increases, so does the area, where it can be seen that the power decreases with increasing area. In reality, only extending the height would result in a larger mass, which can be seen in Figure 4.27. By comparing the two graphs it is clear that while a larger contact surface area is preferred, the mass plays a larger role in determining the power demand.

The power needed for different materials shown in Figure 4.23 indicated that aluminium is the preferable choice as the conductor material. This is because the power required is the lowest of the three options, which is primarily due to the induction heating efficiency, also referred to as the conversion efficiency. Even though the efficiencies used were rough estimates, they have an overarching effect on the power requirements.

For the induction heating system to be efficient, a material is preferred that has a high electric resistivity such as steel. Copper and aluminium are less common because of their low electrical

resistivity meaning that the heat created by the Joule effect due to resistance will dissipate and a higher amount of power is needed to heat the material, which also relates to their high conductivity. As a result, they will take longer to heat and will necessitate more power to reach the same temperature.

The heat generated by induction is only produced locally, thus heating up an entire material will require the locally produced heat to spread via conduction. For the transfer of heat a conductive material is preferable but for induction heating a material with a lower conductivity is preferable. Although the model currently presents aluminium as the favourable conductor material, not all aspects of induction heating were taken into account.

Aspects that were neglected include the skin effect, which would affect the heat flow through the entire system if only the exterior of the core is heated. This means that heat transfer could take significantly longer as conduction would take longer with a lower internal energy over the same power input. As it was not modelled, it is unknown how the skin effect would have affected the heat transfer through the conductor to the permanent magnet.

Another variable plotted against the power was the Curie temperature, which was given a range from 200 - 400 °C⁻¹ and is shown in Figure 4.24. This is because the exact material properties of the NdFeB magnet are unknown and it is therefore interesting to see what the required power would be for different Curie temperatures, where a few values can be seen in 4.5. The main finding is that there is a linear relationship between the Curie temperature and power, where the gradient gets steeper with decreasing heating times.

To reach a higher temperature it is logical that a larger amount of power is needed, however it is interesting to see the gradient increase for the heating times. This is in line with the results in Figure 4.22, where the power ranges less with time as time increases, meaning that the shorter the heating time the more sensitive the power is to other variables. This can also be seen in the plot of the contact surface area with power in Figure 4.26. In both plots, the orange and green line for $t = 360$ and 600 s are substantially closer to each other than the blue line where $t = 120$ s.

5.1.0.2 | Analysis of model

Overall, the orders of magnitude found for the power requirements and temperature gradients of the model are realistic. Nonetheless, the design of an induction heating system is far more complex than conveyed in the results. The simplified model does not go into the shape of the conductor, distance of the coils to the conductor, number of windings, diameter of the coil, distance of windings to each other and so on.

Based on the model, it is possible that the induction and conduction heating concept could work. However, the model is highly dependent on heat transfer through multiple materials across different distances. This study only looked at one possible option for thermal demagnetisation by combining induction with conduction. There are nonetheless, many other options that can be considered such as direct induction where the induction coils are directly applied to the permanent magnet.

Although this was initially considered, the core concept developed was more tangible as it was less dependent on in-depth knowledge of induction heating systems to develop. Direct heating via induction could be a viable option that may have lower power losses as it can be directly applied to the surface of the material. Additionally the material is highly magnetic and thus could benefit from both Joule heating and hysteresis losses simultaneously. The only challenge could be the skin effect as the heat may not penetrate to the core of the magnet.

The disassembly concept developed focuses on the demagnetisation of the permanent magnets from the rotor before disassembly to decrease the disassembly time and improve the ease of disassembly. If the concept can successfully heat the magnets in the given time then the disassembly time of a generator could be improved from 2 days per generator to 8 hours such that an entire OWF can be disassembled in 23-49 days.

It takes half a day to assemble an entire nacelle but it takes 2 days to disassembly just the generator. This shows that the disassembly is significantly more challenging than the assembly and could be faster. Seeing as half a day is 12 hours, it seems would that disassembly could be done within 8 hours as disassembly is usually less precise. Looking at the assembly times in practice, the calculated disassembly times could be realistic as they are not exceptionally fast compared to assembly.

5.1.1 | Implications of results

The benefits of the concept is that it has many variables, such as the shape, materials and orientation. Putting the core in a vertical position as seen in Figure 4.19a would be the orientation that is most applicable to other generator diameters as well, since it is less sensitive to curvature and more dependent on the height of the magnets and construction of the casing. As such, the vertical position is likely the best orientation for the magnet from a efficiency and feasibility perspective.

From a scalability perspective, the sane core set-up can be applied throughout an entire OWF but ideally could also be applied to different types of OWT. For this, the assumption would be that most OWTs of the same magnitude have similar layouts and constructions, with small discrepancies in the details. The nacelle visited at Cuxhaven for example was not the CW OWT but a pretty much identical one, meaning the concept could be applicable to two OWF. Moreover, there is also a possibility that the SGRE 6, 7, 8, 11 and 14 MW OWTs all follow similar structures. The numbers mentioned during an interview with Elmedin who is experience in working with 6,7 and 8 MW DD OWTs were of a similar scale of the CW OWT.

If the magnets could be demagnetised in such a way that they can be non-destructively disassembled in a time efficient manner, this would have a positive impact on the recovery grade of the recycled material. This could potentially accelerate the economic incentive to recycle and disassemble permanent magnets, as it is currently still very labour intensive and time consuming. Developing an automatable process for disassembly means that the industry can retrieve the materials with less effort for a higher return on their investment.

5.2 | Future research

The simplified basic model gives a first impression of the behaviour of the materials and the sensitivity to various factors. The first step to improve this study would be to further develop the theoretical model into a more detailed model that accounts for more thermal phenomena such as heat loss due to convection, radiation and to the surrounding. At the same time, the time dependence of various material properties could be taken into account to improve its accuracy. The shape factor of the core and the adhesives and coatings inside the coating could also be included. Moreover, obtaining the exact dimensions and properties of the materials would also increase the accuracy.

There are many aspects of the induction heating system that can be optimised. The shape for example was mentioned, but another consideration could also be a hollow core, which would maximise surface area and minimise mass. This could also take into account the skin depth of induction heating, although it is unsure how the material would behave as a hollow material might be more susceptible to thermal expansion and deforming.

The model focuses on the fact that the permanent magnet has to reach the Curie temperature, in accordance with most literature. According to a study by [Bahl et al. \(2020\)](#), it is not necessary to reach the Curie temperature for 90% demagnetisation. Since this was not modelled or calculated in this study, it should be noted as an important factor as the Curie temperature is one of the leading variables in the thermal model used. Furthermore, it would be interesting to test what percentage of demagnetisation is required for the magnets to be removable. This would entail that the magnetic fields and forces need to be calculated along with the remanence after exposure to a varying temperatures.

Another consideration is how long the permanent magnet has to stay at the Curie temperature and whether or not this influences the demagnetisation. [Bahl et al. \(2020\)](#)'s study uses multiple heating cycles and heats the magnet for up to 1 hour, although the demagnetisation does not appear to be linked to the heating time but predominantly to the temperature. It unclear why the material was heated in several cycles, possibly to control the heating as direct induction can work relatively quickly.

This would be an advantage of the combination of induction and conduction, because the temperature increase would be gradual and could be more controlled. Nonetheless, this cannot be verified unless the model is further developed or tested in a lab. Another reason is also because this subject and approach is new and combines materials science with electrical engineering, there are not a lot of existing examples to build on. Therefore, a practical experiment would be the best way to go from this point forward.

The best way to observe the behaviour of the materials would be to replicate the concept and test it in real life. This could help verify whether or not it is technically feasible to heat up a U shaped conductor with induction as well as whether or not sufficient heat can be transferred to the permanent magnet in a casing. For the practical experiment, it would also be necessary to

come up with a method to hold and position the core against the magnet, as this was not included in the scope of the study. It is also likely that other barriers and factors may come to light when trying to set-up the experiment, which would again provide more valuable insights.

5.2.1 | Alternative set-ups

There are also other possible ways to thermally demagnetise the permanent magnets that could be explored. These are shown in Figure 5.1 and 5.2, which show a core with two sets of copper windings with the idea to combine induction heating and an opposing magnetic field to demagnetise at a higher efficiency and an example of direct induction with the coils held close to the magnet respectively. It should be noted that these ideas are merely concepts that arose in the process of this study and that the theoretical basis of these ideas is not yet substantiated properly. It would therefore be interesting to also consider alternative options for thermal demagnetisation.

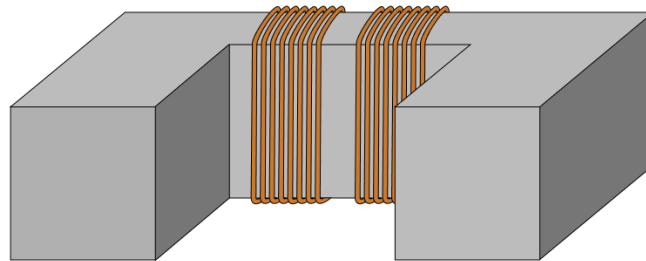


Figure 5.1: Induction heating combined with an opposite magnetic field through two sets of copper wires wrapped around a U shaped core.

Other areas worth exploring include complete thermal demagnetisation in a large furnace, which was not included in this study due to the logistical challenges. It would be interesting to determine the power requirements and time taken to heat up an entire structure and also insightful as to how this could be realised logistically. The major disadvantage is that with the growing size of OWTs, there may be a limit for which a large furnace is physically possible. Notwithstanding, many DD OWTs that are being built or have been built recently are still under the dimensions of the CW OWT, such that a method for complete thermal demagnetisation could also be applicable to most earlier generation DD OWTs.

Besides thermal demagnetisation there is also the option of non-thermal demagnetisation with an opposite magnetic field. This was not explored in much detail because this study focused on the comparison to the WEEE recycling route, in which thermal demagnetisation is dominant. It is

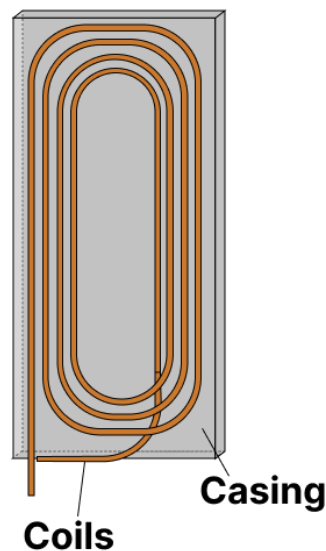


Figure 5.2: Direct induction heating by placing coils near the permanent magnet.

possible that an opposite magnetic field for an OWT is possible, by for example using the inner stator to generator the opposing field. This is another topic that would need additional attention.

5.3 | Recommendations and limitations

This study explored a completely new area of materials science, with a primary focus on disassembly. The cross-section with magnetism and heat transfer, which do not necessarily fall directly under materials science means that a lot of new knowledge had to be obtained from other fields. On the one hand, this makes this study unique as it brings together three fields but on the other hand, this limited the depth to which the study could for testing the theories.

Many of the topics raised in the future recommendations in Section ?? arose during the study with people unable to answer the questions. From the materials science perspective thermal demagnetisation for the disassembly of permanent magnets do not fall under their expertise, while from an electrical engineering perspective this topic also does not fall under their expertise. For this reason, there was a very limited amount of literature to consult and within the TU Delft, there were only two professors that were somewhat knowledgeable on the topic.

This limitation also means that there is an opportunity for increased collaboration among academics across these scientific fields, which would be even better if they were able to work together with the industry. The biggest challenge therein lies in the competition on the market which has driven a very strict protection of intellectual property, which is one of the other limitations of this study. This could also be an explanation as to why research on the most recent OWTs is very limited and why accurate and precise data on the properties and characteristics of OWTs are difficult to find.

Due to the high levels of confidentiality, this study was based on the information provided by the case companies, collected from interviews and desk research. The site visit to Cuxhaven and interviews with various employees at the case company provided invaluable insights and more information than is publicly available. Nevertheless, specific quantitative data on dimensions, materials and other properties was omitted. Fortunately, this study consisted primarily of the development of a concept for disassembly such that precise data was not crucial.

The study aimed to develop a new concept for the disassembly of permanent magnets from OWTs through local thermal demagnetisation. As this is a very new field, this also means that the concept had to be developed based on limited examples from literature and knowledge from experts. Therefore, the concept should predominantly be perceived as a first step towards demagnetisation rather than an ideal solution.

Many assumptions were made in the development of this concept that need to be considered due to the lack of available knowledge, such that it had to be developed from scratch. Throughout the study, as many of the assumptions as possible have been explicitly described and mentioned. However due to the cross-over of three fields, it is possible that there was insufficient knowledge on a specific field to take a particular theory or principle into account that was not mentioned. Nonetheless, each assumption made also provides an opportunity for future research as these can be studied further and looked into in more detail.

It would have been ideal to get an actual permanent magnet from the case company to conduct an experiment and measure the properties. This was not possible due to time constraints and confidentiality. A recommendation would be to allow future studies to use a real magnet as a sample to test the demagnetisation and the heating method for example. Since the heating method used by [Bahl et al. \(2020\)](#) was relatively large in comparison to WEEE, but not necessarily representative of a real magnet since it did not have a casing and was a single block whose dimensions were also inconsistent with the dimensions for the CW OWT.

The aim of this study was to determine a disassembly method to enable the preferred recycling route, which was stated to be magnet-to-magnet. In this study the option for direct reuse was eliminated, while there is a possibility that this is desirable in the future. [Hogberg et al. \(2017\)](#) suggests a method for the direct reuse of rare earth permanent magnets through segmentation into 200 smaller poles. For the CW OWT the permanent magnets are segmented in 6 blocks, it is possible that trends will move towards smaller poles which could facilitate direct reuse, which was not considered in this study.

In the future it might be possible that the permanent magnet design and assembly of OWTs change or that permanent magnets may be eliminated all together, as a result of the industry's eagerness to move away from dependencies on CRMs such as REEs. While the concept may be applicable to the current generation of OWTs, it is possible that it will only be relevant for a limited amount of time. Regardless of the future developments, if the current production of OWTs driven by permanent magnet generators, there should be sufficient incentive to recycle the valuable materials.

As for the academic quality of the results, the model uses a very basic model for heat transfer

across a composite material. To improve the academic quality a more advanced model could have been made or the system could have been reproduced in a finite element modelling software such as COMSOL or Ansys. Prior to the illustrations, SolidWorks was used to model the assembly, unfortunately the program did not function properly and was therefore not imported to COMSOL.

5.4 | Conclusion

The research objective of this study was to determine how permanent magnets can be disassembled from OWT generators to facilitate an efficient recycling process for the effective recovery of REES based on the established WEEE recycling system.

From WEEE it is known that a higher degree of liberation of materials leads to a better quality recycled product. To achieve the best possible outcome for magnet-to-magnet recycling of permanent magnets from OWTs they need to be extracted and separated from other materials as much as possible. As such, disassembly is a critical factor for the liberation of the permanent magnets in OWTs to enable magnet-to-magnet recycling.

An overview of the preferred recycling route is shown in Figure 5.3, which also include subsequent steps after disassembly, where the scope of this study is limited to focusing on the demagnetisation and disassembly as they are the first steps that enable the subsequent steps.

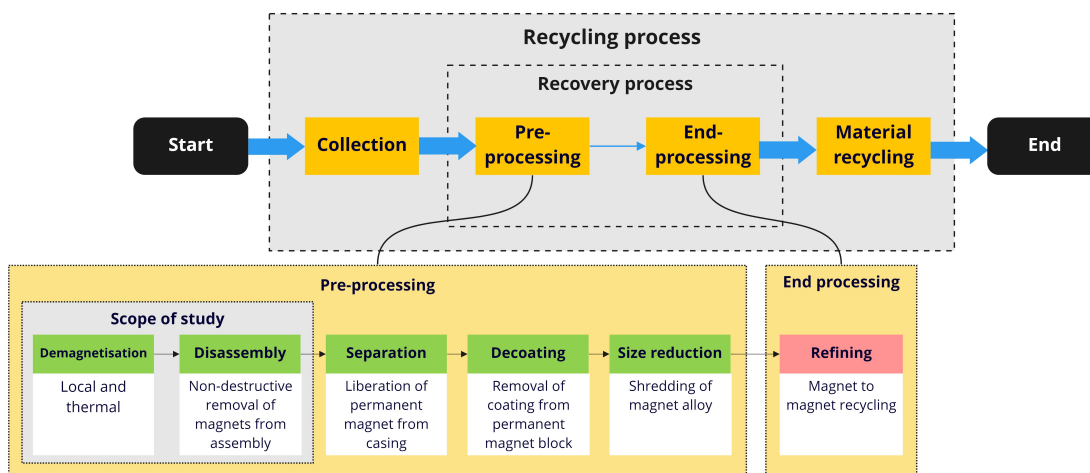


Figure 5.3: Overview of the preferred recycling route for permanent magnets from OWTs.

Based on the assembly and existing disassembly practices for permanent magnets from OWTs, the biggest challenge is the fact that they are currently removed in a magnetised state. While this is possible and common practice for permanent magnets in WEEE, it is evident that the process is tedious and complex for larger permanent magnets. Due to the difference in magnet volume and quantity per product in comparison to WEEE, the magnetic forces between the magnets and effects of the magnet field in the assembly need to be taken into consideration during disassembly.

Permanent magnets from WEEE are usually thermally demagnetised after disassembly and size reduction in a furnace. Thermal demagnetisation is preferred over non-thermal because heating the magnet above the Curie temperature is independent of the direction of the magnetic field, shape or size. Local thermal demagnetisation provides a flexible heating option that can be applied to magnets across the entire generator and has the least logistical challenges. As such, a combination of thermal and local demagnetisation would be preferable.

Due to the presence of a vast amount of electrical components in the OWT nacelles, a comparison to WEEE seemed like a valuable approach to study the recycling and disassembly of the permanent magnets from OWTs. In hindsight however, the disassembly concept itself is not related to any WEEE process and more time could have been spent on the magnetism and heating aspects rather than the comparison with WEEE. Nevertheless, WEEE was an important starting point in identifying the research topic and substantiating the preferred recycling route.

To disassemble the magnets from OWT generators in a non-destructive manner a concept for local thermal demagnetisation was developed. A U shaped core with a copper winding could be heated via induction and placed against the magnets to transfer heat via conduction, as shown in Figure 5.4. By controlling the power in the coil, the temperature in the core and to the magnet can be controlled.

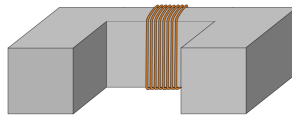


Figure 5.4: Induction heating through copper wires wrapped around a U shaped core.

This demagnetisation concept can be automated and scaled by using the trolleys that are already in place at the assembly site which can insert multiple cores from the top down into the rotor assembly. To keep the magnetic field of the rotor assembly in balance, all the poles of one polarity need to be disassembled first by alternating columns and alternating between opposing sides. To demagnetise multiple magnets simultaneously the core concept can be stacked as shown in Figure 5.5.

Due to the polarity of the magnets, the ideal orientation of the cores would be vertical as shown in Figure 5.6. This means that 6 magnets can be demagnetised per column and 12 magnets can be demagnetised at once, when adding in the opposing side, which can then make 96 rotations to demagnetise the entire assembly in less than four hours.

To determine the power required to heat the magnets to the Curie temperature and the effect of different variables on the demagnetisation concept, a simplified model was constructed. From the model, it was evident that the time taken to heat the conductor had the largest influence over the power requisites of the system. The material chosen for the conductor also had a strong impact on the power, where the aluminium alloy was found to be the most effective. The

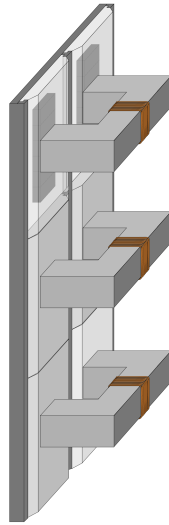


Figure 5.5: Thermal demagnetisation of multiple magnets by utilising multiple cores for induction.

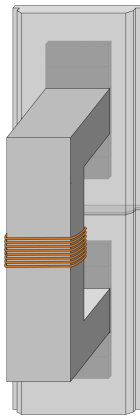


Figure 5.6: Core rotated 90° to contact two magnets in the same column.

power requirements also depended on the contact surface area of the conductor, the mass of the conductor and the Curie temperature.

After the permanent magnet is demagnetised the magnets can be removed from the assembly when they are either hot or cold. The advantage of removing the magnets when they are hot is that they are completely demagnetised and not susceptible to re-magnetisation during their movements. On the other hand, the thermal expansion of the magnet may cause the magnets to expand within the slots, making it difficult to get them out.

If the magnets are to cool first, the magnets may be subjected to re-magnetisation due to the surrounding magnetic field of the rotor assembly. Moreover, the remanence may also cause forces to act between the magnet and the rotor assembly. However, the extent to which re-

magnetisation and remanence hinder the actual disassembly process is something that could be studied as this would also determine whether or not it is a prerequisite for the magnet to reach the Curie temperature to be disassembled.

Prior to developing this concept it was unexpected that the field of magnetism, materials and heat transfer would come together so closely, which appear to be segregated in the academic world. There were many interesting phenomena that could have been interesting from a materials science perspective, such as magneto crystalline anisotropy, that could also have provided insights into demagnetisation. However, since the combinations of these fields appeared to be fairly new, the model and concept had to be developed at a very level. Nevertheless, there is potential to dive into the crystallographic structure of materials and the magnetic domains to see how they come together.

As a result of this high level approach, many effects and factors were neglected and should be taken into consideration in future studies. Due to the lack of literature and knowledge on this field the best place to start for a successive study be through practical experimentation, to determine whether the concept is at all feasible before spending time getting into the precise details.

This concept provides a first approach to local thermal demagnetisation to enable the disassembly of permanent magnets from OWTs but is also very limited to demonstrating just one of the many possibilities for demagnetisation or disassembly. Alternative options such as direct induction, combined thermal and non-thermal techniques or complete thermal demagnetisation in an industrial furnace could be explored.

In the long term the goal is to maintain resources for as long as possible towards a circular economy, therefore other options than recycling such as direct reuse should also be considered. For direct reuse, thermal demagnetisation would not be preferred due to its irreversible nature and thus other solutions for mechanical disassembly of non-thermal demagnetisation should be considered. However, all of the proposed solutions are concocted based on a fixed design.

Ideally, the permanent magnet generators should move towards design for disassembly with the challenges found in this study in mind. How can the design of the generator and the assembly, or the design of the magnet facilitate the disassembly and enable an efficient recycling route? Design parameters should take into account whether the magnets can be moved while magnetised and if not, how the design can accommodate the thermal expansion caused by heating for example.

This study aimed to provide a solution as to how the permanent magnets can be disassembled from the generator of an OWT to enable their efficient recycling. This can be done by local thermal demagnetisation using a U shaped core heated by induction, such that the heat is transferred by conduction. All in all it is only one solution to the bigger picture to reduce the environmental impacts of OWTs and retain the value and reduce the exhaustion of REEs, such that circular design principles may stimulate an entirely different direction such as direct reuse rather than recycling.

Python

A.1 | Properties database

```
1 import numpy as np
2 from matplotlib import pyplot as plt
3
4 """Define functions"""
5
6 def volume (x,y,z):
7     return x * y * z
8
9 T_amb = 293 # [K]
10
11 """
12 Set material properties
13 """
14
15 #304 Steel
16 rho_304 = 7817 # [kgm^-3]
17 k_304 = 14.4 # [Wm^-1K^-1]
18 c_304 = 461 # [Jkg^-1K^-1]
19
20
21 #316 Steel
22 rho_316 = 8060 # [kgm^-3]
23 k_316 = 16.3 # [Wm^-1K^-1]
24 c_316 = 500 # [Jkg^-1K^-1]
25 n_316 = 0.5
26
27 #NdFeB Magnet
28 rho_nd = 7500 # [kgm^-3]
29 k_nd = 7.6 # [Wm^-1K^-1]
30 c_nd = 460 # [Jkg^-1K^-1]
31 Tc_nd = 583 # [K]
```

```

32
33
34 #Copper alloy
35 rho_cu = 8600 # [kgm^-3]
36 k_cu = 83 # [Wm^-1K^-1]
37 c_cu = 410 # [Jkg^-1K^-1]
38 n_cu = 0.15
39
40 #Aluminium alloy
41 rho_al = 2787 # [kgm^-3]
42 k_al = 164 # [Wm^-1K^-1]
43 c_al = 833 # [Jkg^-1K^-1]
44 n_al = 0.4
45
46
47 """
48 Set properties of the components
49 """
50
51 #Permanent magnets"
52
53 x_p = 0.055 # [m]
54 y_p = 0.014 # [m]
55 z_p = 0.025 # [m]
56 V_p = volume(x_p, y_p, z_p) # [m^3]
57
58 rho_p = rho_nd # [kgm^-3]
59 k_p = k_nd # [Wm^-1K^-1]
60 c_p = c_nd # [Jkg^-1K^-1]
61 m_p = V_p * rho_p # [Kg]
62 Tc_p = Tc_nd # [K]
63
64
65 #Magnet casing"
66
67 x_cs = 0.055 # [m]
68 y_cs = 0.014 # [m]
69 z_cs = 0.220 # [m]
70
71 rho_cs = rho_304 # [kgm^-3]
72 k_cs = k_304 # [Wm^-1K^-1]
73 c_cs = c_304 # [Jkg^-1K^-1]
74
75 #Conductor material properties"
76
77 #Part A: Front section in contact with casing
78 x_cda = 0.055 # [m]
79 y_cda = 0.050 # [m]
80 z_cda = 0.220 # [m]
81 V_cda = x_cda * y_cda * z_cda # [m^3]

```

```

82
83 #Part B: Back section being heated via induction
84 x_cdb = 0.135 # [m]
85 y_cdb = 0.050 # [m]
86 z_cdb = 0.220 # [m]
87 V_cdb = x_cdb * y_cdb * z_cdb # [m^3]
88
89 A_cd = x_cda * z_cda # [m^2]
90 V_cd = 2*V_cda + V_cdb # [m^3]
91
92
93 # Number of permanent magnets per casing
94 N_p = 6
95 m_ptot = N_p * m_p # [kg]
96 V_ptot = N_p * V_p # [m^3]
97
98 #Calculate geometry of magnet casing
99 #Part A: Backplate
100 x_csa = 0.125 # [m]
101 y_csa = 0.007 # [m]
102 z_csa = z_cs # [m]
103 V_csa = x_csa * y_csa * z_csa # [m^3]
104
105 #Part B: Frontplate midsection
106 x_csb = 0.115 # [m]
107 y_csb = 0.014 # [m]
108 z_csb = z_cs # [m]
109 V_csb = (x_csb * y_csb * z_csb) - V_ptot # [m^3]
110
111 #Part C: Frontplate topsection
112 x_csc = 0.095 # [m]
113 y_csc = 0.014 # [m]
114 z_csc = z_cs # [m]
115 V_csc = x_csc * y_csc * z_csc # [m^3]
116
117 # Total geometry of casing
118 V_cstot = V_csa + V_csb + V_csc # [m^3]
119 m_cstot = V_cstot * rho_cs # [kg]
120 m_pcstot = m_ptot + m_cstot # [kg]

```

A.2 | Variable Curie temperature

```

1 # -*- coding: utf-8 -*-
2 """
3 Created on Sat Aug 13 15:30:07 2022
4
5 @author: FayDeWaal
6 """
7
8 import properties1
9 from properties1 import *
10
11 import pandas as pd
12 import numpy as np
13 from matplotlib import pyplot as plt
14
15 # Mass calculations of materials
16
17 #print("Mass magnets per casing:", round(m_ptot,3), "kg")
18 #print("Mass casing without magnets:", round(m_cstot,3), "kg")
19 #print("Mass casing with magnets:", round(m_pcstot,3), "kg")
20
21
22 # print("Q_p:", round(Q_p * 10**(-3),3), "kJ")
23
24 # Time taken to heat up the permanent magnets
25
26 def curie(Tc_min,Tc_max,t):
27
28     # Energy required to heat all 6 permanent magnets
29
30     Tc_p = np.linspace(Tc_min, Tc_max, Tc_max-Tc_min+1)
31
32     Q_p = m_p * c_p * (Tc_p - T_amb) # [J]
33
34     # Surface area of the conductor against the magnet
35     A = A_cd # [m^2]
36
37     # Heat flow calculations for the permanent magnets
38
39     # Rate of heat transfer per second
40     Qd_p = Q_p / t # [Js^-1]
41     # Rate of heat transfer per area:
42     q_p = Q_p / A # [Jm^-2]
43     # Heat flow per area per second:
44     qd_p = Q_p / (A * t) # [Jm^-2s^-1]
45
46     # print("t:", t, "s")

```

```

47 # print("Qd_p:", round(Qd_p,3), "Js^-1 or W")
48 # print("q_p:", round(q_p * 10**(-3)), "kJm^-2")
49 # print("qd_p:", round(qd_p * 10**(-3)), "kJm^-2")
50
51 # Assume heat flow (Qd) through the material is constant
52
53 # print("Tc_p:", round(Tc_p - 273), "C")
54
55 k_cd = k_al
56 c_cd = c_al
57 rho_cd = rho_al
58
59 m_cda = V_cda * rho_cd # [Kg]
60 m_cdb = V_cdb * rho_cd # [Kg]
61 m_cd = V_cd * rho_cd # [Kg]
62
63
64 # Calculate thermal resistance of permanent magnet
65
66 #L_p is the depth the heat needs to penetrate, we want to reach the curcie
67 # temperature at the core of the magnet
68 L_p = y_p # [m]
69 R_p = k_p * A / L_p # [WK^-1]
70
71 # Temperature at the face of the magnet
72 T_1 = Qd_p / R_p + Tc_p # [K]
73
74 # print("T_1:", round(T_1-273), "C")
75
76 # Calculate thermal resistance of casing
77 L_cs = y_cs # [m]
78 R_cs = k_cs * A / L_cs # [WK^-1]
79
80 # Temperature at the face of the casing
81 T_2 = Qd_p / R_cs + T_1 # [K]
82
83 # print("T_2:", round(T_2-273), "C")
84
85 # Calculate thermal resistance of conductor material part A
86 L_cda = y_cda # [m]
87 R_cda = k_cd * A / L_cda # [WK
88 ^-1]
89
90 # Temperature at the back edge of part A
91 T_3 = Qd_p / R_cda + T_2 # [K]
92
93 # print("T_3:", round(T_3-273), "C")
94
95 # Calculate thermal resistance of conductor material part B
96 L_cdb = x_cdb # [m]

```

```

95     R_cdb = k_cd * A / L_cdb                                     # [WK
    ^-1]
96
97     # Temperature at the back edge of part A
98     T_4 = Qd_p / R_cdb + T_3                                   # [K]
99
100    # print("T_4:", round(T_4-273), "C")
101
102
103    # Energy required to heat conductor material
104
105    Q_cdb = m_cdb * c_cd * (T_4 - T_amb)                       #[J]
106
107    # print("Q_cdb:", round(Q_cdb * 10**(-3),3), "kJ")
108
109    # Time taken to heat up the conductor material
110    ti = 360                                                    #[s]
111
112    # Heat flow calculations for the inductor
113
114    # Rate of heat transfer per second
115    Qd_i = Q_cdb / ti                                         #[Js^-1]
116    # Rate of heat transfer per area:
117    q_i = Q_cdb / A                                           #[Jm^-2]
118    # Heat flow per area per second:
119    qd_i = Q_cdb / (A * ti)                                   #[Jm^-2s^-1]
120
121    # print("ti:", ti, "s")
122    # print("Qd_i:", round(Qd_i,3), "Js^-1 or W")
123    # print("q_i:", round(q_i * 10**(-3)), "kJm^-2")
124    # print("qd_i:", round(qd_i * 10**(-3)), "kJm^-2")
125
126    # Power needed in the coil
127
128    #Thermal and electrical efficiency
129
130    # n_el = 0.8
131    #n_th = 0.7
132
133    n = n_al
134    # print("n_i:", round(n_i,3), "%")
135
136    P_i = Qd_i / n                                             #[Js^-1]
137
138    # For the plot
139    Tc_p1 = Tc_p - 273
    #[%]
140    P_i1 = P_i * 10 ** (-3)                                    #[W]
141
142    return Tc_p1, P_i1

```

```
143
144 Tc_p1, P_i1 = curie(473, 673, 60)
145 Tc_p2, P_i2 = curie(473, 673, 120)
146 Tc_p3, P_i3 = curie(473, 673, 180)
147
148 #print("P_i:", round(P_i2(110),3), "Js^-1 or W")
149
150 plt.plot(Tc_p1,P_i1, label = 'Time = 60s')
151 plt.plot(Tc_p2,P_i2, label = 'Time = 120s')
152 plt.plot(Tc_p3,P_i3, label = 'Time = 180s')
153 plt.title("Power needed based on Curie Temperature")
154 plt.xlabel("Temperature [C]")
155 plt.ylabel("Power (kW)")
156 plt.legend()
157 plt.savefig('curietemp1.png')
158 plt.show()
159
160 Time = pd.DataFrame({'Temp [C]': Tc_p2, 'Power [W]': P_i2.round(3)})
161 Time.to_excel("curie1.xlsx")
```

Bibliography

- Amato, A., Becci, A., Birloaga, I., De Michelis, I., Ferella, F., Innocenzi, V., Ippolito, N. M., Pillar Jimenez Gomez, C., Vegliò, F., and Beolchini, F. (2019). Sustainability analysis of innovative technologies for the rare earth elements recovery. *Renewable and Sustainable Energy Reviews*, 106:41–53.
- Ambaye, T. G., Vaccari, M., Castro, F. D., Prasad, S., and Rtimi, S. (2020). Emerging technologies for the recovery of rare earth elements (REEs) from the end-of-life electronic wastes: a review on progress, challenges, and perspectives. *Environmental Science and Pollution Research* 2020 27:29, 27(29):36052–36074.
- Andersen, P. D., Bonou, A., Beauson, J., and Brønsted, P. (2014). Recycling of wind turbines. *DTU International Energy Report 2014*, 13(July):91–98.
- Arora, A. (2018). Optical and electric field control of magnetism. *University of Potsdam*, pages 11–20.
- Arrobas, D. L. P., Hund, K. L., McCormick, M. S., Ningthoujam, J., and Drexhage, J. R. (2017). The Growing Role of Minerals and Metals for a Low Carbon Future. Technical report, The World Bank Group, Washington.
- Azuma, D. (2018). Magnetic materials. *Wide Bandgap Power Semiconductor Packaging: Materials, Components, and Reliability*, pages 97–107.
- Bahl, C. R., Eder, M. A., Boland, G., and Abrahamsen, A. B. (2020). A Simple Method for Demagnetizing Large NdFeB Permanent Magnets. *IEEE Transactions on Magnetics*, 56(8).
- Batinic, B., Vaccari, M., Savvilitidou, V., Kousaiti, A., Gidakos, E., Marinkovic, T., and Fiore, S. (2018). Applied WEEE pre-treatment methods: Opportunities to maximizing the recovery of critical metals. *Article in Global Nest Journal*, 20(4):706–711.
- Binnemans, K., Jones, P. T., Blanpain, B., Van Gerven, T., Yang, Y., Walton, A., and Buchert, M. (2013). Recycling of rare earths: a critical review. *Journal of Cleaner Production*, 51:1–22.
- Bonou, A., Laurent, A., and Olsen, S. I. (2016). Life cycle assessment of onshore and offshore wind energy-from theory to application. *Applied Energy*, 180:327–337.
- BVG Associates (2019). Guide to an offshore wind farm. Technical report, The Crown Estate, Offshore Renewable Energy Catapult, Swindon.
- Caglayan, D. G., Ryberg, D. S., Heinrichs, H., Linßen, J., Stolten, D., and Robinius, M. (2019). The techno-economic potential of offshore wind energy with optimized future turbine designs in Europe. *Applied Energy*, 255.

- Campell, P. (1994). *Permanent Magnet Materials and Their Application*, volume 1. Cambridge University, New York, 1 edition.
- Carrara, T., Dias, A., Eur, C., and Nd Pr Dy Tb, E. (2020). Ag Ga Ge Si Cd In Se Raw materials demand for wind and solar PV technologies in the transition towards a decarbonised energy system. Technical report, European Commission Joint Research Centre (JRC), Petten.
- Chen, R. W., Navin-Chandra, D., and Prinz, F. B. (1994). A Cost-Benefit Analysis Model of Product Design for Recyclability and its Application. *IEEE TRANSACTIONS ON COMPONENTS, PACKAGING, AND MANUFACTURING TECHNOLOGY-PART A*, 17(4).
- Constantinides, S. (2022). Permanent magnet coatings and testing procedures. *Modern Permanent Magnets*, pages 371–402.
- CrossWind (2022). The Wind farm.
- Cui, J. and Forssberg, E. (2003). Mechanical recycling of waste electric and electronic equipment: a review. *Journal of Hazardous Materials*, 99(3):243–263.
- Dallos, J. (2019). Brazing 101: Induction Heating.
- Desai, A. and Mital, A. (2003). Evaluation of disassemblability to enable design for disassembly in mass production. *International Journal of Industrial Ergonomics*, 32(4):265–281.
- Diehl, O., Schönfeldt, M., Brouwer, E., Dirks, A., Rachut, K., Gassmann, J., Güth, K., Buckow, A., Gauß, R., Stauber, R., and Gutfleisch, O. (2018). Towards an Alloy Recycling of Nd–Fe–B Permanent Magnets in a Circular Economy. *Journal of Sustainable Metallurgy*, 4(2):163–175.
- Du, X. and Graedel, T. E. (2011). Global Rare Earth In-Use Stocks in NdFeB Permanent Magnets. *Journal of Industrial Ecology*, 15(6):836–843.
- European Commission (2021). Waste from Electrical and Electronic Equipment (WEEE).
- European WEEE registers network (2018). WEEE2 – Definition and Understanding of the 6 Categories. Technical report, European WEEE registers network.
- Evangelopoulos, P., Kantarelis, E., and Yang, W. (2019). Waste Electric and Electronic Equipment: Current Legislations, Waste Management, and Recycling of Energy, Materials, and Feedstocks. *Sustainable Resource Recovery and Zero Waste Approaches*, pages 239–266.
- Farina, A. and Anctil, A. (2022). Material consumption and environmental impact of wind turbines in the USA and globally. *Resources, Conservation and Recycling*, 176:105938.
- Forti, V., Balde, C. P., Keuhr, R., and Bel, G. (2020). The Global E-waste Monitor 2020. Technical report, United Nations University (UNU)/United Nations Institute for Training and Research (UNITAR), Bonn/Geneva/Rotterdam.
- Garcia-Teruel, A., Rinaldi, G., Thies, P. R., Johanning, L., and Jeffrey, H. (2022). Life cycle assessment of floating offshore wind farms: An evaluation of operation and maintenance. *Applied Energy*, 307:118067.
- Guo, X., Zhang, Y., and Xu, K. (2016). Metallurgical Recovery of Metals from Waste Electrical and Electronic Equipment (WEEE) in PRC. *Metal Sustainability: Global Challenges, Consequences, and Prospects*, pages 151–168.
- Harivardhini, S., Murali Krishna, K., and Chakrabarti, A. (2017). An Integrated Framework for supporting decision making during early design stages on end-of-life disassembly. *Journal of Cleaner Production*, 168:558–574.
- Hernandez C, O. M., Shadman, M., Amiri, M. M., Silva, C., Estefen, S. F., and La Rovere, E. (2021). Environmental impacts of offshore wind installation, operation and maintenance, and decommissioning activities: A case study of Brazil. *Renewable and Sustainable Energy Reviews*, 144.

- Hicks, C., Dietmar, R., and Eugster, M. (2005). The recycling and disposal of electrical and electronic waste in China—legislative and market responses. *Environmental Impact Assessment Review*, 25(5):459–471.
- Hogberg, S., Bendixen, F. B., Mijatovic, N., Bech Jensen, B., and Holboll, J. (2016). Influence of demagnetization-temperature on magnetic performance of recycled Nd-Fe-B magnets. *Proceedings - 2015 IEEE International Electric Machines and Drives Conference, IEMDC 2015*, pages 1242–1246.
- Hogberg, S., Holboll, J., Mijatovic, N., Jensen, B. B., and Bendixen, F. B. (2017). Direct Reuse of Rare Earth Permanent Magnets - Coating Integrity. *IEEE Transactions on Magnetics*, 53(4).
- Ibanescu, D., Cailan (Gavrilescu), D., Teodosiu, C., and Fiore, S. (2018). Assessment of the waste electrical and electronic equipment management systems profile and sustainability in developed and developing European Union countries. *Waste Management*, 73:39–53.
- Ilankoon, I. M., Ghorbani, Y., Chong, M. N., Herath, G., Moyo, T., and Petersen, J. (2018). E-waste in the international context - A review of trade flows, regulations, hazards, waste management strategies and technologies for value recovery. *Waste Management*, 82:258–275.
- Ito, A. and Tanaka, K. (2014). Applications of Carbon Nanotubes and Graphene in Spin Electronics. *Carbon Nanotubes and Graphene: Edition 2*, pages 253–278.
- Izatt, R. M. (2016). *Metal Sustainability: Global Challenges, Consequences and Prospects*. John Wiley & Sons Ltd, Utah, first edition.
- Jensen, J. P. and Remmen, A. (2017). Enabling Circular Economy Through Product Stewardship. *Procedia Manufacturing*, 8:377–384.
- Jensen, P. D., Purnell, P., and Velenturf, A. P. M. (2020). Highlighting the need to embed circular economy in low carbon infrastructure decommissioning: The case of offshore wind. *Sustainable Production and Consumption*, 24:266–280.
- Jin, H., Afunoy, P., Dove, S., Furlan, G., Zakotnik, M., Yih, Y., and Sutherland, J. W. (2018). Life Cycle Assessment of Neodymium-Iron-Boron Magnet-to-Magnet Recycling for Electric Vehicle Motors. *Environmental Science and Technology*, 52(6):3796–3802.
- Johnson, J., Harper, E. M., Lifset, R., and Graedel, T. E. (2007). Dining at the periodic table: Metals concentrations as they relate to recycling. *Environmental Science and Technology*, 41(5):1759–1765.
- Jowitt, S. M., Werner, T. T., Weng, Z., and Mudd, G. M. (2018). Recycling of the rare earth elements. *Current Opinion in Green and Sustainable Chemistry*, 13:1–7.
- Kapustka, K., Ziegmann, G., Klimecka-Tatar, D., and Nakonczy, S. (2020). Process Management and Technological Challenges in the Aspect of Permanent Magnets Recovery-the Second Life of Neodymium Magnets Establishment of Design Catalog for Vacuum-Insulating Fiber Composite Sandwich Materials View project. *Manufacturing Technology*, 20(5):617–624.
- Kasper, A. C., Bernardes, A. M., and Veit, H. M. (2011). Characterization and recovery of polymers from mobile phone scrap. *Waste Management and Research*.
- Kasper, A. C., Juchneski, N. C. d. F., and Veit, H. M. (2015). Mechanical Processing. *Topics in Mining, Metallurgy and Materials Engineering*, pages 19–38.
- Kaya, M. (2016). Recovery of metals and nonmetals from electronic waste by physical and chemical recycling processes. *Waste Management*, 57:64–90.
- Kim, J., Guillaume, B., Chung, J., and Hwang, Y. (2015). Critical and precious materials consumption and requirement in wind energy system in the EU 27. *Applied Energy*, 139(2015):327–334.

- Kopacek, B. (2017). Intelligent disassembly of components from printed circuit boards to enable re-use and more efficient recovery of critical metals. *2016 Electronics Goes Green 2016+, EGG 2016*.
- Kreith, F., Manglik, R. M., and Bohn, M. S. (2010). *Principles of Heat Transfer*. Cengage Learning, Stamford, 2 edition.
- Kumar, R. (2021). Tertiary and quaternary recycling of thermoplastics by additive manufacturing approach for thermal sustainability. *Materials Today: Proceedings*, 37(Part 2):2382–2386.
- Li, C., Mogollón, J. M., Tukker, A., Dong, J., von Terzi, D., Zhang, C., and Steubing, B. (2022). Future material requirements for global sustainable offshore wind energy development. *Renewable and Sustainable Energy Reviews*, 164:112603.
- Li, D., Li, Y., Pan, D., Zhang, Z., and Choi, C. J. (2019a). Prospect and status of iron-based rare-earth-free permanent magnetic materials. *Journal of Magnetism and Magnetic Materials*, 469:535–544.
- Li, J., Barwood, M., and Rahimifard, S. (2015). An automated approach for disassembly and recycling of Electric Vehicle components. *2014 IEEE International Electric Vehicle Conference, IEVC 2014*.
- Li, Z., Kedous-Lebouc, A., Dubus, J. M., Garbuio, L., and Personnaz, S. (2019b). Direct reuse strategies of rare earth permanent magnets for PM electrical machines – an overview stu. *The European Physical Journal Applied Physics*, 86(2):20901.
- Liu, P., Meng, F., and Barlow, C. Y. (2019). Wind turbine blade end-of-life options: An eco-audit comparison. *Journal of Cleaner Production*, 212:1268–1281.
- Lixandru, A., Venkatesan, P., Jönsson, C., Poenaru, I., Hall, B., Yang, Y., Walton, A., Güth, K., Gauß, R., and Gutfleisch, O. (2017). Identification and recovery of rare-earth permanent magnets from waste electrical and electronic equipment. *Waste Management*, 68:482–489.
- Maisel, F., Chancerel, P., Dimitrova, G., Emmerich, J., Nissen, N. F., and Schneider-Ramelow, M. (2020). Preparing WEEE plastics for recycling – How optimal particle sizes in pre-processing can improve the separation efficiency of high quality plastics. *Resources, Conservation and Recycling*, 154:104619.
- Majumdar, S., Majumdar, H., Österbacka, R., and McCarthy, E. (2016). Organic Spintronics. *Reference Module in Materials Science and Materials Engineering*.
- Marconi, M., Germani, M., Mandolini, M., and Favi, C. (2018). Applying data mining technique to disassembly sequence planning: a method to assess effective disassembly time of industrial products. <https://doi.org/10.1080/00207543.2018.1472404>, 57(2):599–623.
- Marra, A., Cesaro, A., and Belgiorno, V. (2018). Separation efficiency of valuable and critical metals in WEEE mechanical treatments. *Journal of Cleaner Production*, 186:490–498.
- Möller, B., Hong, L., Lonsing, R., and Hvelplund, F. (2012). Evaluation of offshore wind resources by scale of development. *Energy*, 48(1):314–322.
- München, D. D., Stein, R. T., and Veit, H. M. (2021). Rare Earth Elements Recycling Potential Estimate Based on End-of-Life NdFeB Permanent Magnets from Mobile Phones and Hard Disk Drives in Brazil. *Minerals 2021, Vol. 11, Page 1190*, 11(11):1190.
- München, D. D. and Veit, H. M. (2017). Neodymium as the main feature of permanent magnets from hard disk drives (HDDs). *Waste Management*, 61:372–376.
- Murugappan, R. M. and Karthikeyan, M. (2021). Microbe-assisted management and recovery of heavy metals from electronic wastes. *Environmental Management of Waste Electrical and Electronic Equipment*, pages 65–88.
- Muthu, S. S., Li, Y., Hu, J. Y., and Mok, P. Y. (2012). Recyclability Potential Index (RPI): The concept and quantification of RPI for textile fibres. *Ecological Indicators*, 18:58–62.

- Nababan, D. C., Mukhlis, R., Durandet, Y., Pownceby, M. I., Prentice, L., and Rhamdhani, M. A. (2021). Mechanism and microstructure evolution of high temperature oxidation of end-of-life NdFeB rare earth permanent magnets. *Corrosion Science*, 182:109290.
- Nakamura, H. (2018). The current and future status of rare earth permanent magnets. *Scripta Materialia*, 154:273–276.
- Nelen, D., Manshoven, S., Peeters, J. R., Vanegas, P., D'Haese, N., and Vrancken, K. (2014). A multidimensional indicator set to assess the benefits of WEEE material recycling. *Journal of Cleaner Production*, 83:305–316.
- Ni'am, A. C., Wang, Y. F., Chen, S. W., and You, S. J. (2019). Recovery of rare earth elements from waste permanent magnet (WPMs) via selective leaching using the Taguchi method. *Journal of the Taiwan Institute of Chemical Engineers*, 97:137–145.
- Nijkerk, A. A., Dalmijn, W. L., and Dutch National Reuse of Waste Research Programme (NOH) (2001). *Handbook of recycling techniques. 5th edition*. Nijkerk Consultancy, Den Haag, 5th edition.
- Nlebedim, I. C. and King, A. H. (2018). Addressing Criticality in Rare Earth Elements via Permanent Magnets Recycling. *JOM*, 70(2):115–123.
- Omodara, L., Pitkäaho, S., Turpeinen, E. M., Saavalainen, P., Oravisjärvi, K., and Keiski, R. L. (2019). Recycling and substitution of light rare earth elements, cerium, lanthanum, neodymium, and praseodymium from end-of-life applications - A review. *Journal of Cleaner Production*, 236:117573.
- Önal, M. A. R., Dewilde, S., Degri, M., Pickering, L., Saje, B., Riaño, S., Walton, A., and Binnemans, K. (2020). Recycling of bonded NdFeB permanent magnets using ionic liquids. *Green Chemistry*, 22(9):2821–2830.
- Ortegon, K., Nies, L. F., and Sutherland, J. W. (2013). Preparing for end of service life of wind turbines. *Journal of Cleaner Production*, 39:191–199.
- Pan, X., Wong, C. W., and Li, C. (2022). Circular economy practices in the waste electrical and electronic equipment (WEEE) industry: A systematic review and future research agendas. *Journal of Cleaner Production*, 365:132671.
- Paredes-Sánchez, J. P., Villicaña-Ortíz, E., and Xiberta-Bernat, J. (2015). Materials use in electricity generators in wind turbines – state-of-the-art and future specifications. *Journal of Cleaner Production*, 87(1):275–283.
- Peelman, S., Venkatesan, P., Abrahami, S., and Yang, Y. (2018). Recovery of REEs from End-of-Life Permanent Magnet Scrap Generated in WEEE Recycling Plants. In *The Minerals, Metals and Materials*, pages 2619–2631. Springer, Cham.
- Pérez-Belis, V., Bovea, M. D., and Ibáñez-Forés, V. (2015). An in-depth literature review of the waste electrical and electronic equipment context: Trends and evolution. *Waste Management and Research*, 33(1):3–29.
- Popov, V. V., Grilli, M. L., Koptug, A., Jaworska, L., Katz-Demyanetz, A., Klobčar, D., Balos, S., Postolnyi, B. O., and Goel, S. (2021). Powder Bed Fusion Additive Manufacturing using Critical Raw Materials: a review. *Materials*, 14(909):1–37.
- Rademaker, J. H., Kleijn, R., and Yang, Y. (2013). Recycling as a strategy against rare earth element criticality: A systemic evaluation of the potential yield of NdFeB magnet recycling. *Environmental Science and Technology*, 47(18):10129–10136.
- Ramprasad, C., Gwenzi, W., Chaukura, N., Izyan Wan Azelee, N., Upamali Rajapaksha, A., Naushad, M., and Rangabhashyam, S. (2022). Strategies and options for the sustainable recovery of rare earth elements from electrical and electronic waste. *Chemical Engineering Journal*, 442:135992.
- RF Heating Consult (2022). Induction heating .
- Ruan, J. and Xu, Z. (2016). Constructing environment-friendly return road of metals from e-waste: Combination of physical separation technologies. *Renewable and Sustainable Energy Reviews*, 54:745–760.

- Rudnev, V., Loveless, D., and Cook, R. L. (2017). *Handbook of Induction Heating*.
- Sabaghi, M., Cai, Y., Mascle, C., and Baptiste, P. (2015). Sustainability assessment of dismantling strategies for end-of-life aircraft recycling. *Resources, Conservation and Recycling*, 102:163–169.
- Saraswati, N. (2020). Life cycle assessment of offshore wind farm (a Dutch case study). Technical report, TNO, Petten.
- Sechovský, V. (2001). Magnetism in Solids: General Introduction. *Encyclopedia of Materials: Science and Technology*, pages 5018–5032.
- Sethurajan, M., van Hullebusch, E. D., Fontana, D., Akcil, A., Deveci, H., Batinic, B., Leal, J. P., Gasche, T. A., Ali Kucuker, M., Kuchta, K., Neto, I. F., Soares, H. M., and Chmielarz, A. (2019). Recent advances on hydrometallurgical recovery of critical and precious elements from end of life electronic wastes - a review. <https://doi.org/10.1080/10643389.2018.1540760>, 49(3):212–275.
- Shittu, O. S., Williams, I. D., and Shaw, P. J. (2021). Global E-waste management: Can WEEE make a difference? A review of e-waste trends, legislation, contemporary issues and future challenges. *Waste Management*, 120:549–563.
- Siemens Gamesa (2014). Environmental Product Declaration SG 8.0-167 DD. Technical report, Siemens Gamesa Renewable Energy S.A., Vizcaya.
- Smith, G., Garrett, C., and Gibberd, G. (2015). Logistics and Cost Reduction of Decommissioning Offshore Wind Farms. *EWEA Offshore 2015*, 44(March):0–10.
- Sodhi, R., Sonnenberg, M., and Das, S. (2010). Evaluating the unfastening effort in design for disassembly and serviceability. <https://doi-org.tudelft.idm.oclc.org/10.1080/0954482031000150152>, 15(1):69–90.
- Song, X., Zhou, W., Pan, X., and Feng, K. (2014). Disassembly sequence planning for electro-mechanical products under a partial destructive mode. *Assembly Automation*, 34(1):106–114.
- Sprecher, B., Xiao, Y., Walton, A., Speight, J., Harris, R., Kleijn, R., Visser, G., and Kramer, G. J. (2014). Life cycle inventory of the production of rare earths and the subsequent production of NdFeB rare earth permanent magnets. *Environmental Science and Technology*, 48(7):3951–3958.
- Swain, N. and Mishra, S. (2019). A review on the recovery and separation of rare earths and transition metals from secondary resources. *Journal of Cleaner Production*, 220:884–898.
- Tabelin, C. B., Park, I., Phengsaart, T., Jeon, S., Villacorte-Tabelin, M., Alonzo, D., Yoo, K., Ito, M., and Hiroyoshi, N. (2021). Copper and critical metals production from porphyry ores and E-wastes: A review of resource availability, processing/recycling challenges, socio-environmental aspects, and sustainability issues. *Resources, Conservation and Recycling*, 170:105610.
- Tanskanen, P. (2013). Management and recycling of electronic waste. *Acta Materialia*, 61(3):1001–1011.
- Tao, F., Bi, L., Zuo, Y., and Nee, A. Y. (2018). Partial/Parallel Disassembly Sequence Planning for Complex Products. *Journal of Manufacturing Science and Engineering, Transactions of the ASME*, 140(1).
- Tazi, N., Kim, J., Bouzidi, Y., Chatelet, E., and Liu, G. (2019). Waste and material flow analysis in the end-of-life wind energy system. *Resources, Conservation and Recycling*, 145(February):199–207.
- Thompson, D., Hyde, C., Hartley, J. M., Abbott, A. P., Anderson, P. A., and Harper, G. D. (2021). To shred or not to shred: A comparative techno-economic assessment of lithium ion battery hydrometallurgical recycling retaining value and improving circularity in LIB supply chains. *Resources, Conservation and Recycling*, 175:105741.
- Topham, E., McMillan, D., Bradley, S., and Hart, E. (2019). Recycling offshore wind farms at decommissioning stage. *Energy Policy*, 129(September 2018):698–709.

- Tota-Maharaj, K. and McMahon, A. (2021). Resource and waste quantification scenarios for wind turbine decommissioning in the United Kingdom. *Waste Disposal & Sustainable Energy*, 3(2):117–144.
- Tunsu, C. (2018). Hydrometallurgy in the recycling of spent NdFeB permanent magnets. *Waste Electrical and Electronic Equipment Recycling: Aqueous Recovery Methods*, pages 175–211.
- Ueberschaar, M., Geiping, J., Zamzow, M., Flamme, S., and Rotter, V. S. (2017). Assessment of element-specific recycling efficiency in WEEE pre-processing. *Resources, Conservation and Recycling*, 124:25–41.
- United Nations Environmental Program (2018). E-Waste 2.0.
- van der Tempel, J. (2006). *Design of Support Structures for Offshore Wind Turbines*. PhD thesis, Delft University of Technology.
- Vanegas, P., Peeters, J. R., Cattrysse, D., Tecchio, P., Ardente, F., Mathieux, F., Dewulf, W., and Duflou, J. R. (2018). Ease of disassembly of products to support circular economy strategies. *Resources, Conservation and Recycling*, 135:323–334.
- Wang, S., Wang, S., and Liu, J. (2019). Life-cycle green-house gas emissions of onshore and offshore wind turbines. *Journal of Cleaner Production*, 210:804–810.
- WBCSD (2019). Circular Transition Indicators. Technical Report July, World Business Council Sustainable Development.
- Williams, I. D. (2016). Global metal reuse, and formal and informal recycling from electronic and other high-tech wastes. *Metal Sustainability: Global Challenges, Consequences, and Prospects*, pages 23–47.
- Worrell, E. and Reuter, M. A. (2014). Definitions and Terminology. *Handbook of Recycling: State-of-the-art for Practitioners, Analysts, and Scientists*, pages 9–16.
- Yang, J., Chang, Y., Zhang, L., Hao, Y., Yan, Q., and Wang, C. (2018). The life-cycle energy and environmental emissions of a typical offshore wind farm in China. *Journal of Cleaner Production*, 180:316–324.
- Yang, Y., Walton, A., Sheridan, R., Güth, K., Gauß, R., Gutfleisch, O., Buchert, M., Steenari, B. M., Van Gerven, T., Jones, P. T., and Binnemans, K. (2017). REE Recovery from End-of-Life NdFeB Permanent Magnet Scrap: A Critical Review. *Journal of Sustainable Metallurgy*, 3(1):122–149.